EVALUATION OF BEAM ANGLE SCORING USING MCNP AND APPLIED TO IMRT

A Thesis
Presented to
The Academic Faculty

by

Scott Sample

In Partial Fulfillment
of the Requirements for the Degree
Masters of Science in Medical Physics in the
School of Mechanical Engineering

Georgia Institute of Technology
May 2007

EVALUATION OF BEAM ANGLE SCORING USING MCNP AND APPLIED TO IMRT

Approved by:

Dr. Cassiano de Oliveira, Advisor
School of Mechanical Engineering
Georgia Institute of Technology

Dr. Nolan Hertel
School of Mechanical Engineering
Georgia Institute of Technology

Dr. Timothy Fox
School of Mechanical Engineering
Georgia Institute of Technology

Dr. Eric Elder
School of Mechanical Engineering
Georgia Institute of Technology

Date Approved: March 14, 2007

ACKNOWLEDGEMENTS

I would like to thank everyone who has helped me with numerous questions I have had during the processes of writing this thesis. Particularly I want to thank Dr. Cassiano de Oliveira for taking the time to find a thesis topic when I barely even had an idea of what is medical physics, and then his support while I pursued my thesis. I would not have been able to complete this thesis without his help. In addition, I want to thank Dr. Tim Fox and Dr. Eric Elder for their advice and access to their facilities at Emory to perform my numerous IMRT calculations. I want to thank Dr. Nolan Hertel for basically teaching me MCNP. It certainly made my job a lot easier than attempting to learn MCNP by myself. Furthermore, I would like to thank my classmates for their help and advice while pursuing my thesis, particularly Jared Hoover and Jose Ignacio Damian Marquez. Lastly, I want to thank my family for their support and understanding in everything that I have done.

TABLE OF CONTENTS

LIST OF TABLES

LIST OF FIGURES

LIST OF SYMBOLS

F4	MCNP Cell Tally
DF0	MCNP Dose Function Card
H*(10)	Ambient Dose Equivalent
CFn	MCNP Cell Flagging Tally
DE0	MCNP Dose Energy Card
°	Degree
sela	Angle Exclusion Variable a
selb	Angle Exclusion Variable b
wt(1)	Weighting for Critical Structure Dose Tally Results

LIST OF ABBREVIATIONS

IMRT	Intensity-Modulated Radiation Therapy
BEV	Beams-Eye-View
MCNP	Monte Carlo N-Particle Transport Code
Linac	Linear Accelerator
DVH	Dose Volume Histogram
cDVH	Cumulative Dose Volume Histogram
AAPM	American Association of Physicists in Medicine
Gy	Gray
cm	Centimeter
2-D	Two Dimensional
3-D	Three Dimensional
CT	Computed Tomography
g	Gram
MV	Megavoltage
ICRP	International Commission on Radiological Protection
FOM	Figure of Merit
R	Relative Error
T	Time

SUMMARY

Equispaced beam arrangements are typically used for IMRT plans. This beam arrangement provides adequate dose coverage to the target while sparing dose to other structures. However, an equispaced beam arrangement may not provide the "best" dose coverage to the target while sparing dose to the other structures.

Beam angle optimization attempts to optimize the beam directions to produce a "better" IMRT plan; this is achieved by increasing dose to the target while minimizing dose to the remaining structures. Most methods of beam angle optimization attempt to optimize the beam angles and the beam intensity profiles to find an optimal set of beam angles. This thesis attempts to optimize the beam angles without determining the beam intensity profiles. An MCNP simulation is run to score the beam directions; the simulation is run as an adjoint problem to reduce simulation time, with the target as the source and the detectors scoring the dose for the gantry angles of the beam. Then, an optimization algorithm is run to select a set of beam angles for an optimized IMRT plan. The optimized IMRT plan is compared to an equispaced IMRT plan on a commercial treatment planning system to determine if this method of beam angle optimization is "better" than using an equispaced beam arrangement.

The results of this thesis indicate that the coupling of an MCNP simulation for scoring with an optimization algorithm to select beam angles will produce a "better" IMRT plan than an equispaced IMRT plan. Three different geometries were used and for all geometries, the optimized IMRT plan had a higher average dose to the target while maintaining or increasing dose sparing to the critical structure and normal tissue.

CHAPTER 1

INTRODUCTION

In Intensity-Modulated Radiation Therapy (IMRT) planning, the planner usually selects a set of gantry angles based on the planners' empiric knowledge and intuition, as well as through the use of visualization tools in the treatment planning systems like beams-eye-view (BEV)[1]. The treatment planning system will then optimize the intensity profiles of the beams by inverse planning methods that use dose constraints and goals to optimize the beam intensity profiles[2]. Once the beam profiles are optimized, a more rigorous dose calculation is performed to determine the dose distribution of the IMRT plan. The planner then evaluates the IMRT plan to determine if the prescribed dose goal and constraints are achieved. If the dose goals and constraints are not achieved the planner continues through trial and error to achieve the desired dose goals and constraints. This is an inefficient method of IMRT planning and it does not ensure that an optimal solution is achieved because the optimal solution may use beam directions that are counter-intuitive and will travel through a critical structure before going through the target[3]. However, computer optimization can quantitatively select the optimal beam directions to achieve the prescribed dose goals and constraints rather than intuitively attempting to achieve the prescribed dose goals and constraints through trial and error.

Current commercial treatment planning systems only optimize the intensity profile of the pre-selected beam directions. However, beam angle optimization methods attempt to optimize the beam profiles along with the gantry angle of the beam. This greatly increases the potential solution space since the beam direction is not static, and requires assumptions to reduce the computation time such as increasing the step size for beam angle selection, using 2-D target geometries, and/or simplified dose calculation for beam profile optimization: no lateral scatter of beam, parallel beam geometry, and

homogeneous medium. One approach attempts to modify both the gantry angle of the beam direction and the beam intensity profile to determine an optimal set of beam angles. Typically, inverse planning algorithms are used as the optimization method. "Number and orientations of beams in intensity-modulated radiation treatments," by Jorg Stein, is one example of this method[4]. The beam intensity profiles are optimized using inverse planning, which is similar to how commercial treatment planning systems optimize the beam intensity profiles, and an exhaustive search or simulated annealing is used to select the optimal set of beam directions. Andrei Pugachev's approach to beam angle optimization attempts to select beam directions by calculating the maximum beam intensity profiles for the prescribed dose constraints[5]. Here the beam directions are optimized using a scoring function that will select the beam with the highest score. This approach is different because it does not attempt to optimize the beam intensity profile but rather to determine which beam directions are most effective at delivering the dose. One more approach to beam angle optimization, "Beam orientation optimization in intensity-modulated radiation treatment planning" also by Andrei Pugachev, separates the optimization of the beam intensity profiles and the selection of beam directions[6]. The beam orientations are selected using simulated annealing sampling and then the beam intensity profiles are calculated using filtered back projecting (inverse planning). All of these approaches attempt to optimize the beam intensity profiles to determine the optimal set of beam directions.

This thesis does not attempt to optimize the beam intensity profiles. However, it does attempt to select beam directions that will provide a "better" IMRT plan than an IMRT plan with equispaced beams; an equispaced beam arrangement is the current standard for IMRT plans because it sufficiently accomplishes the prescribed dose goals and constraints[7]. MCNP is used to score the beam directions. The MCNP simulation is set up as an adjoint problem with the target as the source and the beam directions as the detectors that score the dose from the source; this is performed to reduce the simulation

time. In addition, particles traveling through a critical structure are flagged in MCNP and scored by the detectors as well. Then an optimization algorithm is performed on the results of the MCNP simulation to select the optimal set of beam directions. Lastly, a commercial treatment planning system is used to compare an equispaced IMRT plan to the optimized IMRT plan.

CHAPTER 2

BACKGROUND

2.1 MCNP

MCNP is a general Monte Carlo N-Particle transport code. It can be used for neutron, photon, electron transport, or coupled neutron/photon/electron transport. For this thesis, only coupled photon transport is considered. Furthermore, MCNP can arrange arbitrary geometry configurations for simulation of radiation transport, which can account for incoherent and coherent scattering, fluorescent emission after photoelectric absorption, absorption in pair production with local emission of annihilation radiation and bremsstrahlung for photon transports, and a continuous-slowing-down model for electrons including positrons, k x-rays and bremsstrahlung[8]. In addition, the particles can be tallied to determine the flux of particles through a given region: volume, surface or point. The radiation source card in MCNP can define the particle produced and its energy spectrum as well as the direction of the source. Ultimately, MCNP allows the user to simulate radiation transport and tally the results of the simulation by using input cards that define the geometry, particle characteristics, materials, and type of tally desired. Great care is required in defining a MCNP simulation because the simulation is only as accurate as the input definition of the simulation[9].

2.2 IMRT

IMRT is able to modulate the intensity of the radiation beam for each field, allowing any number of both high and low intensity areas within the field[10]. The intensity modulation of the field is generally accomplished by using a multi-leaf

collimator (MLC). The movement of the MLC leaves across the linear accelerator (Linac) beam modulates the field. This modulation of the field gives IMRT the potential to achieve a higher degree of target conformity and/or normal tissue sparing; this is especially true for target volumes and/or critical structures with complex and/or concave shapes[11]. However, the higher degree of conformity results in lower uniformity to the target volume, as well as the potential for hot spots in normal tissue compared to conventional plans.

The modulation of the beam fields is accomplished through optimization algorithms. Typically, inverse planning algorithms are used to design the optimum non-uniform beam intensity profiles for IMRT. In inverse planning, the planner specifies beam directions (gantry angles), target dose constraints/goals, and dose constraints/goals for critical structures as well as weights for the different constraints/goals[12]. The optimization algorithm then adjusts the beam intensities for the given beam directions iteratively to achieve the target and critical structure dose constraints/goals. The planner reviews the optimized dose distribution and can adjust the dose constraints/goals as well as the weight of the constraints/goals to satisfy the prescribed dose to the target volume and/or critical structure[13]. After optimizing the intensity profiles of the beams, the leaf motions that modify the intensity profiles of the beam are determined. Then a more accurate dose calculation is performed such as kernel-based models that directly compute the dose by taking into account beam energy, geometry, beam modifiers, patient contour, and electron density distributions[14]. The beam intensity profile optimization uses approximations like simplified dose calculation methods (e.g. correction-based models like pencil beam) and reduced number of dose points inside calculation volumes to reduce calculation time[15].

2.3 IMRT Plan Evaluation

Optimized IMRT plans are evaluated differently than conventional or other conformal plans. In conventional plans, the un-modulated fields ensure uniform dose to the target volume with the exception of the periphery of the target/beam where penumbra effects of the target occur. Generally, the margins used for the target volume in conventional plans ensure that the penumbra effect will be outside of the actual target volume. IMRT plans have reduced margins and increased conformation of the beam to the target through beam intensity modulation. While this allows for greater conformation of dose to the target, the uniformity of the dose to the target for IMRT plans is usually worse than plans with uniform beams and can produce cold spots within the target volume rather than on the periphery[16]. Furthermore, the increased conformation to the target from beam modulation leads to an increase of hot spots both inside and outside the target volume. Therefore, in analyzing IMRT treatment plans it is important that the planner looks at the minimum and maximum dose for all the contoured structures to determine dose uniformity to the target as well as detect the presence of hot spots. In addition, treatment planners utilize dose volume histograms (DVH) to ensure the prescribed dose is achieved for the treatment plan. Ideally, for an IMRT treatment plan, the planner wants to have 100% of the target volume to receive the prescribed dose to the target. Furthermore, the planner wants the normal tissue and critical structures to receive no dose to 100% of the volume or at least to minimize the dose as much as possible to the normal tissue and critical structure volumes. By doing this, the planner increases the likelihood of tumor control while minimizing normal tissue complication. AAPM guidelines for IMRT plan evaluation are in "Guidance document on delivery, treatment planning, and clinical implementation of IMRT: Report of the IMRT subcommittee of the AAPM radiation therapy committee" [17].

CHAPTER 3

METHODOLOGY

This thesis attempts to model the geometry of a Linac. The target is placed in the center of a ring of cells representing different Linac gantry angles. However, the MCNP simulation performs as an adjoint problem rather than a forward problem; instead of the Linac gantry angles being the source, the target is the source and the Linac gantry angles are the target. An adjoint problem allows the MCNP simulation to be run once for a given target rather than running a new simulation for each Linac gantry angle. Thus, the MCNP simulation time is significantly reduced.

3.1 MCNP Simulation

3.1.1 Geometry

A ring of detectors was created in MCNP to simulate different gantry positions around a target in the center. The forty-eight detectors have a width and length of 12 cm, due to limitations in leaf movement for the multi-leaf collimator (MLC), and a depth of 1 cm. Furthermore, the inner faces of the detectors were located 100 cm from the isocenter to mimic the way the linear accelerator head rotates about the isocenter. Each detector represents a 7.5° increment of the gantry position.

After the detectors were created, then the phantom was formed. The phantom consists of a 30 cm x 30 cm x 30 cm cube. Inside the phantom, the target was created; three different target geometries were simulated. The three target geometries were based off an IMRT optimization paper, “Optimizing the Delivery of Radiation Therapy to

Cancer Patients," by Shepard, et al, and the three geometries are shown in the Figure 3.1[18].

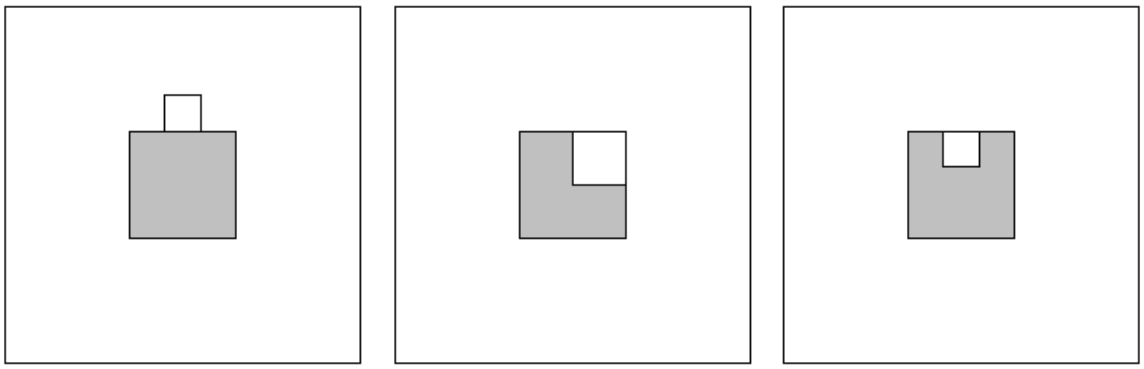

Figure 3.1: MCNP simulation target geometries

The three target geometries consist of a square target with a smaller square outside but next to the target, an L-shaped target, and a U-shaped target. The un-shaded areas in the figure above represent a critical structure that is to be avoided during treatment. The shaded areas represent the target to be treated. The geometries are increasingly difficult to solve, with the U-shaped target having the most complex geometry. The MCNP problem is bounded by a 120 cm sphere to reduce computation time. An example of the MCNP simulation geometry for the U-shaped target is shown in Figure 3.2.

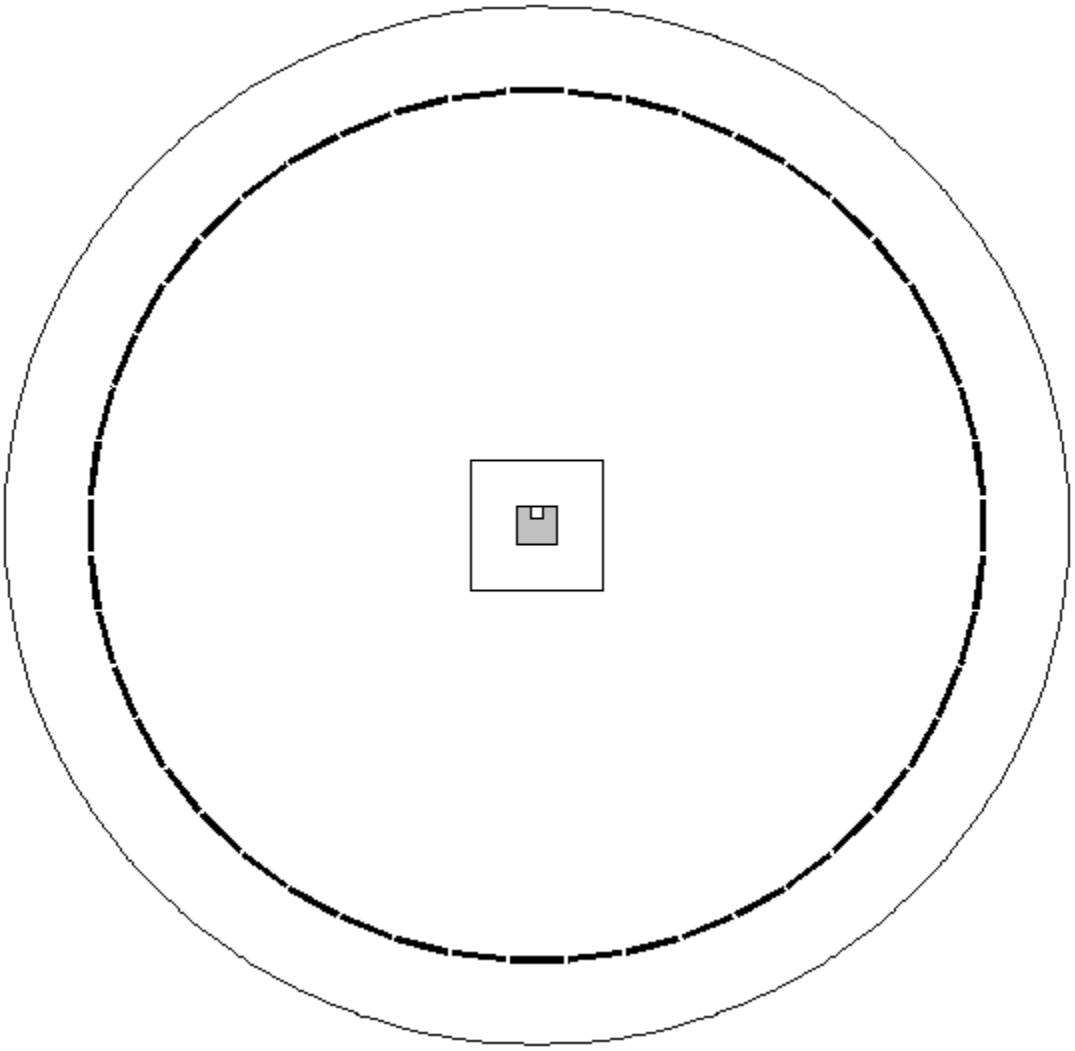

Figure 3.2: MCNP simulation geometry for a U-shaped target

The outer circle in Figure 3.2 represents the outer boundary of the simulation. The ring of blocks just inside of the outer circle represents the detectors. Next, the largest square represents the 30 cm x 30 cm x 30 cm water phantom. The remaining objects in the figure represent the target and the critical structure. The figure above is to scale.

The problems used in this thesis are essentially 2-D geometries, although they are represented in a 3-D space. These target geometries are used due to their simplicity and ease of simulation within MCNP. However, there are programs like Scan2MCNP that can convert complex geometries, such as CT images, into MNCP.

3.1.2 Material

Two materials are specified for the MCNP simulation: water and air. The molecular ratio of two hydrogen atoms to one oxygen atom is used for water, with a density of 1 g/cm^3. Chilton's definition of air is used: 75.52 % nitrogen, 23.19 % oxygen and 1.29 % argon by weight with a density of .001205 g/cm^3 [19]. Everything inside of the phantom, including the target and critical structures, is defined as water. The volume between the phantom and the outer spherical boundary in the MCNP simulation is defined as air; this volume includes the detectors. The volume outside the spherical boundary is defined as null to stop further interactions; consequently, reducing the computation time for the simulation.

3.1.3 Source

Due to the computational time required for Monte Carlo simulations, the radiation source was defined as the target rather than running a different simulation for each gantry angle. Furthermore, the source is isotropic so that radiation is directed toward all detectors equally. The source definition in MCNP used a referenced space phase data for a 6 MV beam on a Varian 2100 series linear accelerator that was determined by Sung Hyun Cho at MD Anderson[20]. A table of the spectrum used for the source is in Appendix A. The source spectrum was measured 100 cm from the linear accelerator source for a 10 cm x 10 cm field along the central axis. Although this method of defining a source does not exactly model the way radiation will actually travel, it does provide a way to compare the dose score for different gantry angles. This is the ultimate goal of the MCNP simulation; that is, to be able to use MCNP simulation results to determine the optimal beam angles for IMRT treatment plan.

3.1.4 Detector

The detectors represent different gantry angles for the linear accelerator head. In the MCNP simulation, they score the fluence of particles that travel through the detector. A cell tally, F4 tally, is used for the detector volumes to score the fluence. In MCNP, the cell tally is a track length estimator "which is generally quite reliable because there are frequently many tracks in a cell (compared to the number of collisions) leading to many contributions to this tally"[21]. It is important that the tracks be scored instead of collisions since the medium of the tally cell is air, which has a significantly reduced number of collisions as compared to a denser material like water. In addition, some mathematical operations are performed within the MCNP simulation to calculate the dose delivered to a detector. The default output for the tally in MCNP is a normalized fluence over a range of energies; the sum of the fluence for all the energy bins is equal to unity. However, a dose function card, DF0, can be used to modify tallies by converting flux to dose using a conversion factor[22]. For this thesis, the conversion coefficients for the ambient dose equivalent, *H*(10)*, are found in Table A.21 of ICRP 74 and were used to modify the tally[23]. In addition, the energy bins of the tallies were modified using the dose energy card, DE0, to match the energy values of the conversion coefficients. Furthermore, particles that travel through certain cells, like critical structures, can be flagged, using a CFn card, to determine their dose contribution to a tally[24]. Ultimately, the tallies are used to score the dose to the detector and dose from particles that travel through a critical structure. The dose values from the tallies of the detectors can then be compared to determine which selection of beam angles will provide the optimal delivery of dose to the target while minimizing dose to the critical structure.

3.1.5 MCNP Simulation Settings

Many of the default settings are used for the MCNP simulations. The mode of particle transport was set for photon and electron interactions; neutron interactions were ignored. Only geometrical limitations are used for variance reduction of the MCNP simulation. In addition, while time is not a consideration statistical precision of results is important for comparison of the detector tallies; enough particle histories are performed to achieve statistical reliability of the tally results.

An example of an MCNP simulation performed is in Appendix B.

3.2 Matlab Algorithm

A Matlab algorithm was developed to select beam angle directions by using dose values from the MCNP simulation for detectors representing gantry angle of beams. The combined dose value for a given beam angle is a combination of the dose value given to the detector less a weighted value of the critical structure dose to the detector. The weighting to the critical structure can be varied to obtain an optimal solution for the algorithm. Furthermore, certain beam directions should be excluded when selecting the next beam angle to avoid beams intersecting in normal tissue. This idea has been incorporated within the algorithm. Both beam angles close to the selected beam and beam angles opposing the selected beam are excluded from selection to prevent overlapping of beams in normal tissue. Lastly, two different beam angle optmization methods were used to select the set of beam angles.

3.2.1 Method 1

The Method 1 beam angle optimization algorithm selects the seven beam angles by exhaustively searching the combined dose values for all beam angles. After searching all the beam angles, then the beam angle with the largest combined dose value is selected.

This beam angle is then stored and certain beam angles are excluded according to the exclusion rules within the algorithm; the beam angles that are excluded can be changed by two angle exclusion variables, **sela** and **selb**, within the algorithm. The algorithm then proceeds to search the combined dose values of the beam angles, selecting the largest combined dose value that is not on the list of excluded beam angles. This process repeats until seven beam angles are selected. This method is good for determining which individual beam angles will best deliver dose to the tumor while reducing dose to critical structures. A flow diagram of the Method 1 algorithm is in Appendix C.

3.2.2 Method 2

The Method 2 beam angle optimization algorithm attempts to select seven beam angles that have the largest aggregate dose value. Unlike Method 1, Method 2 uses random numbers to select the seven beam angles. A number of bins equal to the number of beam angles are created, and the bins are assigned a range of values from zero to one. The range of the bins are the same, although they will not correspond to same values; for example, bin 1 corresponds to the range 0 to 0.1, bin 2 corresponds to the range 0.1 to 0.2, etc... Consequently, a random number generator is used to select a bin by determining which bin contains the generated random number. Upon selection of the bin, the beam angle is then determined. Then, as in Method 1, certain beam angles are excluded according to the exclusion rules within the algorithm. The algorithm then proceeds to select another beam angle using a randomly generated number; so long as the new beam angle is not an excluded beam angle. This process continues until seven beam angles are selected. Next, the aggregate dose value of the beam angles is totaled and stored along with the seven beam angles selected. Then seven more beam angles are selected using the same process as before. If the aggregate dose value of the seven beam angles is larger than the previously stored beam angles, the new aggregate dose value is stored along with its corresponding beam angles. This process will continue until a

certain number of failed attempts to find a larger aggregate dose value occurs; then the algorithm ends. This method does a better job at determining which arrangement of beam angles will generate the largest aggregate dose value. A flow diagram of the Method 2 algorithm is in Appendix D.

3.3 Treatment Planning System

A treatment planning system is used to calculate dose for given field arrangements. Eclipse, a commercial treatment planning system by Varian Medical Systems, Inc., was used to calculate the dose to the target, the critical structures, and the remaining volume. Eclipse can perform IMRT fluence optimization and then calculate the dose to the defined volumes.

To start, a 30 cm x 30 cm x 30 cm water phantom is created in Eclipse. Next, the tumor and critical structures are contoured depending on the geometry of the problem. Seven fields are created from the seven beam angles selected using the Matlab beam angle optimization algorithm. The photon transportation algorithm is selected; in this thesis, the AAA algorithm is selected because it accounts for secondary scatter, as where the Pencil Beam algorithm just accounts for primary attenuation. In addition, the calculation grid must be set; the default of 5 mm is used for the calculation grid to reduce computation time. Furthermore, the plan is normalized so that the isocenter receives 100% of the dose and the heterogeneity correction is turned on. Then the fluences are optimized using the IMRT optimization function. Dose constraints are used to achieve dose goals to the contoured volumes. A target dose of 45 Gy is used for the target volume with 100% of the target volume receiving 43 Gy and 0% receiving 47 Gy as the dose constraints. The critical structure volume was given a dose constraint of no more than 15% of the volume receiving 30 Gy. The priorities for the dose constraints were set to be equal. These dose constraints were used for all IMRT optimizations in Eclipse.

Upon completion of the IMRT optimization, the dose is calculated and the cumulative dose volume histograms (cDVHs) are formed to determine dose distribution to target, critical structure, and the remaining volume called the body. The cDVHs are used to compare different plans to determine which plans provide a "better" dose distribution. In addition, Eclipse calculates the minimum and maximum dose to the different volumes to show the degree of hot and cold spots.

CHAPTER 4

RESULTS

4.1 MCNP DATA

One hundred million particle histories were run for each of the MCNP simulations. This number of histories was used because the figure of merit (FOM) value in the MCNP output file for the simulation began to level off. Furthermore, the relative error, R, which is related to the FOM by $FOM \equiv \frac{1}{R^2 T}$, is less than 0.004 or 0.4% for all detectors in all the MCNP simulations[25]. The MCNP manual gives a set of guidelines for interpreting the relative error, stating that for tally results of $R < 0.05$, the results are generally reliable[26]. Ten statistical tests are preformed by the MCNP simulation to indicate the reliability of the tally results[27]. In addition, an analysis was performed on the validity of MCNP simulation results by looking at the geometry of the results. Polar graphs for each of the target geometries were created from the MCNP simulation detector dose values, and the polar graphs are shown in the following figures.

4.1.1 Square Target Geometry

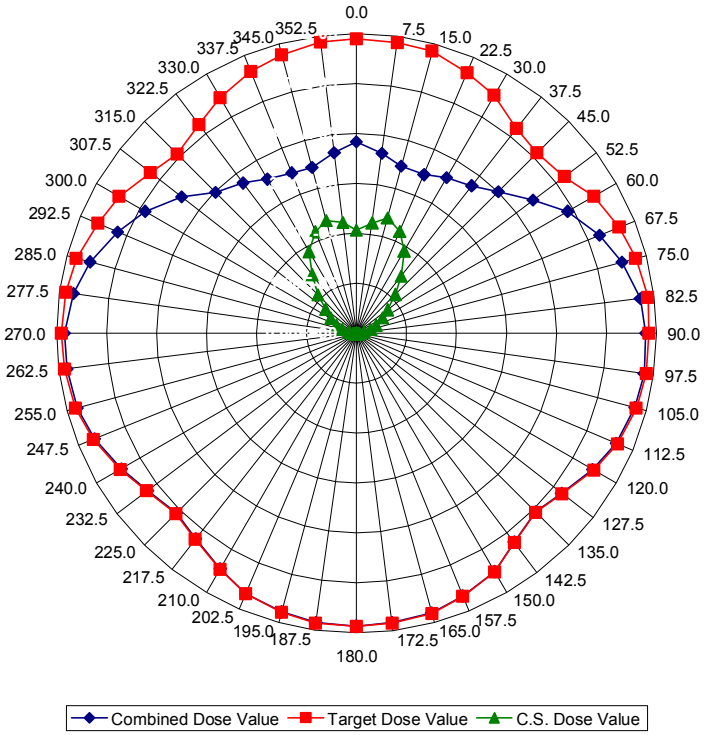

Figure 4.3: Polar graph of MCNP simulation data for square target geometry

The polar graph of the target dose value in Figure 4.1 follows the prediction for a square water phantom. The smallest target dose occurs at the corners of the phantom, which corresponds to detector angles of 45°, 135°, 225°, and 315° on the polar graph, because at those angles the photons must travel the longest average distance through the water phantom to reach the detector. Consequently, the largest target dose value occurs at 0°, 90°, 180°, and 270°, the angles where the photons have the shortest average distance to travel through the phantom. Furthermore, the critical structure dose values of the detectors are larger at angles where the critical structure is between the isocenter and the detector. The combined dose value is the target dose value subtracted by the critical structure dose value for each detector.

4.1.2 L-Shaped Target Geometry

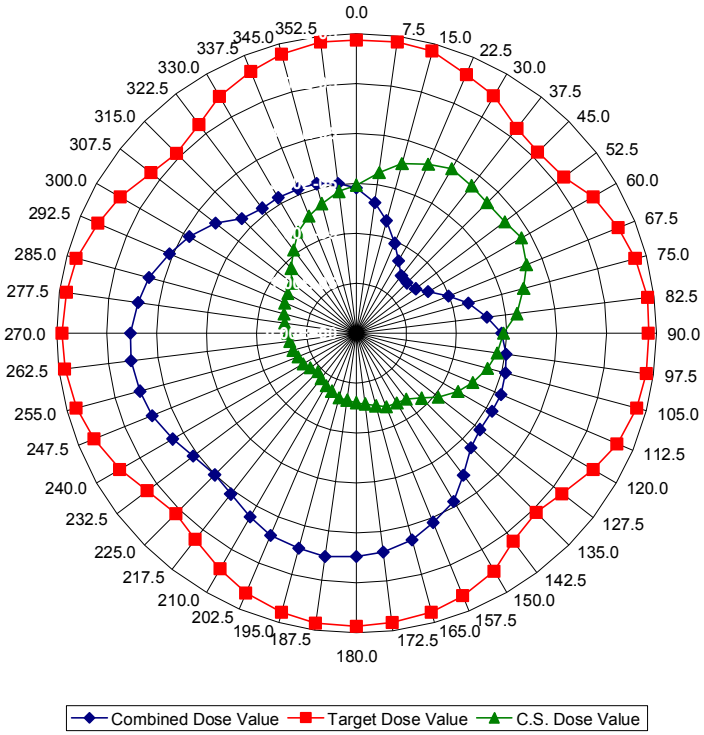

Figure 4.4: Polar graph of MCNP simulation data for L-shaped target geometry

Figure 4.2 shows the polar graph of the MCNP simulation for the L-shaped target geometry. The target dose values follow the same trend as the square target geometry because water phantom and source geometries in the MCNP simulation are the same. However, the critical structure dose values are significantly different between the two target geometries because of the different locations of the critical structure. The critical structure dose values in the polar graph indicate that the critical structure is located at the upper right quadrant of the square for the L-shaped target geometry, which corresponds to the MCNP simulation geometry. Consequently, the combined dose value is lower for detector values in the upper right quadrant.

4.1.3 U-Shaped Target Geometry

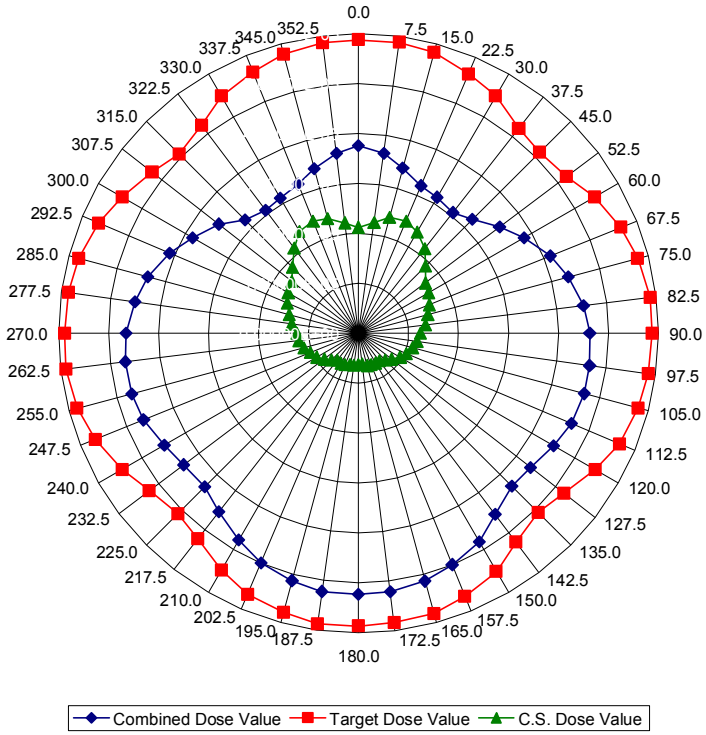

Figure 4.5: Polar graph of MCNP simulation data for U-shaped target geometry

The results of the MCNP simulation for U-shaped target geometry, shown in Figure 4.3, indicate that the combined dose value is lower for the angles where the beam goes through the critical structure. This result is to be expected since the beam angles are penalized for photons that travel through the critical structure, and indicates that the critical structure is located in the center of the target edge inside the target, as modeled in the MCNP simulation.

The polar graphs for the three MCNP simulation geometries indicate that setup of the MCNP simulation results are geometrically correct. Furthermore, the ten statistics tests in the MCNP simulation results indicate that results of simulation tallies, e.g. the recorded dose values, should be reliable. The tally results of the MCNP simulation are in Appendix E.

4.2 Matlab Beam Selection Algorithm

The results of the Matlab beam selection algorithms are shown in the following tables. Each table represents different target geometries from the MCNP simulation and the algorithm method; furthermore, each table indicates the value of the angle exclusion variables, **sela** and **selb**. These variables are the primary method of altering the beam selection algorithm. Combinations of angle exclusion variable values were used to determine which angle exclusion variable value combination would select the optimal beam angles for an IMRT treatment of the target. Ideally, one angle exclusion variable value combination will select the optimal beam angles for all geometries. In addition, the weighting of the critical structure dose value can be varied using the **wt(1)** variable in the algorithm. However, the **wt(1)** variable was set to a value of 1 for all optimizations.

4.2.1 Method 1

Table 4.1: Matlab Beam Angle Selection for Square Target Geometry (Method 1)

Angle Exclusion Variables		Beam Angle 1	Beam Angle 2	Beam Angle 3	Beam Angle 4	Beam Angle 5	Beam Angle 6	Beam Angle 7	Total Combined Dose Value
sela	selb								
2	0	0.0	270.0	82.5	22.5	337.5	292.5	105.0	3.9991E-04
2	1	0.0	270.0	75.0	22.5	337.5	292.5	52.5	3.9650E-04
2	2	0.0	270.0	22.5	337.5	67.5	292.5	315.0	3.9425E-04
3	0	0.0	270.0	82.5	30.0	330.0	300.0	112.5	3.9152E-04
3	1	0.0	270.0	75.0	30.0	105.0	330.0	300.0	3.9361E-04

Table 4.1 shows the beam angles selected using the Method 1 Matlab algorithm. The beam angles are listed in order of their selection by the algorithm: beam angle 1 represents the beam angle with largest combined dose value; beam angle 2 has the next largest combined dose value, etc. A comparison of the beam angles for the different angle exclusion variable combinations shows that many of the beam angles are the same, meaning this method will give similar results over a large range of combinations for the angle exclusion variables.

Table 4.2: Matlab Beam Angle Selection for L-Shaped Target Geometry (Method 1)

Angle Exclusion Variables		Beam Angle 1	Beam Angle 2	Beam Angle 3	Beam Angle 4	Beam Angle 5	Beam Angle 6	Beam Angle 7	Total Combined Dose Value
sela	selb								
2	1	82.5	7.5	105.0	345.0	30.0	60.0	127.5	2.9707E-04
3	1	82.5	7.5	52.5	337.5	112.5	142.5	307.5	2.7583E-04
3	2	82.5	7.5	52.5	337.5	112.5	210.0	135.0	2.2991E-04
4	1	82.5	7.5	45.0	330.0	120.0	165.0	285.0	2.7020E-04

The result of the Matlab beam angle optimization algorithm using Method 1 for the L-Shaped target geometry, which is shown in the table above, is similar to the results of the square-shaped geometry. For different combinations of angle exclusion variables, the selection of beam angles is similar although not exactly the same.

Table 4.3: Matlab Beam Angle Selection for U-Shaped Target Geometry (Method 1)

Angle Exclusion Variables		Beam Angle 1	Beam Angle 2	Beam Angle 3	Beam Angle 4	Beam Angle 5	Beam Angle 6	Beam Angle 7	Total Combined Dose Value
sela	selb								
2	1	0.0	22.5	337.5	285.0	75.0	307.5	52.5	3.3349E-04
3	1	0.0	30.0	330.0	285.0	75.0	120.0	240.0	3.1875E-04
3	2	0.0	30.0	330.0	285.0	75.0	232.5	127.5	3.1299E-04

The results of the Method 1 Matlab algorithm for the U-shaped target geometry in Table 4.3 show that Method 1 is limited in selecting different beam angles; therefore, changing the angle exclusion variables will not provide a large range of choices. Although it may appear that the combinations of the angle exclusion variables are limited, this is due to the fact that for larger values of **sela** and/or **selb** the algorithm is not able to select seven beam angles because of the exclusion of angles. Furthermore, the algorithm is written in such a way that it will pick the best beam angles in order of availability with no attempt to select the combination of beam angles that will provide optimal beam angles. Another method was developed to account for this deficiency in the method.

4.2.2 Method 2

Table 4.4: Matlab Beam Angle Selection for Square Target Geometry (Method 2)

Angle Exclusion Variables		Beam Angle 1	Beam Angle 2	Beam Angle 3	Beam Angle 4	Beam Angle 5	Beam Angle 6	Beam Angle 7	Total Combined Dose Value
sela	**selb**								
2	0	7.5	30.0	75.0	97.5	270.0	292.5	345.0	4.0109E-04
2	1	7.5	30.0	67.5	97.5	262.5	292.5	345.0	3.9874E-04
3	0	0.0	30.0	67.5	97.5	262.5	292.5	330.0	3.9567E-04
3	1	0.0	30.0	67.5	97.5	262.5	292.5	330.0	3.9567E-04
3	2	0.0	30.0	75.0	120.0	232.5	277.5	330.0	3.7750E-04
4	0	30.0	67.5	105.0	240.0	277.5	315.0	352.5	3.8318E-04
4	1	30.0	75.0	112.5	240.0	277.5	315.0	352.5	3.8180E-04
4	2	22.5	75.0	120.0	180.0	232.5	277.5	337.5	3.6080E-04
5	0	22.5	67.5	112.5	180.0	240.0	285.0	337.5	3.6710E-04
5	1	22.5	75.0	120.0	180.0	240.0	285.0	337.5	3.6467E-04
5	2	22.5	75.0	120.0	180.0	232.5	277.5	337.5	3.6080E-04

Table 4.4 shows a larger combination of angle exclusion variables used in Method 2 than in Method 1. The use of more combinations is a result of the algorithm's ability to have larger values for **sela** and **selb** as well as the ability of the algorithm to select a greater variety of beam angles based on the value of **sela** and **selb**. Although combinations with similar **sela** and **selb** values have similar beam angle values, these values change as the combinations vary. The most notable trend in Table 4.4 is that as **sela** and **selb** values increase, the beam angles are grouped further apart, and become similar to an equispaced beam arrangement. In addition, larger angle exclusion variable values of **sela** and **selb** were not used because the algorithm was not able to select seven beam angles because the variables were too restrictive.

Table 4.5: Matlab Beam Angle Selection for L-Shaped Target Geometry (Method 2)

Angle Exclusion Variables		Beam Angle 1	Beam Angle 2	Beam Angle 3	Beam Angle 4	Beam Angle 5	Beam Angle 6	Beam Angle 7	Total Combined Dose Value
sela	selb								
2	1	0.0	22.5	45.0	67.5	90.0	112.5	337.5	2.9970E-04
2	2	0.0	22.5	45.0	67.5	90.0	112.5	337.5	2.9970E-04
3	1	0.0	30.0	60.0	90.0	120.0	165.0	330.0	2.8347E-04
3	2	15.0	45.0	75.0	120.0	172.5	277.5	330.0	2.6749E-04
5	1	22.5	82.5	127.5	172.5	247.5	292.5	337.5	2.4730E-04
5	2	22.5	90.0	135.0	180.0	247.5	292.5	337.5	2.4280E-04

Table 4.5 shows that the application of the Method 2 algorithm for the L-Shaped target geometry yielded similar results to the square-shaped geometry. The beam angles selected are different due to the different geometries, but the trends of the angle exclusion variable combinations are the same.

Table 4.6: Matlab Beam Angle Selection for U-Shaped Target Geometry (Method 2)

Angle Exclusion Variables		Beam Angle 1	Beam Angle 2	Beam Angle 3	Beam Angle 4	Beam Angle 5	Beam Angle 6	Beam Angle 7	Total Combined Dose Value
sela	selb								
2	0	0.0	22.5	67.5	90.0	270.0	292.5	337.5	3.3779E-04
2	1	7.5	30.0	75.0	270.0	292.5	322.5	345.0	3.3679E-04
3	0	0.0	30.0	67.5	97.5	262.5	292.5	330.0	3.3159E-04
3	1	0.0	30.0	67.5	97.5	262.5	292.5	330.0	3.3159E-04
3	2	0.0	30.0	75.0	120.0	232.5	277.5	330.0	3.1595E-04
4	0	22.5	60.0	97.5	180.0	270.0	307.5	345.0	3.1953E-04
4	1	15.0	60.0	97.5	180.0	262.5	300.0	337.5	3.1935E-04
5	0	22.5	67.5	112.5	180.0	240.0	285.0	337.5	3.1040E-04
5	1	22.5	75.0	120.0	180.0	240.0	285.0	337.5	3.0781E-04
5	2	22.5	75.0	120.0	180.0	232.5	277.5	337.5	3.0500E-04

In Table 4.6, a larger range of exclusion variable combinations was used for the U-Shaped target geometry because of the difficulty of the geometry. Again, for similar **sela** and **selb** values, the beam angles are also similar, but the beam angles change as the **sela** and **selb** values diverge from other combinations. Furthermore, as **sela** and **selb** values increase the beam distance between beam angles increases and becomes closer to an equispaced beam arrangement.

The Method 2 version of the Matlab algorithm selects the optimal combination of beam angles to achieve the largest total combined dose, as where the Method 1 algorithm only looks at selecting the next largest combined dose value of the beam angle. For both methods, the separation between beam angles is increased by increasing the value of the angle exclusion variables: **sela** and **selb**. However, Method 1 algorithm will not change as much as Method 2 algorithm.

4.3 Dose Calculation

An equispaced IMRT plan was used as the control for comparison of the optimized IMRT plan using MCNP simulation data. The goal of this thesis is to produce a plan that has lower dose to critical structures and normal tissue, and a higher dose to the target volume. In other words, the IMRT plan should have the largest dose separation possible between the critical structure and the target volume, so the dose to the target can be escalated while delivering the same or less dose to the critical structure. Furthermore, when comparing plans, the maximum dose to the normal tissue, critical structure, and target volume should be kept to a minimum to reduce hot spots and ensure uniformity of dose to the target volume. In addition, the minimum dose to the target volume needs to be close to the target dose to prevent cold spots and ensure dose uniformity. Consequently, the "better" IMRT plan will have a more uniform dose to the target with either greater dose sparing of the critical structure and normal tissue and/or escalated dose to the target, e.g. a higher mean target dose.

However, during the process of developing an optimization method to select beam angles, multiple methods and different variable values were used to select the optimal beam angles. The upcoming sections will determine which method and which combination of angle exclusion variables provide the optimal beam angle solution as compared to the equispaced beam arrangement traditionally used in IMRT.

4.3.1 Method 1

Five angle exclusion variable combinations were used for the square target geometry. The optimized IMRT plans for all five angle exclusion variable combinations have greater dose sparing of the normal tissue and the critical structure than the equispaced IMRT plan, with varying degrees of dose sparing between IMRT plans. In general, the equispaced IMRT plan has a higher mean dose than the five optimized IMRT plans. In addition, the equispaced IMRT plan has lower maximum dose values than the optimized IMRT plans for some of the structures. However, the "best" optimized IMRT plan has increased dose sparing of normal tissue and critical structure, and lower maximum dose values for all three structures: target volume, critical structure, and normal tissue. Furthermore, the mean dose to the target for the optimized IMRT plan is slightly less than the equispaced IMRT plan, but dose escalation of the optimized IMRT plan can produce an IMRT plan that still has increased dose sparing to the normal tissue and the critical structure while having the same mean dose to the target as the equispaced IMRT plan. The cDVH of the optimized IMRT plan versus the equispaced IMRT plan is shown in Figure 4.4.

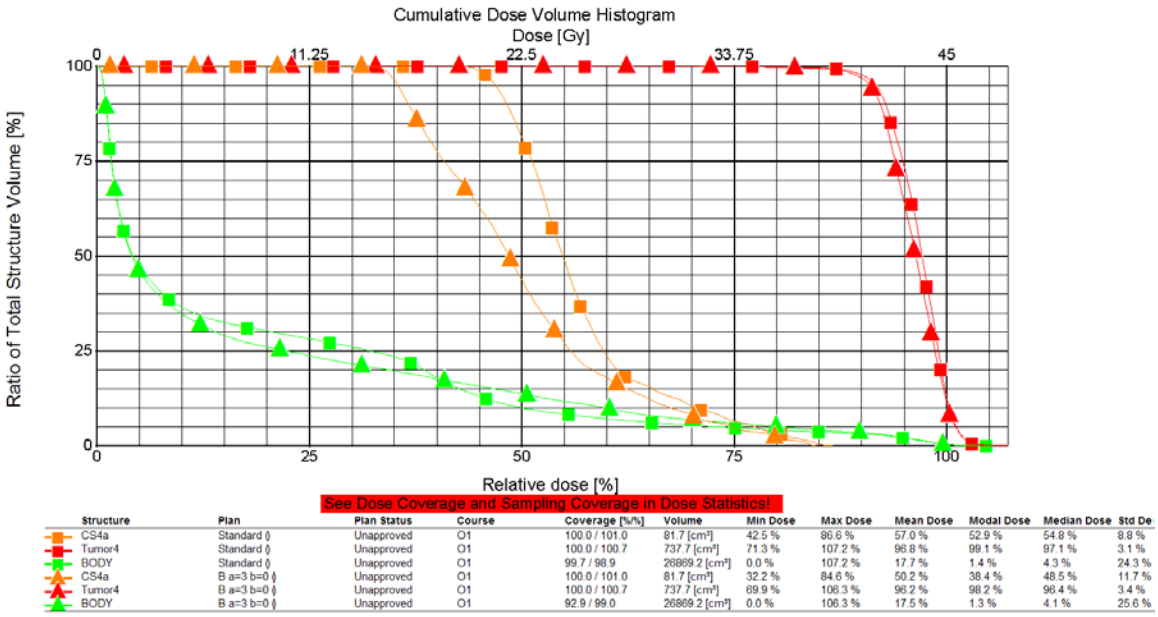

Figure 4.6: cDVH of equispaced IMRT plan vs.. Method 1, with sela=3 and selb=0, optimized IMRT plan for square target geometry

Figure 4.4 compares an equispaced IMRT plan and the beam arrangement that was selected using the Method 1 algorithm with angle exclusion variables: **sela**=3 and **selb**=0. The triangle data points represent the optimized IMRT plan and the square data points represent the equispaced IMRT plan; the green data points represent the normal tissue and the orange data points represent the critical structure; the red data points represent the target volume. The cDVHs for the other angle exclusion variable combinations are in Appendix F.

Four angle exclusion variable combinations were used for the L-Shaped target geometry. Unlike the square target geometry, one of the angle exclusion variable combinations produced a "worse" optimized IMRT plan than the equispaced IMRT plan. However, the other three plans are "better"; the target volume has a higher mean dose and there is greater dose sparing of the normal tissue. Two of the three optimized IMRT plans have greater dose sparing of the critical structure while the other plan has dose sparing similar to the equispaced plan, e.g. the cDVHs are similar. The "best" optimized IMRT plan uses angle exclusion variables: **sela**=3 and **selb**=2. This plan has a lower maximum dose than the equispaced IMRT plan for all three structures, indicating that there are reduced hot spots and a more uniform dose to the target volume. The cDVHs for the four optimized IMRT plans are in Appendix F.

Three combinations of the angle exclusion variables were used for the U-Shaped target geometry. However, none of the combinations produced an optimized IMRT plan that is better than the equispaced IMRT plan. One of the optimized IMRT plans is close, with similar or slightly better cDVHs for the three structures, but the maximum dose to the structures is significantly higher than the equispaced IMRT plan. This inability to produce an optimized IMRT plan "better" than the equispaced IMRT plan is a result of the difficult geometry of the target and critical structure, because the critical structure is inside the U-shaped target. The cDVHs for the U-Shaped target geometry are in Appendix F.

The Method 1 algorithm tends to select beam angles that are concentrated closely together. This works well when the critical structure is outside the target, like the square target geometry, or located at the corner of the target, like the L-Shaped target geometry, but does not work as well when the critical structure is located centrally inside the target, like the U-Shaped target geometry. In other words, Method 1 algorithm is less effective in selecting beam angle arrangement as the target and critical structure geometry becomes more complex. A different method must be used to select the beam angles for the optimized IMRT plans.

4.3.2 Method 2

A larger number of beam angle exclusion variable combinations were used for the Method 2 algorithm because the algorithm produces more variations as the angle exclusion variables change. Nine combinations were used for the square target geometry; the combinations are in Table 4.1 and the cDVHs for the optimized IMRT plans are in Appendix G. In general, cDVHs for all of the optimized IMRT plans are equal to if not better than the equispaced IMRT plan. However, large values of the beam angle exclusion variables produce higher dose for the hot spots, and the cDVHs for the three structures are only slightly better than the equispaced plan. The beam angle variable combination for the "best" optimized IMRT plan is **sela**=3 and **selb**=0 or **selb**=1, since both algorithm combinations produced the same beam angle solutions. The cDVH of the plan is shown in Figure 4.5.

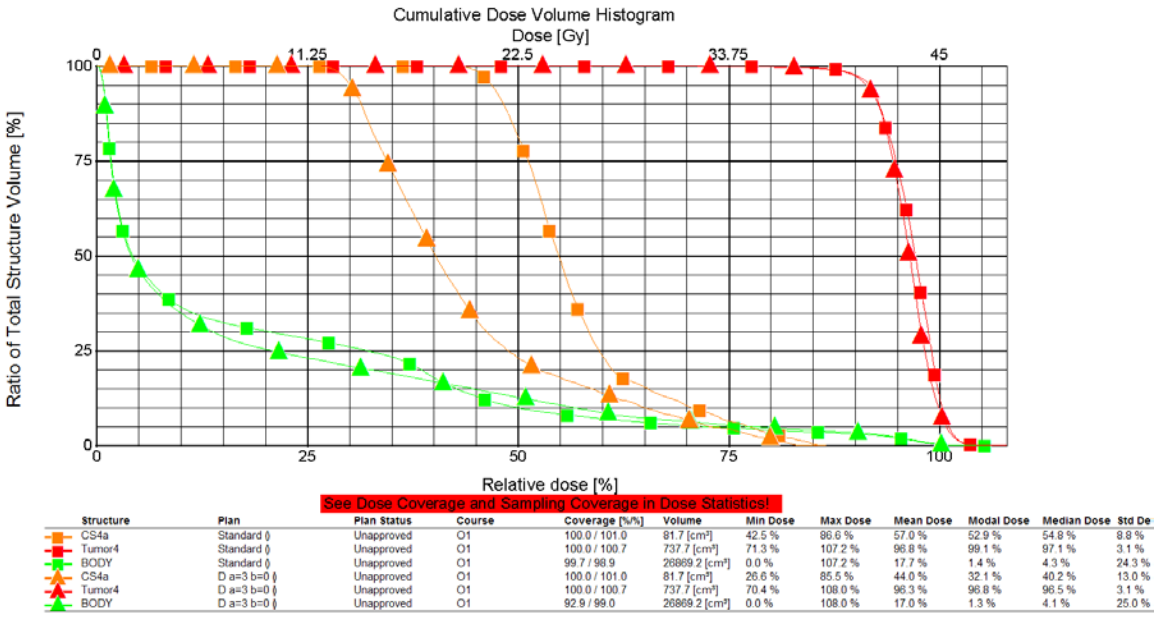

Figure 4.7: cDVH of equispaced IMRT plan vs. Method 2, with sela=3 and selb=0, optimized IMRT plan for square target geometry

The triangle data points in Figure 4.5 represent the optimized IMRT plan and the square data points represent the equispaced IMRT plan. The critical structure cDVH, for the optimized plan, represented by the orange data points, is significantly less than the equispaced plan; this results in greater dose sparing for the optimized plan. The normal tissue cDVH, represented by the green data points, and the target cDVH, represented by the red data points, are slightly less for the optimized IMRT plan. This means that the normal tissue has greater dose sparing but the target also receives a lower mean dose. However, since the critical structure and the normal tissue for the optimized plan have greater dose sparing than the equispaced IMRT plan, then the overall dose can be escalated to achieve a similar target cDVH while still sparing dose to the critical structure and the normal tissue. Ultimately, this means that the optimized IMRT plan using MCNP simulation data with the Method 2 Matlab algorithm produces a "better" IMRT plan than an equispaced IMRT plan.

Six angle exclusion variable combinations were used for the L-Shaped target geometry. None of the combinations produced an optimized IMRT plan that was better than the equispaced IMRT plan; however, two of the combinations produced optimized

IMRT plans that were close to the equispaced IMRT plan. Both optimized IMRT plans have slightly better target and normal tissue cDVHs but the critical structure has less dose sparing than the equispaced IMRT plan. Figure 4.6 shows the cDVHs for **sela**=3 and **selb**=2 angle exclusion variable combination.

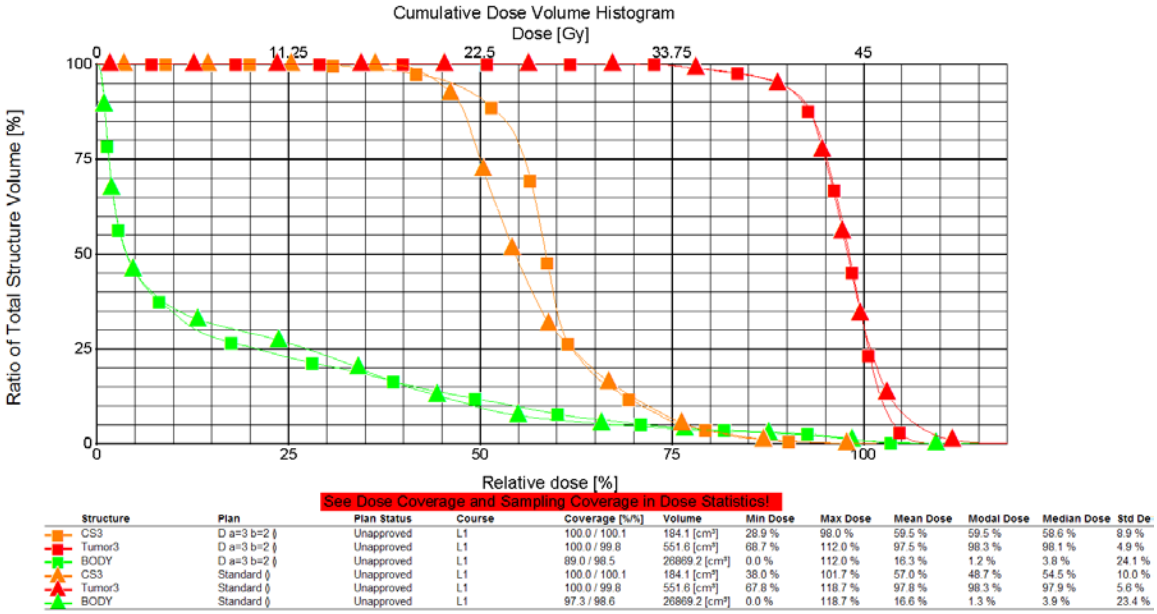

Figure 4.8: cDVH of equispaced IMRT plan vs. Method 2, with sela=3 and selb=2, optimized IMRT plan for L-shaped target geometry

In Figure 4.6, the triangle data points represent the equispaced IMRT plan and the square data points represent the optimized IMRT plan. The target cDVHs, represented by the red line, are similar for the two plans, but the cDVH for the optimized IMRT plan is steeper towards the end. This means that the dose to the target has "better" uniformity than equispaced IMRT plan. In addition, the maximum dose for the optimized IMRT plan is less than the equispaced IMRT plan, further proving that the optimized IMRT plan produces a more uniform dose for the target. However, while the critical structure cDVH is worse for the optimized IMRT plan, the percentage of volume receiving a higher dose occurs only at lower doses and the optimized IMRT plan has a slightly lower volume percentage receiving a higher dose. In addition, the maximum dose for the critical structure is lower for the optimized plan. Overall, the use of the MCNP

simulation with the Method 2 algorithm provides a similar solution to the equispaced IMRT plan.

The U-Shaped target geometry used the same angle exclusion variable combination as the square target geometry, but the U-Shaped target geometry did not produce any optimized IMRT plans that are clearly "better" than the equispaced IMRT plans. However, this could be a result of the number of beam angles available for selection rather than a fault in the Matlab algorithm. The cDVHs for the U-Shaped target geometry is in Appendix G.

4.4 Rotated MCNP Simulation Results

As the target geometry of the phantom becomes more difficult, the ability of the Method 2 optimization algorithm to select seven beam angles becomes more difficult. For the square target geometry, the simplest geometry, all of the optimized IMRT plans are as "good" if not "better" than the equispaced IMRT plan. Then for the L-Shaped target geometry, which is moderately difficult, only two of the optimized IMRT plans are even equal to the equispaced IMRT plan while the other optimized IMRT plans are "worse." None of the optimized IMRT plans for the most difficult geometry, the U-Shaped target geometry, are as "good" as the equispaced IMRT plan. This may be a result of the limited number of beam angles available for selection. So, more MCNP beam angles for each of the geometries were simulated by rotating the phantom in the MCNP simulation by 3.75°, effectively doubling the number of data points available for the Matlab algorithm. The rotated MCNP simulation data is in Appendix E.

The Matlab algorithm was slightly changed to account for the larger data set, and new angle exclusion variables were used to account for the shorter distance between beam angles. The following tables show the angle exclusion variable combinations used and the angles selected by the Matlab algorithm.

Table 4.7: Matlab Beam Angle Selection for Square Target Geometry with Rotated Data (Method 2)

Angle Exclusion Variables		Beam Angle 1	Beam Angle 2	Beam Angle 3	Beam Angle 4	Beam Angle 5	Beam Angle 6	Beam Angle 7	Total Combined Dose Value
sela	selb								
4	2	0.00	18.75	67.50	101.25	270.00	292.50	341.25	4.0170E-04
4	3	0.00	18.75	67.50	97.50	262.50	292.50	337.50	4.0008E-04
5	3	3.75	26.25	67.50	97.50	262.50	296.25	341.25	3.9835E-04
5	4	0.00	22.50	63.75	86.25	285.00	307.50	337.50	3.9600E-04
6	4	0.00	26.25	63.75	101.25	262.50	290.00	333.75	3.9412E-04
6	5	3.75	30.00	56.25	82.50	285.00	311.25	337.50	3.9100E-04

The beam anglesfor the different angle exclusion variable combinations, shown in Table 4.7, are similar for this target geometry. In addition, the angle exclusion variables go up to the equivalent of **sela**=3 and **selb**=2 for MCNP simulation data that does not include the rotated data.

Table 4.8. Matlab Beam Angle Selection for L-Shaped Target Geometry with Rotated Data (Method 2)

Angle Exclusion Variables		Beam Angle 1	Beam Angle 2	Beam Angle 3	Beam Angle 4	Beam Angle 5	Beam Angle 6	Beam Angle 7	Total Combined Dose Value
sela	selb								
4	2	7.50	26.25	45.00	63.75	82.50	101.25	348.75	3.0517E-04
4	3	7.50	26.25	52.50	71.25	90.00	108.75	348.75	3.0489E-04
5	3	3.75	26.25	48.75	71.25	93.75	116.25	341.25	3.0076E-04
5	4	18.75	41.25	63.75	86.25	108.75	333.75	356.25	2.9990E-04
6	4	18.75	45.00	71.25	97.50	123.75	326.25	352.50	2.9256E-04
10	4	18.75	90.00	131.25	176.25	251.25	292.50	337.50	2.4820E-04
11	4	22.50	82.50	127.50	176.25	243.75	288.75	337.50	2.4620E-04
12	4	18.75	67.50	116.25	168.75	228.75	277.50	330.00	2.4360E-04

Table 4.8 shows an increased range of the angle exclusion variable used for the L-Shaped target geometry. The angle exclusion variable, **sela**, was increased to see if an induced quasi-equispaced IMRT plan would produce a "better" IMRT plan. The rest of the angle exclusion variable combinations are the same as the square target geometry, but there is greater variation in the beam angles selected for the L-Shaped target geometry.

Table 4.9. Matlab Beam Angle Selection for U-Shaped Target Geometry with Rotated Data (Method 2)

Angle Exclusion Variables		Beam Angle 1	Beam Angle 2	Beam Angle 3	Beam Angle 4	Beam Angle 5	Beam Angle 6	Beam Angle 7	Total Combined Dose Value
sela	selb								
4	2	11.25	30.00	75.00	270.00	292.50	333.75	352.50	3.4061E-04
4	3	11.25	30.00	63.75	82.50	281.25	333.75	352.50	3.4044E-04
5	3	7.50	30.00	71.25	270.00	292.50	322.50	345.00	3.3675E-04
5	4	7.50	30.00	71.25	270.00	292.50	322.50	345.00	3.3675E-04
6	4	0.00	26.25	56.25	82.50	281.25	307.50	333.75	3.3235E-04
6	5	3.75	30.00	56.25	82.50	285.00	311.25	337.50	3.3196E-04

The same angle exclusion variable combinations in the square target geometry were used for the U-Shaped target geometry found in Table 4.9, but with different beam angle values.

The IMRT plans of the selected beam angles in Table 4.7, Table 4.8, and Table 4.9 were then calculated to determine if increasing the number of beam angle data points would produce an optimized IMRT plan that was equal to if not "better" than an equispaced IMRT plan. After comparing the different optimized IMRT plans, one angle exclusion variable combination produced a consistently "better" optimized IMRT plan than the equispaced IMRT plan for all geometries: **sela** = 6 and **selb** = 4. More importantly, this combination provided a "better" optimized IMRT plan than the equispaced IMRT plan for the U-Shaped target geometry, the most difficult geometry. Furthermore, the angle exclusion variable values are consistent with the variable values found when the rotated MCNP simulation data was not used; the best optimized IMRT plans for all geometries used angle exclusion variable values of **sela** = 3 and the **selb** value ranged from 1 to 2. Remember that angle exclusion variable values of **sela** = 6 and **selb** = 4 for the added rotated MCNP simulation data are equivalent to **sela** = 3 and **selb** = 2 for the MCNP simulation data without the rotated data. A comparison of the cDVHs of the optimized IMRT plan to the equispaced IMRT plan for the three geometries are in the following figures. The red data points represent the cDVH of the target volume; the

orange data points represent the cDVH of the critical structure, and the green data points represent the cDVH of the normal tissue in the following figures.

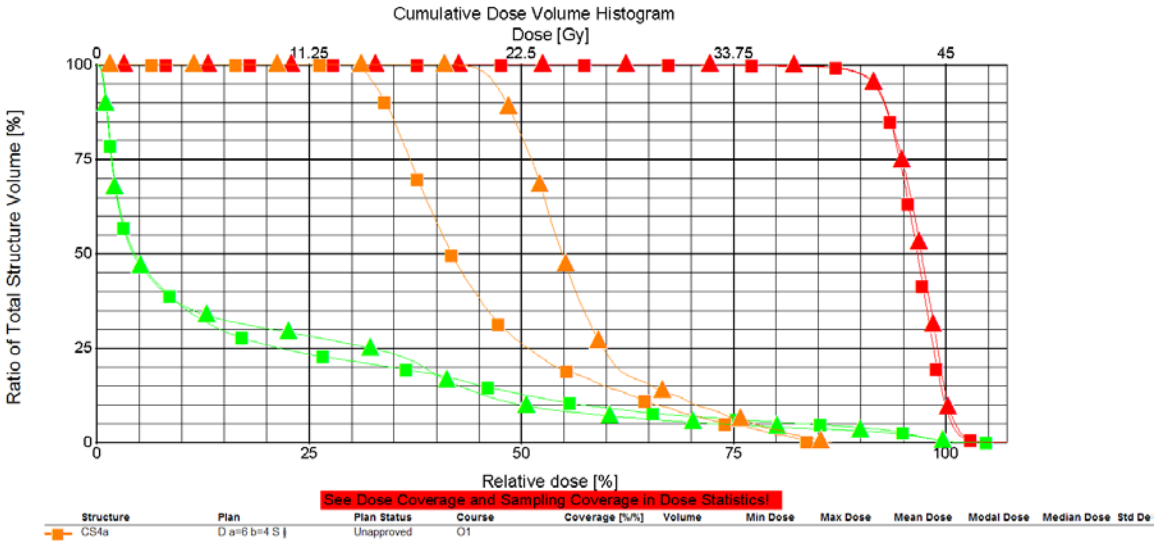

Figure 4.9: cDVH of equispaced IMRT plan vs. optimized IMRT plan using Method 2 algorithm with rotated MCNP simulation data, and sela=6 and selb=4 for the square target geometry

In Figure 4.7, the square data points represent the optimized IMRT plan and the triangle data points represent the equispaced IMRT plan. The cDVHs of the critical structure clearly show significant dose sparing of the critical structure for the optimized IMRT plan compared to the equispaced IMRT plan. The cDVHs of the target show an increase dose to the target for the equispaced IMRT plan. This is confirmed by a larger mean dose for the equispaced IMRT plan. However, the increased dose sparing of the critical structure allows for greater dose escalation of the IMRT plan to achieve a higher mean dose to the target volume with the same or "better" dose sparing of the critical structure as compared to the equispaced plan. In addition, the maximum dose values for the target are similar, meaning the dose uniformity of the plans is comparable, and the maximum dose to the critical structure for the optimized IMRT plan is less than the maximum dose for the equispaced IMRT plan.

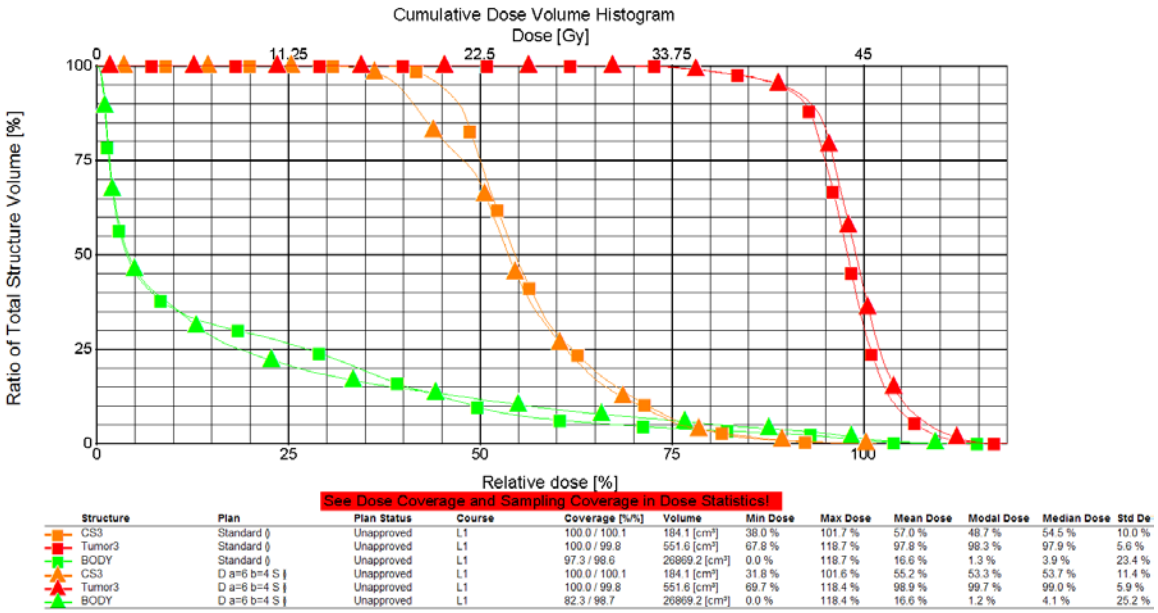

Figure 4.10: cDVH of equispaced IMRT plan vs. optimized IMRT plan using Method 2 algorithm with rotated MCNP simulation data, and sela=6 and selb=4 for the L-shaped target geometry

In Figure 4.8, the triangle data points represent the optimized IMRT plan and the square data points represent the equispaced IMRT plan. The cDVHs of the critical structures show increased dose sparing for the optimized IMRT plan. Furthermore, the optimized IMRT plan has an increased mean dose to the target while having a lower maximum dose to the target. In other words, the optimized IMRT plan already has an escalated dose for the target while still maintaining greater dose sparing to the critical structure, and the dose to the target can further be increased while still maintaining greater dose sparing to the critical structure. In addition, the dose uniformity for the target is "better" in the optimized IMRT plan because the maximum dose to the target is less for the optimized IRMT plan and the minimum dose to the target is higher for the optimized IMRT plan.

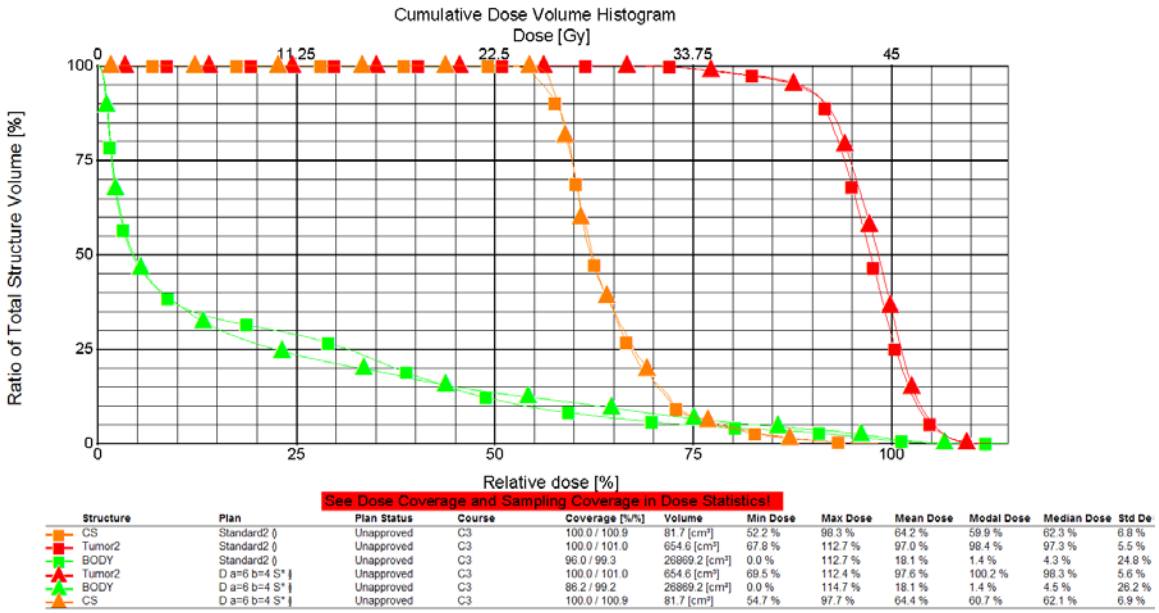

Figure 4.11: cDVH of equispaced IMRT plan vs. optimized IMRT plan using Method 2 algorithm with rotated MCNP simulation data, and sela=6 and selb=4 for the U-shaped target geometry

In Figure 4.9, the triangle data points represent the optimized IMRT plan and the square data points represent the equispaced IMRT plan. The cDVHs of the critical structure for the two IMRT plans are almost identical. However, the mean dose to the critical structure for optimized IMRT plan is slightly higher than the equispaced IMRT plan, but the maximum dose to critical structure is less for the optimized IMRT plan. The mean target dose for the optimized IMRT plan is higher than equispaced IMRT plan. Therefore, the optimized IMRT plan achieves a higher target dose while maintaining similar dose sparing for the critical structure. Furthermore, the optimized IMRT plan has "better" dose uniformity than the equispaced IMRT plan: The maximum dose to the target is lower and the minimum dose to the target is higher for the optimized IMRT plan.

The remainder of the cDVHs for the different beam angle selection variable combinations of the optimized IMRT plans are in Appendix H.

CHAPTER 5

CONCLUSIONS

An effective beam optimization algorithm is necessary in the selection of a set of beam angles. After a series of angle exclusion variable combinations and algorithm methods were tested, a universal beam angle optimization algorithm was achieved, producing "better" IMRT plans than the equispaced IMRT plans for all the target geometries. In addition, some of the other angle exclusion variable combinations produced optimized IMRT plans with similar results as the equispaced IMRT plan. These results indicate that it is possible to develop a beam angle optimization method that is capable of optimizing the beam angles for an IMRT plan without attempting to optimize the beam intensity profiles, which would greatly increase the complexity of the calculation. Furthermore, the results indicate that an adjoint simulation of the target geometry in MCNP is capable of scoring beam directions. Although this thesis used homogeneous water phantoms for the MCNP simulations, MCNP can have heterogeneous phantoms and account for scattering effects, which most beam angle optimization methods ignore during scoring of beam directions. However, the results of this thesis do not indicate if this method is capable of solving more complex 3-D target geometries since the target geometries are essentially 2-D problems solved in a 3-D space. Ultimately, this thesis shows a promising method of optimizing beam directions without having to solve beam intensity profiles with complex optimization algorithms while optimizing the beam directions.

CHAPTER 6

RECOMMENDATIONS

The next step for this method of IMRT beam angle optimization is to determine its ability to handle more complex target geometries with the ultimate goal of using CT data for the phantom. The increasing complexity of the phantom may require more beam directions to solve the problem: Possibly the beam angles scored should have a step size of 1°. However, the increased number of beam directions scored will increase the simulation time. Variance reduction should be performed on the MCNP simulations to reduce MCNP simulation time. In addition, "better" optimization algorithms for the selection of the beam directions will be required with an increased number of beam directions to ensure the optimal solution is achieved and reduce the calculation time.

APPENDIX A

MD Anderson Beam Spectrum for a 6 MV Beam with a 10 cm x 10 cm Field Measured 100 cm Away Along the Central Axis

Table A.10: MD Anderson 6 MV beam spectrum for a 10 cm x 10 cm field measured 100 cm away along the central axis

Photon Energy (MeV)	Differential Fluence (photon/cm^2/MeV)	Fluence (photon/cm^2)	Normalized Composition
0.04789	3.52990E-09	1.69040E-10	1.57097E-07
0.07981	1.99410E-09	1.59153E-10	1.47909E-07
0.11174	6.59910E-08	7.37383E-09	6.85288E-06
0.14366	3.39450E-07	4.87654E-08	4.53202E-05
0.17559	1.78390E-06	3.13235E-07	2.91105E-04
0.20751	3.36850E-06	6.98997E-07	6.49614E-04
0.23944	5.52650E-06	1.32327E-06	1.22978E-03
0.27136	6.77950E-06	1.83969E-06	1.70971E-03
0.30329	8.23460E-06	2.49747E-06	2.32103E-03
0.33521	9.05720E-06	3.03606E-06	2.82157E-03
0.36714	9.26310E-06	3.40085E-06	3.16059E-03
0.39906	9.66750E-06	3.85791E-06	3.58535E-03
0.43099	8.82260E-06	3.80245E-06	3.53381E-03
0.46291	9.25100E-06	4.28238E-06	3.97983E-03
0.49484	9.66260E-06	4.78144E-06	4.44364E-03
0.52676	1.07670E-05	5.67162E-06	5.27093E-03
0.55869	9.09250E-06	5.07989E-06	4.72100E-03
0.59061	9.27980E-06	5.48074E-06	5.09353E-03
0.62254	9.17610E-06	5.71249E-06	5.30891E-03
0.65446	9.12680E-06	5.97313E-06	5.55113E-03
0.68639	9.18700E-06	6.30586E-06	5.86036E-03
0.71831	8.76100E-06	6.29311E-06	5.84851E-03
0.75024	9.05230E-06	6.79140E-06	6.31159E-03
0.78216	8.45690E-06	6.61465E-06	6.14733E-03
0.81409	8.32040E-06	6.77355E-06	6.29501E-03
0.84601	8.21400E-06	6.94913E-06	6.45818E-03
0.87794	7.65120E-06	6.71729E-06	6.24272E-03
0.90986	8.00740E-06	7.28561E-06	6.77089E-03
0.94179	7.82070E-06	7.36546E-06	6.84509E-03
0.97371	7.98880E-06	7.77877E-06	7.22921E-03
1.00560	7.41720E-06	7.45874E-06	6.93178E-03
1.03760	7.50520E-06	7.78740E-06	7.23722E-03
1.06950	7.56780E-06	8.09376E-06	7.52194E-03
1.10140	7.03140E-06	7.74438E-06	7.19725E-03
1.13330	7.08800E-06	8.03283E-06	7.46532E-03
1.16530	6.66210E-06	7.76335E-06	7.21487E-03
1.19720	6.58890E-06	7.88823E-06	7.33093E-03
1.22910	7.05920E-06	8.67646E-06	8.06348E-03

Table A.1 (Continued)

1.26100	6.93070E-06	8.73961E-06	8.12217E-03
1.29300	5.98860E-06	7.74326E-06	7.19621E-03
1.32490	6.21430E-06	8.23333E-06	7.65165E-03
1.35680	6.05280E-06	8.21244E-06	7.63224E-03
1.38870	5.86910E-06	8.15042E-06	7.57460E-03
1.42070	5.64600E-06	8.02127E-06	7.45458E-03
1.45260	5.56100E-06	8.07791E-06	7.50721E-03
1.48450	5.85980E-06	8.69887E-06	8.08431E-03
1.51640	5.64920E-06	8.56645E-06	7.96123E-03
1.54840	5.62750E-06	8.71362E-06	8.09801E-03
1.58030	5.41900E-06	8.56365E-06	7.95863E-03
1.61220	5.18890E-06	8.36554E-06	7.77453E-03
1.64410	4.76700E-06	7.83742E-06	7.28372E-03
1.67610	5.46690E-06	9.16307E-06	8.51571E-03
1.70800	4.64380E-06	7.93161E-06	7.37125E-03
1.73990	4.67860E-06	8.14030E-06	7.56519E-03
1.77180	4.96200E-06	8.79167E-06	8.17055E-03
1.80380	4.39520E-06	7.92806E-06	7.36795E-03
1.83570	4.85440E-06	8.91122E-06	8.28165E-03
1.86760	4.86680E-06	9.08924E-06	8.44709E-03
1.89950	4.52310E-06	8.59163E-06	7.98464E-03
1.93150	4.55340E-06	8.79489E-06	8.17354E-03
1.96340	4.01660E-06	7.88619E-06	7.32904E-03
1.99530	4.30980E-06	8.59934E-06	7.99181E-03
2.02720	4.16100E-06	8.43518E-06	7.83924E-03
2.05920	4.16780E-06	8.58233E-06	7.97600E-03
2.09110	3.81260E-06	7.97253E-06	7.40928E-03
2.12300	3.86790E-06	8.21155E-06	7.63141E-03
2.15490	3.65300E-06	7.87185E-06	7.31571E-03
2.18690	3.87010E-06	8.46352E-06	7.86558E-03
2.21880	3.47590E-06	7.71233E-06	7.16746E-03
2.25070	3.58930E-06	8.07844E-06	7.50770E-03
2.28260	3.47410E-06	7.92998E-06	7.36973E-03
2.31460	3.36650E-06	7.79210E-06	7.24160E-03
2.34650	3.18220E-06	7.46703E-06	6.93949E-03
2.37840	3.52490E-06	8.38362E-06	7.79133E-03
2.41030	3.36900E-06	8.12030E-06	7.54661E-03
2.44230	3.32480E-06	8.12016E-06	7.54648E-03
2.47420	3.18470E-06	7.87958E-06	7.32290E-03
2.50610	3.18020E-06	7.96990E-06	7.40683E-03
2.53800	3.09100E-06	7.84496E-06	7.29072E-03
2.57000	2.70880E-06	6.96162E-06	6.46978E-03
2.60190	3.21960E-06	8.37708E-06	7.78524E-03
2.63380	3.03410E-06	7.99121E-06	7.42664E-03
2.66570	3.18320E-06	8.48546E-06	7.88597E-03
2.69770	2.71970E-06	7.33693E-06	6.81859E-03
2.72960	2.74420E-06	7.49057E-06	6.96137E-03

Table A.1 (Continued)

2.76150	3.05470E-06	8.43555E-06	7.83959E-03
2.79340	2.77070E-06	7.73967E-06	7.19287E-03
2.82540	2.58780E-06	7.31157E-06	6.79501E-03
2.85730	2.42190E-06	6.92009E-06	6.43120E-03
2.88920	2.60470E-06	7.52550E-06	6.99383E-03
2.92110	2.57710E-06	7.52797E-06	6.99612E-03
2.95310	2.61140E-06	7.71173E-06	7.16690E-03
2.98500	2.55790E-06	7.63533E-06	7.09590E-03
3.01690	2.41230E-06	7.27767E-06	6.76351E-03
3.04880	2.45960E-06	7.49883E-06	6.96904E-03
3.08080	1.97840E-06	6.09505E-06	5.66444E-03
3.11270	2.24020E-06	6.97307E-06	6.48043E-03
3.14460	2.24810E-06	7.06938E-06	6.56993E-03
3.17650	2.34520E-06	7.44953E-06	6.92323E-03
3.20850	2.02420E-06	6.49465E-06	6.03580E-03
3.24040	1.99960E-06	6.47950E-06	6.02173E-03
3.27230	2.11800E-06	6.93073E-06	6.44108E-03
3.30420	2.02910E-06	6.70455E-06	6.23088E-03
3.33620	1.78570E-06	5.95745E-06	5.53656E-03
3.36810	1.85100E-06	6.23435E-06	5.79390E-03
3.40000	1.97550E-06	6.71670E-06	6.24217E-03
3.43190	1.74000E-06	5.97151E-06	5.54962E-03
3.46390	1.98030E-06	6.85956E-06	6.37494E-03
3.49580	1.69460E-06	5.92398E-06	5.50546E-03
3.52770	1.92140E-06	6.77812E-06	6.29925E-03
3.55960	1.81190E-06	6.44964E-06	5.99398E-03
3.59160	1.81790E-06	6.52917E-06	6.06789E-03
3.62350	1.87160E-06	6.78174E-06	6.30262E-03
3.65540	1.57280E-06	5.74921E-06	5.34304E-03
3.68730	1.80750E-06	6.66479E-06	6.19393E-03
3.71930	1.81440E-06	6.74830E-06	6.27154E-03
3.75120	1.61190E-06	6.04656E-06	5.61938E-03
3.78310	1.41430E-06	5.35044E-06	4.97243E-03
3.81500	1.59370E-06	6.07997E-06	5.65042E-03
3.84700	1.58550E-06	6.09942E-06	5.66850E-03
3.87890	1.61930E-06	6.28110E-06	5.83735E-03
3.91080	1.51760E-06	5.93503E-06	5.51573E-03
3.94270	1.57340E-06	6.20344E-06	5.76518E-03
3.97470	1.53950E-06	6.11905E-06	5.68675E-03
4.00660	1.81410E-06	7.26837E-06	6.75487E-03
4.03850	1.32910E-06	5.36757E-06	4.98836E-03
4.07040	1.16240E-06	4.73143E-06	4.39716E-03
4.10240	1.39310E-06	5.71505E-06	5.31129E-03
4.13430	1.18620E-06	4.90411E-06	4.55764E-03
4.16620	1.26220E-06	5.25858E-06	4.88706E-03
4.19810	1.19640E-06	5.02261E-06	4.66776E-03
4.23010	1.27430E-06	5.39042E-06	5.00959E-03

Table A.1 (Continued)

4.26200	1.15400E-06	4.91835E-06	4.57087E-03
4.29390	1.29470E-06	5.55931E-06	5.16655E-03
4.32580	1.15810E-06	5.00971E-06	4.65578E-03
4.35780	1.17550E-06	5.12259E-06	4.76069E-03
4.38970	1.23810E-06	5.43489E-06	5.05092E-03
4.42160	1.12040E-06	4.95396E-06	4.60397E-03
4.45350	1.11190E-06	4.95185E-06	4.60200E-03
4.48550	1.22930E-06	5.51403E-06	5.12446E-03
4.51740	1.08960E-06	4.92216E-06	4.57441E-03
4.54930	1.26070E-06	5.73530E-06	5.33011E-03
4.58120	9.95930E-07	4.56255E-06	4.24021E-03
4.61320	9.95370E-07	4.59184E-06	4.26743E-03
4.64510	9.12580E-07	4.23903E-06	3.93954E-03
4.67700	1.06110E-06	4.96276E-06	4.61215E-03
4.70890	8.96010E-07	4.21922E-06	3.92114E-03
4.74090	9.89200E-07	4.68970E-06	4.35838E-03
4.77280	7.98290E-07	3.81008E-06	3.54090E-03
4.80470	8.68680E-07	4.17375E-06	3.87888E-03
4.83660	8.84540E-07	4.27817E-06	3.97592E-03
4.86860	9.89060E-07	4.81534E-06	4.47514E-03
4.90050	8.59230E-07	4.21066E-06	3.91318E-03
4.93240	8.24850E-07	4.06849E-06	3.78105E-03
4.96430	7.18630E-07	3.56749E-06	3.31545E-03
4.99630	7.70310E-07	3.84870E-06	3.57679E-03
5.02820	7.73680E-07	3.89022E-06	3.61538E-03
5.06010	6.60140E-07	3.34037E-06	3.10438E-03
5.09200	8.29630E-07	4.22448E-06	3.92602E-03
5.12400	7.23490E-07	3.70716E-06	3.44525E-03
5.15590	6.21600E-07	3.20491E-06	2.97848E-03
5.18780	6.03970E-07	3.13328E-06	2.91191E-03
5.21970	7.10210E-07	3.70708E-06	3.44518E-03
5.25170	5.14240E-07	2.70063E-06	2.50984E-03
5.28360	5.89130E-07	3.11273E-06	2.89282E-03
5.31550	5.63730E-07	2.99651E-06	2.78481E-03
5.34740	5.83130E-07	3.11823E-06	2.89793E-03
5.37940	5.24340E-07	2.82063E-06	2.62136E-03
5.41130	5.28690E-07	2.86090E-06	2.65878E-03
5.44320	4.97150E-07	2.70609E-06	2.51490E-03
5.47510	4.53210E-07	2.48137E-06	2.30606E-03
5.50710	4.33250E-07	2.38595E-06	2.21739E-03
5.53900	4.65550E-07	2.57868E-06	2.39650E-03
5.57090	4.18850E-07	2.33337E-06	2.16852E-03
5.60280	3.65940E-07	2.05029E-06	1.90544E-03
5.63480	3.07330E-07	1.73174E-06	1.60940E-03
5.66670	4.33120E-07	2.45436E-06	2.28096E-03
5.69860	3.44670E-07	1.96414E-06	1.82537E-03
5.73050	3.60270E-07	2.06453E-06	1.91867E-03

Table A.1 (Continued)

5.76250	3.61650E-07	2.08401E-06	1.93677E-03
5.79440	3.11710E-07	1.80617E-06	1.67857E-03
5.82630	2.70070E-07	1.57351E-06	1.46234E-03
5.85820	3.21690E-07	1.88452E-06	1.75138E-03
5.89020	3.31820E-07	1.95449E-06	1.81640E-03
5.92210	3.02770E-07	1.79303E-06	1.66636E-03
5.95400	2.27980E-07	1.35739E-06	1.26149E-03
5.98590	1.71820E-07	1.02850E-06	9.55835E-04
6.01790	2.25540E-07	1.35728E-06	1.26139E-03
6.04980	1.49840E-07	9.06502E-07	8.42458E-04
6.08170	1.18330E-07	7.19648E-07	6.68805E-04
6.11360	7.99840E-08	4.88990E-07	4.54443E-04
6.14560	5.88310E-08	3.61552E-07	3.36008E-04
6.17750	5.15790E-08	3.18629E-07	2.96118E-04
6.20940	8.29460E-09	5.15045E-08	4.78657E-05
6.24130	1.65680E-08	1.03406E-07	9.61003E-05
6.27330	1.29470E-08	8.12204E-08	7.54823E-05
6.30520	1.53450E-08	9.67533E-08	8.99178E-05
6.36900	7.82010E-09	4.98062E-08	4.62875E-05

APPENDIX B

MCNP Simulation

```
c  Shaped Problem
c   Inverse Problem Treating the Tumor Volume as the Source
c
c   The "body" is a box phantom of water.
c   The "tumor" is a C-shaped volume located at the origin (SAD setup).
c   The "critical structure" is in the center of the C-shaped volume of tumor, forming a cube.
c   The detection volumes are located in a circle 100 cm from the origin.
c   The detectors are every 7.5 degrees (48 detectors total).
c
c   **********Particle Histories: 100000000**********
c
c   Energy bins set up according to Ambient Dose Equivalent H*(10)) found in
c      ICRP 74.
c   Using 6MV beam data from MD ANDERSON as source definition.
c   Turned on calculation of Ambient Dose Equivialent
c   The "source" includes the tumor and the critical structure.
c   Particles that travel through the "critical structure" are flagged.
c
c   All preceding input files will have different water phantom locations, to change position of tumor.
c                              Isocentric
c
c   *Had to change the random number seed to go past 2e6 particle histories.
c
c ********************************************************************************
c   Cell Card ------------------------------------------------------------
    1     1      -1 -1  $ TUMOR 1.1 (WATER)
    2     1      -1 -2  $ TUMOR 1.2 (WATER)
    3     1      -1 -3  $ TUMOR 1.3 (WATER)
    4     1      -1 -10  $ CRITICAL STRUCTURE (WATER)
   10     1       -1 1 2 3 10 -20  $ BODY VOLUME (WATER)
   20     2 -0.001205 20 -99 41 42 43 44 45 46 47 48 49 50 51 52 53 54 55 56 57
           58 59 60 61 62 63 64 65 66 67 68 69 70 71 72 73 74 75 76 77 78 79
           80 81 82 83 84 85 86 87 88
   41     2 -0.001205 -41  $ DETECTOR VOL 1 (AIR)
   42     2 -0.001205 -42  $ DETECTOR VOL 2 (AIR)
   43     2 -0.001205 -43  $ DETECTOR VOL 3 (AIR)
   44     2 -0.001205 -44  $ DETECTOR VOL 4 (AIR)
   45     2 -0.001205 -45  $ DETECTOR VOL 5 (AIR)
   46     2 -0.001205 -46  $ DETECTOR VOL 6 (AIR)
   47     2 -0.001205 -47  $ DETECTOR VOL 7 (AIR)
   48     2 -0.001205 -48  $ DETECTOR VOL 8 (AIR)
   49     2 -0.001205 -49  $ DETECTOR VOL 9 (AIR)
   50     2 -0.001205 -50  $ DETECTOR VOL 10 (AIR)
   51     2 -0.001205 -51  $ DETECTOR VOL 11 (AIR)
   52     2 -0.001205 -52  $ DETECTOR VOL 12 (AIR)
   53     2 -0.001205 -53  $ DETECTOR VOL 13 (AIR)
   54     2 -0.001205 -54  $ DETECTOR VOL 14 (AIR)
   55     2 -0.001205 -55  $ DETECTOR VOL 15 (AIR)
   56     2 -0.001205 -56  $ DETECTOR VOL 16 (AIR)
   57     2 -0.001205 -57  $ DETECTOR VOL 17 (AIR)
   58     2 -0.001205 -58  $ DETECTOR VOL 18 (AIR)
   59     2 -0.001205 -59  $ DETECTOR VOL 19 (AIR)
   60     2 -0.001205 -60  $ DETECTOR VOL 20 (AIR)
   61     2 -0.001205 -61  $ DETECTOR VOL 21 (AIR)
   62     2 -0.001205 -62  $ DETECTOR VOL 22 (AIR)
   63     2 -0.001205 -63  $ DETECTOR VOL 23 (AIR)
   64     2 -0.001205 -64  $ DETECTOR VOL 24 (AIR)
   65     2 -0.001205 -65  $ DETECTOR VOL 25 (AIR)
   66     2 -0.001205 -66  $ DETECTOR VOL 26 (AIR)
   67     2 -0.001205 -67  $ DETECTOR VOL 27 (AIR)
   68     2 -0.001205 -68  $ DETECTOR VOL 28 (AIR)
   69     2 -0.001205 -69  $ DETECTOR VOL 29 (AIR)
   70     2 -0.001205 -70  $ DETECTOR VOL 30 (AIR)
   71     2 -0.001205 -71  $ DETECTOR VOL 31 (AIR)
   72     2 -0.001205 -72  $ DETECTOR VOL 32 (AIR)
   73     2 -0.001205 -73  $ DETECTOR VOL 33 (AIR)
   74     2 -0.001205 -74  $ DETECTOR VOL 34 (AIR)
   75     2 -0.001205 -75  $ DETECTOR VOL 35 (AIR)
   76     2 -0.001205 -76  $ DETECTOR VOL 36 (AIR)
   77     2 -0.001205 -77  $ DETECTOR VOL 37 (AIR)
```

```
  78    2 -0.001205 -78  $ DETECTOR VOL 38 (AIR)
  79    2 -0.001205 -79  $ DETECTOR VOL 39 (AIR)
  80    2 -0.001205 -80  $ DETECTOR VOL 40 (AIR)
  81    2 -0.001205 -81  $ DETECTOR VOL 41 (AIR)
  82    2 -0.001205 -82  $ DETECTOR VOL 42 (AIR)
  83    2 -0.001205 -83  $ DETECTOR VOL 43 (AIR)
  84    2 -0.001205 -84  $ DETECTOR VOL 44 (AIR)
  85    2 -0.001205 -85  $ DETECTOR VOL 45 (AIR)
  86    2 -0.001205 -86  $ DETECTOR VOL 46 (AIR)
  87    2 -0.001205 -87  $ DETECTOR VOL 47 (AIR)
  88    2 -0.001205 -88  $ DETECTOR VOL 48 (AIR)
  99    0        99  $ BOUNDARY VOLUME (NULL)

c ***************************************************************************
c  Suface Card ------------------------------------------------------------
   1      box -4.5 -4.5 -4.5 0 9 0 5.99999 0 0 0 0 9  $ TUMOR 1.1
   2      box 1.5 -4.5 1.5 0 9 0 3 0 0 0 0 3  $ TUMOR 1.2
   3      box 1.5 -4.5 -4.5 0 9 0 3 0 0 0 0 2.99999  $ TUMOR 1.3
  10      box 1.5 -4.5 -1.5 0 9 0 3 0 0 0 0 2.99999  $ CRITICAL STRUCTURE
  20      box -15 -15 -15 0 30 0 30 0 0 0 0 30  $ BODY BOUNDARY (CUBE)
c  Set up the linac surface so that it corresponts with size of the tumor
c ************************1st Quadrant************************************
c  Detector Vol 1 @ 0 deg
  41      box 100 -6 -5.999999 0 12 0 0 0 12 1 0 0
c  Detector Vol 2 @ 7.5 deg
  42      box 99.92764 -6 7.103951 0 12 0 -1.566314 0 11.89734 0.991445 0
            0.130526
c  Detector Vol 3 @ 15 deg
  43      box 98.1455 -6 20.08635 0 12 0 -3.105828 0 11.59111 0.965926 0
            0.258819
c  Detector Vol 4 @ 22.5 deg
  44      box 94.68405 -6 32.72507 0 12 0 -4.5922 0 11.08655 0.92388 0
            0.382683
c  Detector Vol 5 @ 30 deg
  45      box 89.60254 -6 44.80385 0 12 0 -5.999999 0 10.3923 0.866025 0 0.5
c  Detector Vol 6 @ 37.5 deg
  46      box 82.9879 -6 56.11602 0 12 0 -7.305136 0 9.520238 0.793353 0
            0.608761
c  Detector Vol 7 @ 45 deg
  47      box 74.95332 -6 66.46804 0 12 0 -8.48528 0 8.48528 0.707107 0
            0.707107
c  Detector Vol 8 @ 52.5 deg
  48      box 65.63626 -6 75.68277 0 12 0 -9.520238 0 7.305136 0.608761 0
            0.793353
c  Detector Vol 9 @ 60 deg
  49      box 55.19615 -6 83.60254 0 12 0 -10.3923 0 5.999999 0.5 0 0.866025
c  Detector Vol 10 @ 67.5 deg
  50      box 43.81162 -6 90.09185 0 12 0 -11.08655 0 4.5922 0.382683 0
            0.92388
c  Detector Vol 11 @ 75 deg
  51      box 31.67746 -6 95.03967 0 12 0 -11.59111 0 3.105828 0.258819 0
            0.965926
c  Detector Vol 12 @ 82.5 deg
  52      box 19.00129 -6 98.36133 0 12 0 -11.89734 0 1.566631 0.130526 0
            0.991445
c ************************2nd Quadrant************************************
c  Detector Vol 13 @ 90 deg
  53      box 5.999999 -6 100 0 12 0 -12 0 0 0 0 1
c  Detector Vol 14 @ 97.5 deg
  54      box -7.103951 -6 99.92764 0 12 0 -11.89734 0 -1.566631 -0.130526 0
            0.991445
c  Detector Vol 15 @ 105 deg
  55      box -20.08635 -6 98.1455 0 12 0 -11.59111 0 -3.105828 -0.258819 0
            0.965926
c  Detector Vol 16 @ 112.5 deg
  56      box -32.72507 -6 94.68405 0 12 0 -11.08655 0 -4.5922 -0.382683 0
            0.92388
c  Detector Vol 17 @ 120 deg
  57      box -44.80385 -6 89.60254 0 12 0 -10.3923 0 -5.999999 -0.5 0
            0.866025
c  Detector Vol 18 @ 127.5 deg
  58      box -56.11602 -6 82.9879 0 12 0 -9.520238 0 -7.305136 -0.608761 0
            0.793353
c  Detector Vol 19 @ 135 deg
  59      box -66.46804 -6 74.95332 0 12 0 -8.48528 0 -8.48528 -0.707107 0
            0.707107
c  Detector Vol 20 @ 142.5 deg
  60      box -75.68277 -6 65.63626 0 12 0 -7.305136 0 -9.520238 -0.793353 0
            0.608761
c  Detector Vol 21 @ 150 deg
```

```
  61      box -83.60254 -6 55.19615 0 12 0 -5.999999 0 -10.3923 -0.866025 0
            0.5
c  Detector Vol 22 @ 157.5 deg
  62      box -90.09185 -6 43.81162 0 12 0 -4.5922 0 -11.08655 -0.92388 0
            0.382683
c  Detector Vol 23 @ 165 deg
  63      box -95.03967 -6 31.67746 0 12 0 -3.105828 0 -11.59111 -0.965926 0
            0.258819
c  Detector Vol 24 @ 172.5 deg
  64      box -98.36133 -6 19.00129 0 12 0 -1.566314 0 -11.89734 -0.991445 0
            0.130526
c ********************3rd Quadrant****************************************
c  Detector Vol 25 @ 180 deg
  65      box -100 -6 5.999999 0 12 0 0 0 -12 -1 0 0
c  Detector Vol 26 @ 187.5 deg
  66      box -99.92764 -6 -7.103951 0 12 0 1.566314 0 -11.89734 -0.991445 0
            -0.130526
c  Detector Vol 27 @ 195 deg
  67      box -98.1455 -6 -20.08635 0 12 0 3.105828 0 -11.59111 -0.965926 0
            -0.258819
c  Detector Vol 28 @ 202.5 deg
  68      box -94.68405 -6 -32.72507 0 12 0 4.5922 0 -11.08655 -0.92388 0
            -0.382683
c  Detector Vol 29 @ 210 deg
  69      box -89.60254 -6 -44.80385 0 12 0 5.999999 0 -10.3923 -0.866025 0
            -0.5
c  Detector Vol 30 @ 217.5 deg
  70      box -82.9879 -6 -56.11602 0 12 0 7.305136 0 -9.520238 -0.793353 0
            -0.608761
c  Detector Vol 31 @ 225 deg
  71      box -74.95332 -6 -66.46804 0 12 0 8.48528 0 -8.48528 -0.707107 0
            -0.707107
c  Detector Vol 32 @ 232.5 deg
  72      box -65.63626 -6 -75.68277 0 12 0 9.520238 0 -7.305136 -0.608761 0
            -0.793353
c  Detector Vol 33 @ 240 deg
  73      box -55.19615 -6 -83.60254 0 12 0 10.3923 0 -5.999999 -0.5 0
            -0.866025
c  Detector Vol 34 @ 247.5 deg
  74      box -43.81162 -6 -90.09185 0 12 0 11.08655 0 -4.5922 -0.382683 0
            -0.92388
c  Detector Vol 35 @ 255 deg
  75      box -31.67746 -6 -95.03967 0 12 0 11.59111 0 -3.105828 -0.258819 0
            -0.965926
c  Detector Vol 36 @ 262.5 deg
  76      box -19.00129 -6 -98.36133 0 12 0 11.89734 0 -1.566631 -0.130526 0
            -0.991445
c ************************4th Quadrant************************************
c  Detector Vol 37 @ 270 deg
  77      box -5.999999 -6 -100 0 12 0 12 0 0 0 0 -1
c  Detector Vol 38 @ 277.5 deg
  78      box 7.103951 -6 -99.92764 0 12 0 11.89734 0 1.566631 0.130526 0
            -0.991445
c  Detector Vol 39 @ 285 deg
  79      box 20.08635 -6 -98.1455 0 12 0 11.59111 0 3.105828 0.258819 0
            -0.965926
c  Detector Vol 40 @ 292.5 deg
  80      box 32.72507 -6 -94.68405 0 12 0 11.08655 0 4.5922 0.382683 0
            -0.92388
c  Detector Vol 41 @ 300 deg
  81      box 44.80385 -6 -89.60254 0 12 0 10.3923 0 5.999999 0.5 0 -0.866025
c  Detector Vol 42 @ 307.5 deg
  82      box 56.11602 -6 -82.9879 0 12 0 9.520238 0 7.305136 0.608761 0
            -0.793353
c  Detector Vol 43 @ 315 deg
  83      box 66.46804 -6 -74.95332 0 12 0 8.48528 0 8.48528 0.707107 0
            -0.707107
c  Detector Vol 44 @ 322.5 deg
  84      box 75.68277 -6 -65.63626 0 12 0 7.305136 0 9.520238 0.793353 0
            -0.608761
c  Detector Vol 45 @ 330 deg
  85      box 83.60254 -6 -55.19615 0 12 0 5.999999 0 10.3923 0.866025 0 -0.5
c  Detector Vol 46 @ 337.5 deg
  86      box 90.09185 -6 -43.81162 0 12 0 4.5922 0 11.08655 0.92388 0
            -0.382683
c  Detector Vol 47 @ 345 deg
  87      box 95.03967 -6 -31.67746 0 12 0 3.105828 0 11.59111 0.965926 0
            -0.258819
c  Detector Vol 26 @ 352.5 deg
  88      box 98.36133 -6 -19.00129 0 12 0 1.566314 0 11.89734 0.991445 0
```

```
             -0.130526
c ********************Outer Boundary*************************************
c   Outer boundary
  99       so 120  $ OUTER BOUNDARY (SPHERE)

mode  p
c
c   Material Card ------------------------------------------------------
m1    1000.                2  $ WATER
      16000.               1
m2    7000.          -0.7552  $ AIR (N,O,Ar - chilton)
      8000.          -0.2319 18000.          -0.0129
imp:p            1 53r                   0  $ 1, 99
c
c   Source Definition ---------------------------------------------------
c
sdef X=d2 Y=d3 Z=d4 erg=d1 par=2          $ Parallelpiped Source Volume
c   *****************6MV Beam Spectrum 100 cm from source****************
si1  0 0.016027 0.048082 0.080137 0.11219 &      $ Photon Energies
0.14425 0.1763 0.20836 0.24041 0.27247 0.30452 0.33658 0.36863 0.40069 &
0.43274 0.4648 0.49685 0.52891 0.56096 0.59302 0.62507 0.65713 0.68918 &
0.72124 0.75329 0.78535 0.8174 0.84946 0.88151 0.91357 0.94562 0.97768 &
1.0097 1.0418 1.0738 1.1059 1.138 1.17 1.2021 1.2341 1.2662 1.2982 1.3303 &
1.3623 1.3944 1.4264 1.4585 1.4906 1.5226 1.5547 1.5867 1.6188 1.6508 &
1.6829 1.7149 1.747 1.7791 1.8111 1.8432 1.8752 1.9073 1.9393 1.9714 &
2.0034 2.0355 2.0675 2.0996 2.1317 2.1637 2.1958 2.2278 2.2599 2.2919 &
2.324 2.356 2.3881 2.4202 2.4522 2.4843 2.5163 2.5484 2.5804 2.6125 &
2.6445 2.6766 2.7086 2.7407 2.7728 2.8048 2.8369 2.8689 2.901 2.933 &
2.9651 2.9971 3.0292 3.0613 3.0933 3.1254 3.1574 3.1895 3.2215 3.2536 &
3.2856 3.3177 3.3497 3.3818 3.4139 3.4459 3.478 3.51 3.5421 3.5741 3.6062 &
3.6382 3.6703 3.7024 3.7344 3.7665 3.7985 3.8306 3.8626 3.8947 3.9267 &
3.9588 3.9908 4.0229 4.055 4.087 4.1191 4.1511 4.1832 4.2152 4.2473 4.2793 &
4.3114 4.3435 4.3755 4.4076 4.4396 4.4717 4.5037 4.5358 4.5678 4.5999 &
4.6319 4.664 4.6961 4.7281 4.7602 4.7922 4.8243 4.8563 4.8884 4.9204 &
4.9525 4.9846 5.0166 5.0487 5.0807 5.1128 5.1448 5.1769 5.2089 5.241 &
5.273 5.3051 5.3372 5.3692 5.4013 5.4333 5.4654 5.4974 5.5295 5.5615 &
5.5936 5.6257 5.6577 5.6898 5.7218 5.7539 5.7859 5.818 5.85 5.8821 5.9141 &
5.9462 5.9783 6.0103 6.0424 6.0744 6.1065 6.1385 6.1706 6.2026 6.2347 &
6.2668 6.2988 6.3309 6.3629 6.395
sp1  0 1.08E-07 1.66E-07 4.12E-06 3.15E-05 &    $ Probabilty of Photon Energy
1.22e-04 3.81E-04 7.95E-04 1.39E-03 1.86E-03 2.43E-03 2.77E-03 3.35E-03 &
3.61e-03 3.92E-03 4.33E-03 4.76E-03 4.79E-03 5.05E-03 5.26E-03 5.51E-03 &
5.67e-03 5.81E-03 5.89E-03 6.08E-03 6.16E-03 6.47E-03 6.72E-03 6.66E-03 &
6.87e-03 6.97E-03 7.14E-03 7.07E-03 7.16E-03 7.31E-03 7.22E-03 7.35E-03 &
7.38e-03 7.63E-03 7.43E-03 7.61E-03 7.73E-03 7.91E-03 7.67E-03 7.75E-03 &
7.93e-03 7.89E-03 8.02E-03 7.86E-03 7.52E-03 7.75E-03 7.90E-03 7.86E-03 &
7.90e-03 8.09E-03 8.01E-03 8.03E-03 7.71E-03 8.05E-03 7.76E-03 7.80E-03 &
7.80e-03 7.87E-03 8.03E-03 7.64E-03 7.78E-03 7.44E-03 7.72E-03 7.52E-03 &
7.86e-03 7.67E-03 7.56E-03 8.07E-03 7.64E-03 7.54E-03 7.47E-03 7.48E-03 &
7.23e-03 7.42E-03 7.27E-03 7.37E-03 7.25E-03 7.10E-03 6.78E-03 7.15E-03 &
6.96e-03 7.02E-03 7.22E-03 7.06E-03 7.05E-03 6.85E-03 7.00E-03 6.86E-03 &
7.12e-03 6.63E-03 7.19E-03 6.94E-03 6.41E-03 6.23E-03 6.47E-03 6.36E-03 &
6.32e-03 6.45E-03 6.47E-03 6.00E-03 5.94E-03 6.06E-03 6.38E-03 5.77E-03 &
5.82e-03 6.08E-03 6.29E-03 5.97E-03 5.71E-03 5.84E-03 6.09E-03 5.49E-03 &
5.70e-03 5.59E-03 5.43E-03 5.52E-03 5.73E-03 5.39E-03 5.40E-03 5.29E-03 &
5.17e-03 5.27E-03 5.15E-03 5.35E-03 5.20E-03 5.26E-03 4.83E-03 4.90E-03 &
4.70e-03 5.00E-03 4.58E-03 4.91E-03 4.82E-03 4.73E-03 4.67E-03 4.60E-03 &
4.48e-03 4.59E-03 4.18E-03 4.33E-03 4.02E-03 4.39E-03 4.15E-03 3.97E-03 &
4.44e-03 3.99E-03 3.92E-03 3.59E-03 3.76E-03 3.61E-03 3.54E-03 3.82E-03 &
3.83e-03 3.68E-03 3.28E-03 3.07E-03 3.48E-03 3.49E-03 2.89E-03 2.80E-03 &
2.99e-03 3.25E-03 2.67E-03 2.78E-03 2.94E-03 2.68E-03 2.98E-03 2.36E-03 &
2.59e-03 2.17E-03 2.17E-03 2.29E-03 2.15E-03 1.94E-03 1.89E-03 2.06E-03 &
1.73e-03 1.74E-03 1.46E-03 1.36E-03 1.56E-03 1.02E-03 1.13E-03 1.11E-03 &
9.32e-04 7.28E-04 6.67E-04 4.45E-04 3.97E-04 2.04E-04 1.50E-04 5.55E-05 &
2.71e-05 1.03E-05 1.74E-05 6.28E-06
c   ***************************Source Parameters*****************************
si2  -4.49999 4.49999                  $ X-axis limits
sp2  0 1                          $ Uniform Probability
si3  -4.49999 4.49999                  $ Y-axis limits
sp3  0 1                          $ Uniform Probability
si4  -4.49999 4.49999                  $ Z-axis limits
sp4  0 1                          $ Uniform Probability
c
c   Tally Card ----------------------------------------------------------
c
c f2:p 1
c fc2  Ambient Dose Equivalent (pSv) Over Tumor Surface
c
c f4:p 1
c fc4  Ambient Dose Equivalent (pSv) Over Tumor Volume
```

```
c
c f12:p 30.1                          $ Don't need this tally
c fc12  Ambient Dose Equivalent (pSv) Over Linac Surface
c
fl14:p 41
fc114  Ambient Dose Equivalent (pSv) for Detector 1
cfl14  4   $ Flag particles that travel through the "critical structure"
c
fl24:p 42
fc124  Ambient Dose Equivalent (pSv) for Detector 2
cfl24  4   $ Flag particles that travel through the "critical structure"
c
fl34:p 43
fc134  Ambient Dose Equivalent (pSv) for Detector 3
cfl34  4   $ Flag particles that travel through the "critical structure"
c
fl44:p 44
fc144  Ambient Dose Equivalent (pSv) for Detector 4
cfl44  4   $ Flag particles that travel through the "critical structure"
c
fl54:p 45
fc154  Ambient Dose Equivalent (pSv) for Detector 5
cfl54  4   $ Flag particles that travel through the "critical structure"
c
fl64:p 46
fc164  Ambient Dose Equivalent (pSv) for Detector 6
cfl64  4   $ Flag particles that travel through the "critical structure"
c
fl74:p 47
fc174  Ambient Dose Equivalent (pSv) for Detector 7
cfl74  4   $ Flag particles that travel through the "critical structure"
c
fl84:p 48
fc184  Ambient Dose Equivalent (pSv) for Detector 8
cfl84  4   $ Flag particles that travel through the "critical structure"
c
fl94:p 49
fc194  Ambient Dose Equivalent (pSv) for Detector 9
cfl94  4   $ Flag particles that travel through the "critical structure"
c
f204:p 50
fc204  Ambient Dose Equivalent (pSv) for Detector 10
cf204  4   $ Flag particles that travel through the "critical structure"
c
f214:p 51
fc214  Ambient Dose Equivalent (pSv) for Detector 11
cf214  4   $ Flag particles that travel through the "critical structure"
c
f224:p 52
fc224  Ambient Dose Equivalent (pSv) for Detector 12
cf224  4   $ Flag particles that travel through the "critical structure"
c
f234:p 53
fc234  Ambient Dose Equivalent (pSv) for Detector 13
cf234  4   $ Flag particles that travel through the "critical structure"
c
f244:p 54
fc244  Ambient Dose Equivalent (pSv) for Detector 14
cf244  4   $ Flag particles that travel through the "critical structure"
c
f254:p 55
fc254  Ambient Dose Equivalent (pSv) for Detector 15
cf254  4   $ Flag particles that travel through the "critical structure"
c
f264:p 56
fc264  Ambient Dose Equivalent (pSv) for Detector 16
cf264  4   $ Flag particles that travel through the "critical structure"
c
f274:p 57
fc274  Ambient Dose Equivalent (pSv) for Detector 17
cf274  4   $ Flag particles that travel through the "critical structure"
c
f284:p 58
fc284  Ambient Dose Equivalent (pSv) for Detector 18
cf284  4   $ Flag particles that travel through the "critical structure"
c
f294:p 59
fc294  Ambient Dose Equivalent (pSv) for Detector 19
cf294  4   $ Flag particles that travel through the "critical structure"
c
```

```
f304:p 60
fc304  Ambient Dose Equivalent (pSv) for Detector 20
cf304  4   $ Flag particles that travel through the "critical structure"
c
f314:p 61
fc314  Ambient Dose Equivalent (pSv) for Detector 21
cf314  4   $ Flag particles that travel through the "critical structure"
c
f324:p 62
fc324  Ambient Dose Equivalent (pSv) for Detector 22
cf324  4   $ Flag particles that travel through the "critical structure"
c
f334:p 63
fc334  Ambient Dose Equivalent (pSv) for Detector 23
cf334  4   $ Flag particles that travel through the "critical structure"
c
f344:p 64
fc344  Ambient Dose Equivalent (pSv) for Detector 24
cf344  4   $ Flag particles that travel through the "critical structure"
c
f354:p 65
fc354  Ambient Dose Equivalent (pSv) for Detector 25
cf354  4   $ Flag particles that travel through the "critical structure"
c
f364:p 66
fc364  Ambient Dose Equivalent (pSv) for Detector 26
cf364  4   $ Flag particles that travel through the "critical structure"
c
f374:p 67
fc374  Ambient Dose Equivalent (pSv) for Detector 27
cf374  4   $ Flag particles that travel through the "critical structure"
c
f384:p 68
fc384  Ambient Dose Equivalent (pSv) for Detector 28
cf384  4   $ Flag particles that travel through the "critical structure"
c
f394:p 69
fc394  Ambient Dose Equivalent (pSv) for Detector 29
cf394  4   $ Flag particles that travel through the "critical structure"
c
f404:p 70
fc404  Ambient Dose Equivalent (pSv) for Detector 30
cf404  4   $ Flag particles that travel through the "critical structure"
c
f414:p 71
fc414  Ambient Dose Equivalent (pSv) for Detector 31
cf414  4   $ Flag particles that travel through the "critical structure"
c
f424:p 72
fc424  Ambient Dose Equivalent (pSv) for Detector 32
cf424  4   $ Flag particles that travel through the "critical structure"
c
f434:p 73
fc434  Ambient Dose Equivalent (pSv) for Detector 33
cf434  4   $ Flag particles that travel through the "critical structure"
c
f444:p 74
fc444  Ambient Dose Equivalent (pSv) for Detector 34
cf444  4   $ Flag particles that travel through the "critical structure"
c
f454:p 75
fc454  Ambient Dose Equivalent (pSv) for Detector 35
cf454  4   $ Flag particles that travel through the "critical structure"
c
f464:p 76
fc464  Ambient Dose Equivalent (pSv) for Detector 36
cf464  4   $ Flag particles that travel through the "critical structure"
c
f474:p 77
fc474  Ambient Dose Equivalent (pSv) for Detector 37
cf474  4   $ Flag particles that travel through the "critical structure"
c
f484:p 78
fc484  Ambient Dose Equivalent (pSv) for Detector 38
cf484  4   $ Flag particles that travel through the "critical structure"
c
f494:p 79
fc494  Ambient Dose Equivalent (pSv) for Detector 39
cf494  4   $ Flag particles that travel through the "critical structure"
c
```

```
f504:p 80
fc504  Ambient Dose Equivalent (pSv) for Detector 40
cf504  4   $ Flag particles that travel through the "critical structure"
c
f514:p 81
fc514  Ambient Dose Equivalent (pSv) for Detector 41
cf514  4   $ Flag particles that travel through the "critical structure"
c
f524:p 82
fc524  Ambient Dose Equivalent (pSv) for Detector 42
cf524  4   $ Flag particles that travel through the "critical structure"
c
f534:p 83
fc534  Ambient Dose Equivalent (pSv) for Detector 43
cf534  4   $ Flag particles that travel through the "critical structure"
c
f544:p 84
fc544  Ambient Dose Equivalent (pSv) for Detector 44
cf544  4   $ Flag particles that travel through the "critical structure"
c
f554:p 85
fc554  Ambient Dose Equivalent (pSv) for Detector 45
cf554  4   $ Flag particles that travel through the "critical structure"
c
f564:p 86
fc564  Ambient Dose Equivalent (pSv) for Detector 46
cf564  4   $ Flag particles that travel through the "critical structure"
c
f574:p 87
fc574  Ambient Dose Equivalent (pSv) for Detector 47
cf574  4   $ Flag particles that travel through the "critical structure"
c
f584:p 88
fc584  Ambient Dose Equivalent (pSv) for Detector 48
cf584  4   $ Flag particles that travel through the "critical structure"
c
c ********************Energy Bins*********************************
c
e0  0.01  0.015  0.02  0.03  0.04 0.05  0.06  0.08  0.1  0.15  0.2  &
    0.3     0.4   0.5   0.6  0.8  1.0    1.5   2.0  3.0   4.0  5.0 &
    6.0  8.0  10.0
c  ambient dose equivalent conversion coefficients  ICRP Pub 74
de0  0.01  0.015  0.02  0.03  0.04 0.05  0.06  0.08  0.1  0.15  0.2  &
     0.3     0.4   0.5   0.6  0.8  1.0    1.5   2.0  3.0   4.0  5.0 &
     6.0  8.0  10.0
c in units of pSv-cm2
df0  0.061  0.83  1.05  0.81  0.64  0.55  0.51  0.53  0.61  0.89  &
     1.20  1.80  2.38  2.93  3.44  4.38  5.20  6.90  8.60  11.1  13.4 &
     15.5  17.6  21.6  25.6
c
c   Number Generator / Histories
c
rand  GEN=2 SEEd 46442489987763 STRIDE=3000001
nps   100000000
print
```

APPENDIX C

Method 1 Matlab Algorithm

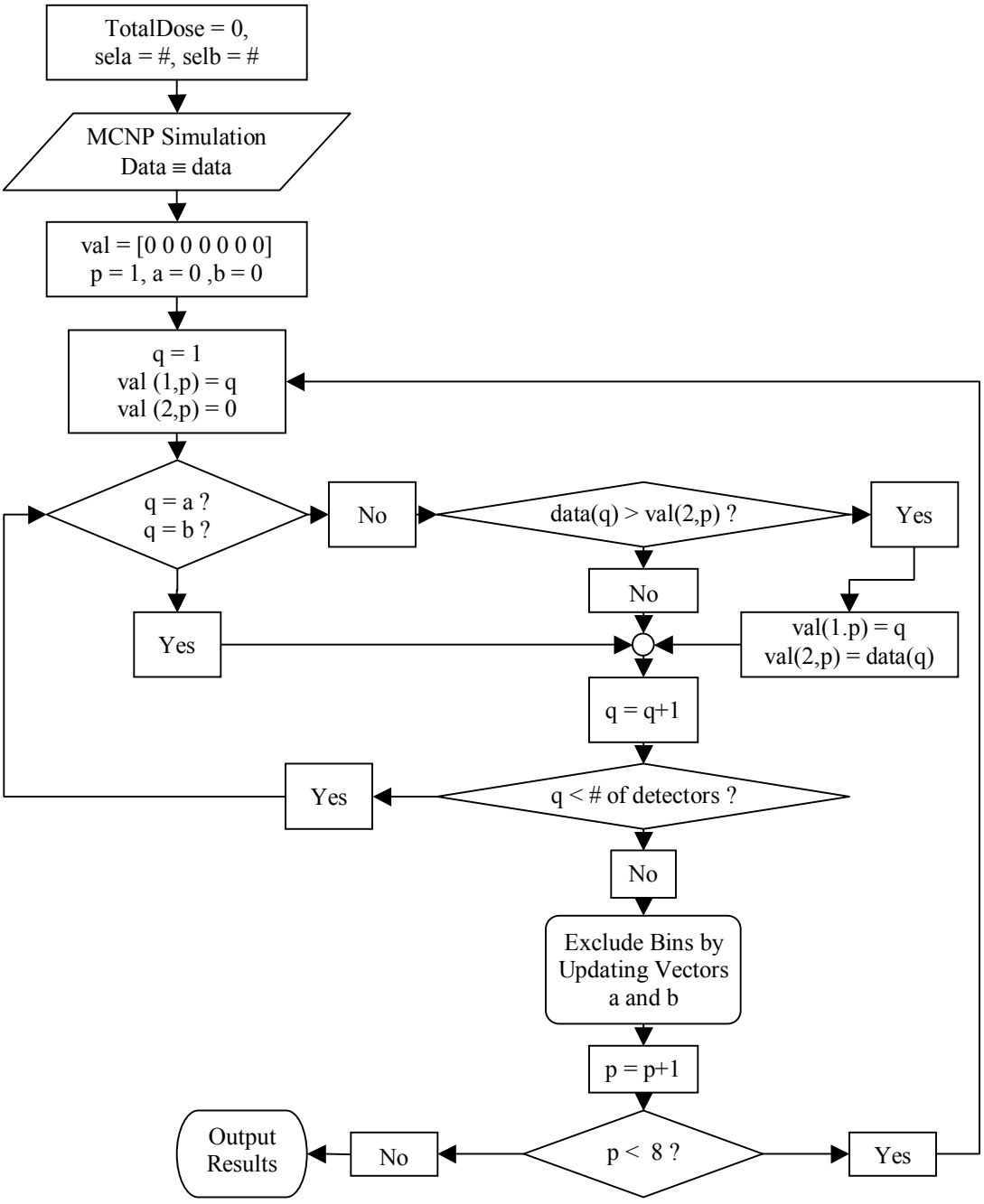

Figure C.1: Flow diagram for Method 1 Matlab Algorithm

Method 1 Matlab Algorithm Example

```
% FILE NAME: c3.o
% SHIFT:    x = 0    y = 0

%Penalty weighting for the flagged values for the critical structure
wt=1;
%Number of angles to discount to the left and right of the selected angle
sela=5;
%Number of angles to discount to the left and right of the opposing angle
selb=0;
%Column of beam angles
angles=[0:7.5:352.5]; angles=transpose(angles);

% MCNP DATA
% Column 1 is dose from source to detector
% Column 2 is dose from source through critical structure to detector
data=[5.87766E-05    2.12138E-05
5.88423E-05          2.23863E-05
5.83017E-05          2.40176E-05
5.64432E-05          2.43540E-05
5.48989E-05          2.34559E-05
5.21127E-05          2.14840E-05
5.12409E-05          1.89958E-05
5.20916E-05          1.67585E-05
5.45308E-05          1.62232E-05
5.65801E-05          1.52572E-05
5.78542E-05          1.43756E-05
5.88338E-05          1.35337E-05
5.86951E-05          1.24221E-05
5.85775E-05          1.19111E-05
5.79140E-05          1.11877E-05
5.67692E-05          1.04385E-05
5.46766E-05          9.63150E-06
5.21003E-05          8.40942E-06
5.08704E-05          7.53146E-06
5.23749E-05          6.95810E-06
5.51502E-05          6.86923E-06
5.68057E-05          6.81878E-06
5.81422E-05          6.70841E-06
5.84256E-05          6.25561E-06
5.86455E-05          6.29074E-06
5.87507E-05          6.50186E-06
5.78734E-05          6.56523E-06
5.67944E-05          6.83996E-06
5.47361E-05          6.92814E-06
5.23202E-05          6.89692E-06
5.10549E-05          7.54961E-06
5.23760E-05          8.56991E-06
5.45559E-05          9.65143E-06
5.67840E-05          1.04180E-05
5.82641E-05          1.12925E-05
5.89380E-05          1.19755E-05
5.88123E-05          1.22921E-05
5.86148E-05          1.34668E-05
5.79729E-05          1.43458E-05
5.64360E-05          1.54710E-05
5.45498E-05          1.62527E-05
5.23865E-05          1.68751E-05
5.07867E-05          1.87363E-05
5.22366E-05          2.14228E-05
5.47991E-05          2.35244E-05
5.64137E-05          2.41676E-05
5.78739E-05          2.37660E-05
5.86118E-05          2.22642E-05];

% Creates another column of detector values that will be used to determine
%       the best angles.
% Is a combination of the the dose from the tumor to the detector with a
```

```
%       penalty for passing through the critical structure.
g=size(data);
h=g(2);
for j=1:h-1
   if j==1
      for i=1:g(1)
         data(i,h+1)=data(i,1)-wt(j)*data(i,j+1);
      end
   else
      for i=1:g(1)
         data(i,h+1)=data(i,h+1)-wt(j)*data(i,j+1);
      end
   end
end
% Initialize variables to run the program
% Val matrix contains detector number and corresponding detector value
val=[0 0 0 0 0 0 0];
% p represents the selection of the pth detector number
p=1;
% a represents detectors that cannot be selected because they are two close
%       to one of the bins already selected
a=0;
% b represents detectors that cannot be selected because they oppose
%       detectors already selected
b=0;
% tem is a temporary file composed of the detector values
tem=data(:,h+1);

% This is the beginning of the optimization routine
% A while loop is used to select 7 detectors
while p<8
   % q represents the detector being analyzed
   q=1;
   % This sets val(1,p) equal to q
   val(1,p)=q;
   % This sets val(2,p) equal to detector value of detector q
   val(2,p)=0;

   % A while loop is used to exhaustively analyze all 48 detectors, with
   %       certain detectors not being allowed according to rules below
   while q<g(1)
      % If the current detector being analyzed is not on the list a of
      %       forbidden detectors, then the progam will procede else the
      %       next bin will be analyzed
      if q~=a
         if q~=b
         % If the value of the detector (q) currently be analyzed is
         %       greater than the the detector with the highest detector
         %       value that has been analyzed then the detector (q) will
         %       replace the previous highest detector value and
         %       detector nubmer.  Otherwise, the next detector will be
         %       analyzed.
            if tem(q) > val(2,p)
               val(2,p)=data(q,h+1);
               val(1,p)=q;
               q=q+1;
               1;
            else
               q=q+1;
               2;
            end
         else
            q=q+1;
         end
      else
         q=q+1;
      end
   end

   % This begins the rules for elimination of detectors that are near
```

```
    %       detectors that have been selected.

    % In this section, once a detector has been selected, the two closest
    %       detectors on either side of the selected detector are excluded
    %       from selection by placing them on detector list a.
    % The list has been made additive, so as each detector is selected the
    %       excluded detectors will be added to this list.
    t=(p-1)*(sela*2+1)+1;
    s=1;
    for n=t:t+(sela*2)
       a(n)=val(1,p)-(sela+1)+s;
       if a(n)<1
          a(n)=a(n)+g(1);
       elseif a(n)>g(1)
          a(n)=a(n)-g(1);
       end
       s=s+1;
    end
    % In this section, once a detector has been selected, the closest
    %       detectors on either side of the detector opposing the selected
    %       detector are excluded from selection by placing them on
    %       detector list b.
    u=(p-1)*(selb*2+1)+1;
    w=1;
    for n=u:u+(selb*2)
       k=val(1,p)+g(1)/2;
       if k>g(1)
          b(n)=k-g(1)-(selb+1)+w;
          if b(n)<1
             b(n)=b(n)+g(1);
          elseif b(n)>g(1)
             b(n)=b(n)-g(1);
          end
       else
          b(n)=k-(selb+1)+w;
          if b(n)<1
             b(n)=b(n)+g(1);
          elseif b(n)>g(1)
             b(n)=b(n)-g(1);
          end
       end
       w=w+1;
    end
    p=p+1;
end

% BinsA are the a list of excluded detectors.
BinsA=a
% BinsB are the b list of excluded detectors.
BinsB=b
% Dose is the detector value of the selected detectors.
Dose=val(2,:)
TotalDose=sum(Dose)
% Detectors is the list of selected detectors
Detectors=val(1,:)
```

APPENDIX D

Method 2 Matlab Algorithm

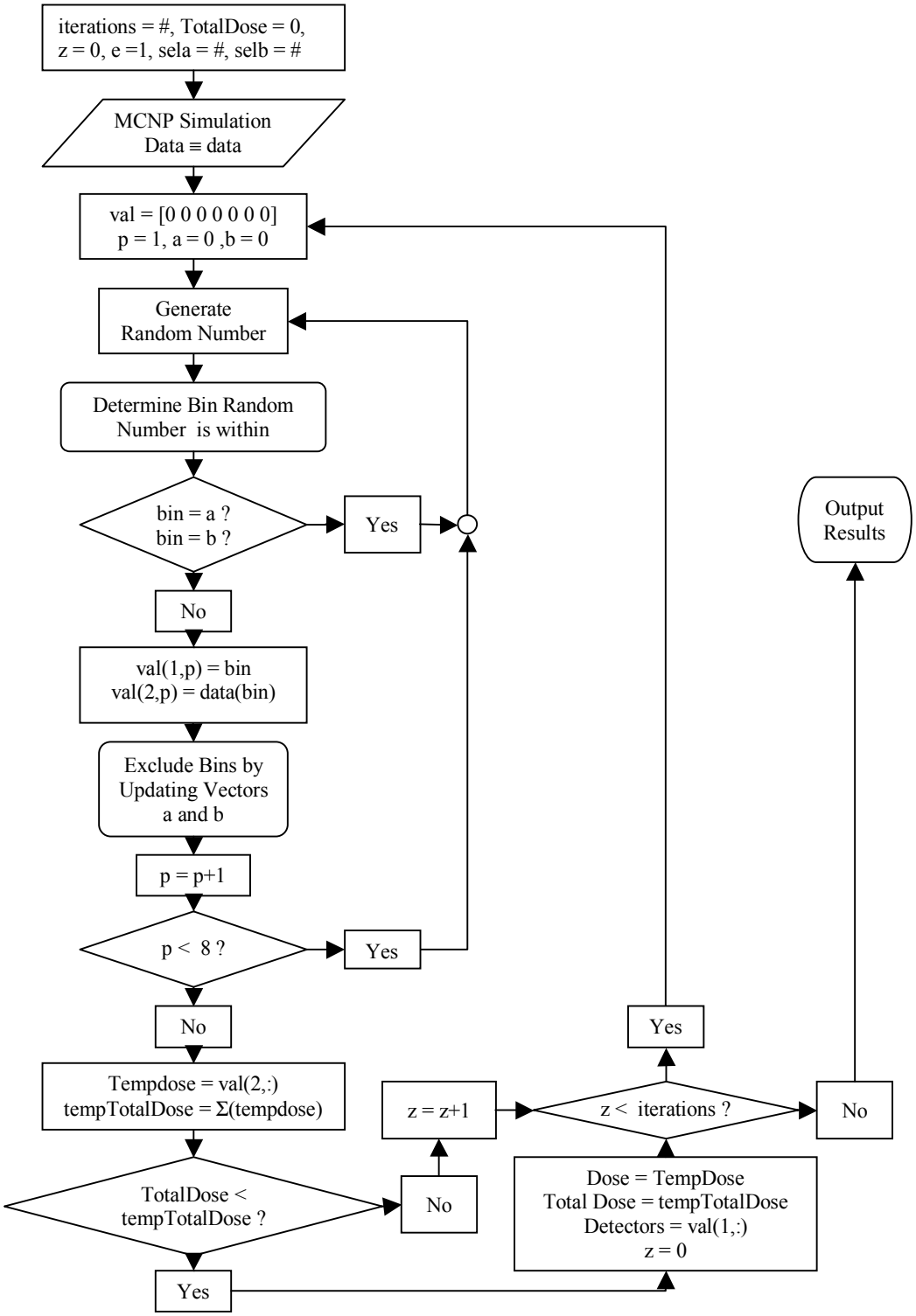

Figure D.1: Flow diagram for Method 2 Matlab Algorithm

Method 2 Matlab Algorithm Example

```
% FILE NAME: c3.o
% SHIFT:    x = 0    y = 0

%%%%%%%%%%%%%%%%%%%%%%%%%%%Changeable Parameters%%%%%%%%%%%%%%%%%%%%%%%%%%%%%%%%%
%Penalty weighting for the flagged values for the critical structure
wt(1)=1;
wt(2)=1;
%Number of angles to discount to the left and right of the selected angle
sela=3;
%Number of angles to discount to the left and right of the opposing angle
selb=2;
%Number of iterations
iterations=1500000;
%%%%%%%%%%%%%%%%%%%%%%%%%%%%%%%%%%%%%%%%%%%%%%%%%%%%%%%%%%%%%%%%%%%%%%%%%%%%%%%%%%%%%%%%%

%Column of beam angles
angles=[0:7.5:352.5]; angles=transpose(angles);


% MCNP DATA
% Column 1 is dose from source to detector
% Column 2 is dose from source through critical structure to detector
data=[5.87766E-05         2.12138E-05
5.88423E-05              2.23863E-05
5.83017E-05              2.40176E-05
5.64432E-05              2.43540E-05
5.48989E-05              2.34559E-05
5.21127E-05              2.14840E-05
5.12409E-05              1.89958E-05
5.20916E-05              1.67585E-05
5.45308E-05              1.62232E-05
5.65801E-05              1.52572E-05
5.78542E-05              1.43756E-05
5.88338E-05              1.35337E-05
5.86951E-05              1.24221E-05
5.85775E-05              1.19111E-05
5.79140E-05              1.11877E-05
5.67692E-05              1.04385E-05
5.46766E-05              9.63150E-06
5.21003E-05              8.40942E-06
5.08704E-05              7.53146E-06
5.23749E-05              6.95810E-06
5.51502E-05              6.86923E-06
5.68057E-05              6.81878E-06
5.81422E-05              6.70841E-06
5.84256E-05              6.25561E-06
5.86455E-05              6.29074E-06
5.87507E-05              6.50186E-06
5.78734E-05              6.56523E-06
5.67944E-05              6.83996E-06
5.47361E-05              6.92814E-06
5.23202E-05              6.89692E-06
5.10549E-05              7.54961E-06
5.23760E-05              8.56991E-06
5.45559E-05              9.65143E-06
5.67840E-05              1.04180E-05
5.82641E-05              1.12925E-05
5.89380E-05              1.19755E-05
5.88123E-05              1.22921E-05
5.86148E-05              1.34668E-05
5.79729E-05              1.43458E-05
5.64360E-05              1.54710E-05
5.45498E-05              1.62527E-05
5.23865E-05              1.68751E-05
5.07867E-05              1.87363E-05
5.22366E-05              2.14228E-05
5.47991E-05              2.35244E-05
5.64137E-05              2.41676E-05
5.78739E-05              2.37660E-05
5.86118E-05              2.22642E-05];

% Creates another column of detector values that will be used to determine
%       the best angles.
% Is a combination of the the dose from the tumor to the detector with a
%       penalty for passing through the critical structure.
% Takes infomation from 'data' (which includes detector dose and dose from
%       critical structures) and creates a column of detector valuesusing
```

```
%       the penalty weight for each of the critical structures that is then
%       used to determine the best beam angles.
g=size(data);
h=g(2);
bins=[1/g(1):1/g(1):1]
for j=1:h-1
   if j==1
      for i=1:g(1)
         data(i,h+1)=data(i,1)-wt(j)*data(i,j+1);
      end
   else
      for i=1:g(1)
         data(i,h+1)=data(i,h+1)-wt(j)*data(i,j+1);
      end
   end
end

% Initialize variables to run the program
% Val matrix contains detector number and corresponding detector value
val=[0 0 0 0 0 0 0];
% p represents the selection of the pth detector number
p=1;
% a represents detectors that cannot be selected because they are two close
%       to one of the bins already selected
a=0;
% b represents detectors that cannot be selected because they oppose
%       detectors already selected
b=0;
% tem is a temporary file composed of the detector values
tem=data(:,h+1);
% Initializes TotalDose variable
TotalDose=0;
% Initializes the variable z (number of histories to recheck solution)
z=0;
% Initializes the variable e (keeps track of all the solutions)
e=1;

% This algorith work by using a random number generator to select the bin.
% If the bin is disallowed according to the rules set forward here then
% another bin is selected using the random number generator.  Once all the
% beam angles have been selected then the Total dose delivered from those
% angles is calculated.  The program then continues to run at least 50
% times or until a group of beam angles are selected with a higher total
% dose.  Then the program restarts an continues to run at least another 50
% times.
while z<iterations
   brk=1;
   while p<8
      % This randomnly selects bins.
      r=rand;
      q=0;
      for i=1:g(1)
         if r<bins(i)
            q=q+1;
         end
      end

      if q~=a
         if q~=b
            % This sets val(1,p) equal to q
            val(1,p)=q;
            % This sets val(2,p) equal to detector value of detector q
            val(2,p)=data(q,h+1);

            % Below are the rules for excluding certain angles

            % In this section, once a detector has been selected, the two closest
            %       detectors on either side of the selected detector are excluded
            %       from selection by placing them on detector list a.
            % The list has been made additive, so as each detector is selected the
            %       excluded detectors will be added to this list.
            t=(p-1)*(sela*2+1)+1;
            s=1;
            for n=t:t+(sela*2)
               a(n)=val(1,p)-(sela+1)+s;
               if a(n)<1
                  a(n)=a(n)+g(1);
               elseif a(n)>g(1)
                  a(n)=a(n)-g(1);
               end
```

```
            s=s+1;
        end
        % In this section, once a detector has been selected, the closest
        %       detectors on either side of the detector opposing the selected
        %       detector are excluded from selection by placing them on
        %       detector list b.
        u=(p-1)*(selb*2+1)+1;
        w=1;
        for n=u:u+(selb*2)
            k=val(1,p)+g(1)/2;
            if k>g(1)
                b(n)=k-g(1)-(selb+1)+w;
                if b(n)<1
                    b(n)=b(n)+g(1);
                elseif b(n)>g(1)
                    b(n)=b(n)-g(1);
                end
            else
                b(n)=k-(selb+1)+w;
                if b(n)<1
                    b(n)=b(n)+g(1);
                elseif b(n)>g(1)
                    b(n)=b(n)-g(1);
                end
            end
            w=w+1;
        end
        p=p+1;
      end
    end
    brk=brk+1;
    if brk > 100
      break
    end
  end
  % Temporary total dose calculation
  tempDose=val(2,:);
  tempTotalDose=sum(tempDose);
  if TotalDose<tempTotalDose
    HistoryDetector(e,:)=val(1,:)
    HistoryTotalDose(e)=tempTotalDose
    e=e+1;
    Dose=tempDose;
    TotalDose=tempTotalDose;
    BinsA=a;
    BinsB=b;
    Detectors=val(1,:);
    z=0;
  else
    z=z+1;
  end
  % This reinitializes all the parameters for the next calculation
  val=[0 0 0 0 0 0 0];
  p=1;
  a=0;
  b=0;
end

HistoryDetector
HistoryTotalDose
% BinsA are the a list of excluded detectors.
BinsA
% BinsB are the b list of excluded detectors.
BinsB
% Dose is the detector value of the selected detectors.
Dose
TotalDose
% Detectors is the list of selected detectors
Detectors
```

APPENDIX E

MCNP Simulation Results

Table E.1: MCNP Simulation Data for Square Geometry

Detector	Angle	Target Dose Value	C.S. Dose Value	Combined Dose Value
1	0.0	5.89578E-05	2.06493E-05	3.83085E-05
2	7.5	5.87552E-05	2.23157E-05	3.64395E-05
3	15.0	5.84919E-05	2.38855E-05	3.46064E-05
4	22.5	5.66288E-05	2.21198E-05	3.45090E-05
5	30.0	5.50341E-05	1.90366E-05	3.59975E-05
6	37.5	5.19807E-05	1.45097E-05	3.74710E-05
7	45.0	5.10842E-05	1.10215E-05	4.00627E-05
8	52.5	5.20487E-05	7.79526E-06	4.42534E-05
9	60.0	5.47971E-05	6.01542E-06	4.87817E-05
10	67.5	5.66984E-05	4.30648E-06	5.23919E-05
11	75.0	5.78603E-05	2.90570E-06	5.49546E-05
12	82.5	5.87265E-05	1.50563E-06	5.72209E-05
13	90.0	5.85254E-05	6.26668E-07	5.78987E-05
14	97.5	5.85398E-05	4.60382E-07	5.80794E-05
15	105.0	5.79800E-05	3.68239E-07	5.76118E-05
16	112.5	5.67611E-05	2.95773E-07	5.64653E-05
17	120.0	5.47681E-05	2.48355E-07	5.45197E-05
18	127.5	5.22063E-05	1.96883E-07	5.20094E-05
19	135.0	5.07302E-05	1.43144E-07	5.05871E-05
20	142.5	5.24882E-05	1.19540E-07	5.23687E-05
21	150.0	5.52820E-05	1.01569E-07	5.51804E-05
22	157.5	5.68468E-05	9.31729E-08	5.67536E-05
23	165.0	5.81597E-05	8.65992E-08	5.80731E-05
24	172.5	5.85160E-05	8.38133E-08	5.84322E-05
25	180.0	5.87444E-05	9.07638E-08	5.86536E-05
26	187.5	5.86245E-05	8.71346E-08	5.85374E-05
27	195.0	5.78890E-05	8.79501E-08	5.78010E-05
28	202.5	5.67124E-05	9.14473E-08	5.66210E-05
29	210.0	5.46055E-05	9.90282E-08	5.45065E-05
30	217.5	5.23424E-05	1.15512E-07	5.22269E-05
31	225.0	5.10622E-05	1.48026E-07	5.09142E-05
32	232.5	5.25256E-05	1.84249E-07	5.23414E-05
33	240.0	5.45593E-05	2.34949E-07	5.43244E-05
34	247.5	5.67755E-05	3.10362E-07	5.64651E-05
35	255.0	5.81924E-05	3.69184E-07	5.78232E-05
36	262.5	5.88376E-05	4.78237E-07	5.83594E-05
37	270.0	5.89873E-05	6.05242E-07	5.83821E-05
38	277.5	5.86841E-05	1.50674E-06	5.71774E-05
39	285.0	5.80235E-05	2.88604E-06	5.51375E-05
40	292.5	5.62766E-05	4.35616E-06	5.19204E-05
41	300.0	5.47596E-05	5.99249E-06	4.87671E-05
42	307.5	5.22078E-05	7.84121E-06	4.43666E-05
43	315.0	5.07939E-05	1.09021E-05	3.98918E-05
44	322.5	5.23261E-05	1.46778E-05	3.76483E-05
45	330.0	5.45055E-05	1.88896E-05	3.56159E-05
46	337.5	5.65277E-05	2.19142E-05	3.46135E-05
47	345.0	5.77789E-05	2.33667E-05	3.44122E-05
48	352.5	5.88251E-05	2.23274E-05	3.64977E-05

Table E.2: Rotated MCNP Simulation Data for Square Geometry

Detector	Angle	Target Dose Value	C.S. Dose Value	Combined Dose Value
1	3.75	5.89851E-05	2.13305E-05	3.76546E-05
2	11.25	5.88482E-05	2.34895E-05	3.53587E-05
3	18.75	5.72930E-05	2.28123E-05	3.44807E-05
4	26.25	5.61146E-05	2.03918E-05	3.57228E-05
5	33.75	5.31342E-05	1.59224E-05	3.72118E-05
6	41.25	5.13971E-05	1.22885E-05	3.91086E-05
7	48.75	5.11217E-05	8.69116E-06	4.24305E-05
8	56.25	5.36600E-05	6.33280E-06	4.73272E-05
9	63.75	5.57682E-05	4.46517E-06	5.13030E-05
10	71.25	5.73576E-05	2.97638E-06	5.43812E-05
11	78.75	5.83845E-05	1.48063E-06	5.69039E-05
12	86.25	5.84565E-05	6.07631E-07	5.78489E-05
13	93.75	5.87186E-05	4.56212E-07	5.82624E-05
14	101.25	5.83064E-05	3.61077E-07	5.79453E-05
15	108.75	5.74147E-05	2.91693E-07	5.71230E-05
16	116.25	5.58367E-05	2.44794E-07	5.55919E-05
17	123.75	5.34772E-05	2.03651E-07	5.32735E-05
18	131.25	5.11032E-05	1.48461E-07	5.09547E-05
19	138.75	5.16711E-05	1.16623E-07	5.15545E-05
20	146.25	5.41452E-05	9.81081E-08	5.40471E-05
21	153.75	5.59771E-05	8.87856E-08	5.58883E-05
22	161.25	5.75637E-05	8.21444E-08	5.74816E-05
23	168.75	5.82427E-05	7.55131E-08	5.81672E-05
24	176.25	5.86434E-05	7.90409E-08	5.85644E-05
25	183.75	5.88049E-05	7.68946E-08	5.87280E-05
26	191.25	5.82381E-05	7.76974E-08	5.81604E-05
27	198.75	5.74320E-05	8.15827E-08	5.73504E-05
28	206.25	5.56601E-05	8.08352E-08	5.55793E-05
29	213.75	5.35135E-05	1.00306E-07	5.34132E-05
30	221.25	5.13600E-05	1.21597E-07	5.12384E-05
31	228.75	5.16160E-05	1.59495E-07	5.14565E-05
32	236.25	5.33548E-05	2.00580E-07	5.31542E-05
33	243.75	5.59441E-05	2.57708E-07	5.56864E-05
34	251.25	5.76201E-05	3.09103E-07	5.73110E-05
35	258.75	5.86335E-05	4.12426E-07	5.82211E-05
36	266.25	5.89049E-05	4.89435E-07	5.84155E-05
37	273.75	5.89013E-05	8.58727E-07	5.80426E-05
38	281.25	5.84269E-05	1.92447E-06	5.65024E-05
39	288.75	5.71370E-05	3.27849E-06	5.38585E-05
40	296.25	5.58517E-05	4.74426E-06	5.11074E-05
41	303.75	5.33822E-05	6.32051E-06	4.70617E-05
42	311.25	5.11076E-05	8.74173E-06	4.23659E-05
43	318.75	5.14039E-05	1.22754E-05	3.91285E-05
44	326.25	5.33352E-05	1.66380E-05	3.66972E-05
45	333.75	5.58138E-05	2.06077E-05	3.52061E-05
46	341.25	5.73284E-05	2.30641E-05	3.42643E-05
47	348.75	5.85387E-05	2.31578E-05	3.53809E-05
48	356.25	5.88635E-05	2.11405E-05	3.77230E-05

Table E.3: MCNP Simulation Data for L-Shaped Geometry

Detector	Angle	Target Dose Value	C.S. Dose Value	Combined Dose Value
1	0.0	5.87342E-05	2.96594E-05	2.90748E-05
2	7.5	5.88737E-05	3.24596E-05	2.64141E-05
3	15.0	5.84819E-05	3.51636E-05	2.33183E-05
4	22.5	5.63265E-05	3.67544E-05	1.95721E-05
5	30.0	5.49024E-05	3.80862E-05	1.68162E-05
6	37.5	5.21145E-05	3.74972E-05	1.46173E-05
7	45.0	5.12769E-05	3.70100E-05	1.42669E-05
8	52.5	5.19113E-05	3.70983E-05	1.48130E-05
9	60.0	5.46543E-05	3.81003E-05	1.65540E-05
10	67.5	5.64720E-05	3.66460E-05	1.98260E-05
11	75.0	5.77322E-05	3.46344E-05	2.30978E-05
12	82.5	5.86656E-05	3.23567E-05	2.63089E-05
13	90.0	5.84340E-05	2.94220E-05	2.90120E-05
14	97.5	5.85998E-05	2.84256E-05	3.01742E-05
15	105.0	5.80706E-05	2.71844E-05	3.08862E-05
16	112.5	5.66472E-05	2.52882E-05	3.13590E-05
17	120.0	5.46794E-05	2.34005E-05	3.12789E-05
18	127.5	5.21736E-05	2.08204E-05	3.13532E-05
19	135.0	5.07861E-05	1.83693E-05	3.24168E-05
20	142.5	5.21444E-05	1.65411E-05	3.56033E-05
21	150.0	5.50462E-05	1.61546E-05	3.88916E-05
22	157.5	5.67702E-05	1.59158E-05	4.08544E-05
23	165.0	5.79102E-05	1.50678E-05	4.28424E-05
24	172.5	5.84156E-05	1.42721E-05	4.41435E-05
25	180.0	5.87048E-05	1.39399E-05	4.47649E-05
26	187.5	5.87088E-05	1.35113E-05	4.51975E-05
27	195.0	5.78662E-05	1.33425E-05	4.45237E-05
28	202.5	5.66087E-05	1.26152E-05	4.39935E-05
29	210.0	5.45890E-05	1.20869E-05	4.25021E-05
30	217.5	5.23611E-05	1.14749E-05	4.08862E-05
31	225.0	5.10920E-05	1.09274E-05	4.01646E-05
32	232.5	5.24772E-05	1.15120E-05	4.09652E-05
33	240.0	5.46583E-05	1.22194E-05	4.24389E-05
34	247.5	5.66683E-05	1.26313E-05	4.40370E-05
35	255.0	5.80006E-05	1.31227E-05	4.48779E-05
36	262.5	5.87813E-05	1.33964E-05	4.53849E-05
37	270.0	5.88859E-05	1.36931E-05	4.51928E-05
38	277.5	5.85576E-05	1.44783E-05	4.40793E-05
39	285.0	5.80256E-05	1.50520E-05	4.29736E-05
40	292.5	5.62782E-05	1.55881E-05	4.06901E-05
41	300.0	5.45958E-05	1.59233E-05	3.86725E-05
42	307.5	5.21413E-05	1.64106E-05	3.57307E-05
43	315.0	5.09273E-05	1.84512E-05	3.24761E-05
44	322.5	5.22626E-05	2.08734E-05	3.13892E-05
45	330.0	5.47418E-05	2.33947E-05	3.13471E-05
46	337.5	5.65166E-05	2.53311E-05	3.11855E-05
47	345.0	5.79024E-05	2.68960E-05	3.10064E-05
48	352.5	5.87957E-05	2.86065E-05	3.01892E-05

Table E.4: Rotated MCNP Simulation Data for L-Shaped Geometry

Detector	Angle	Target Dose Value	C.S. Dose Value	Combined Dose Value
1	3.75	5.90077E-05	3.04479E-05	2.85598E-05
2	11.25	5.89479E-05	3.33397E-05	2.56082E-05
3	18.75	5.69946E-05	3.52696E-05	2.17250E-05
4	26.25	5.61159E-05	3.74109E-05	1.87050E-05
5	33.75	5.33580E-05	3.75326E-05	1.58254E-05
6	41.25	5.16526E-05	3.67665E-05	1.48861E-05
7	48.75	5.10668E-05	3.61565E-05	1.49103E-05
8	56.25	5.35586E-05	3.76142E-05	1.59444E-05
9	63.75	5.55267E-05	3.68341E-05	1.86926E-05
10	71.25	5.70772E-05	3.51726E-05	2.19046E-05
11	78.75	5.82885E-05	3.32180E-05	2.50705E-05
12	86.25	5.83724E-05	3.02596E-05	2.81128E-05
13	93.75	5.87447E-05	2.87715E-05	2.99732E-05
14	101.25	5.82484E-05	2.75921E-05	3.06563E-05
15	108.75	5.73324E-05	2.60051E-05	3.13273E-05
16	116.25	5.56989E-05	2.42685E-05	3.14304E-05
17	123.75	5.33983E-05	2.18279E-05	3.15704E-05
18	131.25	5.11143E-05	1.93815E-05	3.17328E-05
19	138.75	5.14221E-05	1.70919E-05	3.43302E-05
20	146.25	5.38569E-05	1.61477E-05	3.77092E-05
21	153.75	5.58131E-05	1.59436E-05	3.98695E-05
22	161.25	5.73770E-05	1.52552E-05	4.21218E-05
23	168.75	5.81676E-05	1.45625E-05	4.36051E-05
24	176.25	5.86357E-05	1.42307E-05	4.44050E-05
25	183.75	5.88561E-05	1.35979E-05	4.52582E-05
26	191.25	5.82324E-05	1.35151E-05	4.47173E-05
27	198.75	5.73858E-05	1.28589E-05	4.45269E-05
28	206.25	5.56710E-05	1.23567E-05	4.33143E-05
29	213.75	5.35496E-05	1.18401E-05	4.17095E-05
30	221.25	5.14450E-05	1.11156E-05	4.03294E-05
31	228.75	5.16603E-05	1.11612E-05	4.04991E-05
32	236.25	5.33628E-05	1.18331E-05	4.15297E-05
33	243.75	5.58432E-05	1.24077E-05	4.34355E-05
34	251.25	5.74740E-05	1.28981E-05	4.45759E-05
35	258.75	5.85986E-05	1.32795E-05	4.53191E-05
36	266.25	5.88354E-05	1.35404E-05	4.52950E-05
37	273.75	5.87519E-05	1.37941E-05	4.49578E-05
38	281.25	5.84818E-05	1.44120E-05	4.40698E-05
39	288.75	5.70915E-05	1.50562E-05	4.20353E-05
40	296.25	5.56218E-05	1.55856E-05	4.00362E-05
41	303.75	5.33558E-05	1.59966E-05	3.73592E-05
42	311.25	5.13222E-05	1.71867E-05	3.41355E-05
43	318.75	5.13092E-05	1.94041E-05	3.19051E-05
44	326.25	5.35927E-05	2.20118E-05	3.15809E-05
45	333.75	5.55603E-05	2.39582E-05	3.16021E-05
46	341.25	5.73851E-05	2.57014E-05	3.16837E-05
47	348.75	5.84037E-05	2.74251E-05	3.09786E-05
48	356.25	5.86845E-05	2.84245E-05	3.02600E-05

Table E.5: MCNP Simulation Data for U-Shaped Geometry

Detector	Angle	Target Dose Value	C.S. Dose Value	Combined Dose Value
1	0.0	5.87766E-05	2.12138E-05	3.75628E-05
2	7.5	5.88423E-05	2.23863E-05	3.64560E-05
3	15.0	5.83017E-05	2.40176E-05	3.42841E-05
4	22.5	5.64432E-05	2.43540E-05	3.20892E-05
5	30.0	5.48989E-05	2.34559E-05	3.14430E-05
6	37.5	5.21127E-05	2.14840E-05	3.06287E-05
7	45.0	5.12409E-05	1.89958E-05	3.22451E-05
8	52.5	5.20916E-05	1.67585E-05	3.53331E-05
9	60.0	5.45308E-05	1.62232E-05	3.83076E-05
10	67.5	5.65801E-05	1.52572E-05	4.13229E-05
11	75.0	5.78542E-05	1.43756E-05	4.34786E-05
12	82.5	5.88338E-05	1.35337E-05	4.53001E-05
13	90.0	5.86951E-05	1.24221E-05	4.62730E-05
14	97.5	5.85775E-05	1.19111E-05	4.66664E-05
15	105.0	5.79140E-05	1.11877E-05	4.67263E-05
16	112.5	5.67692E-05	1.04385E-05	4.63307E-05
17	120.0	5.46766E-05	9.63150E-06	4.50451E-05
18	127.5	5.21003E-05	8.40942E-06	4.36909E-05
19	135.0	5.08704E-05	7.53146E-06	4.33389E-05
20	142.5	5.23749E-05	6.95810E-06	4.54168E-05
21	150.0	5.51502E-05	6.86923E-06	4.82810E-05
22	157.5	5.68057E-05	6.81878E-06	4.99869E-05
23	165.0	5.81422E-05	6.70841E-06	5.14338E-05
24	172.5	5.84256E-05	6.25561E-06	5.21700E-05
25	180.0	5.86455E-05	6.29074E-06	5.23548E-05
26	187.5	5.87507E-05	6.50186E-06	5.22488E-05
27	195.0	5.78734E-05	6.56523E-06	5.13082E-05
28	202.5	5.67944E-05	6.83996E-06	4.99544E-05
29	210.0	5.47361E-05	6.92814E-06	4.78080E-05
30	217.5	5.23202E-05	6.89692E-06	4.54233E-05
31	225.0	5.10549E-05	7.54961E-06	4.35053E-05
32	232.5	5.23760E-05	8.56991E-06	4.38061E-05
33	240.0	5.45559E-05	9.65143E-06	4.49045E-05
34	247.5	5.67840E-05	1.04180E-05	4.63660E-05
35	255.0	5.82641E-05	1.12925E-05	4.69716E-05
36	262.5	5.89380E-05	1.19755E-05	4.69625E-05
37	270.0	5.88123E-05	1.22921E-05	4.65202E-05
38	277.5	5.86148E-05	1.34668E-05	4.51480E-05
39	285.0	5.79729E-05	1.43458E-05	4.36271E-05
40	292.5	5.64360E-05	1.54710E-05	4.09650E-05
41	300.0	5.45498E-05	1.62527E-05	3.82971E-05
42	307.5	5.23865E-05	1.68751E-05	3.55114E-05
43	315.0	5.07867E-05	1.87363E-05	3.20504E-05
44	322.5	5.22366E-05	2.14228E-05	3.08138E-05
45	330.0	5.47991E-05	2.35244E-05	3.12747E-05
46	337.5	5.64137E-05	2.41676E-05	3.22461E-05
47	345.0	5.78739E-05	2.37660E-05	3.41079E-05
48	352.5	5.86118E-05	2.22642E-05	3.63476E-05

Table E.6: MCNP Simulation Data for U-Shaped Geometry

Detector	Angle	Target Dose Value	C.S. Dose Value	Combined Dose Value
1	3.75	5.89914E-05	2.16214E-05	3.73700E-05
2	11.25	5.87646E-05	2.34400E-05	3.53246E-05
3	18.75	5.71411E-05	2.43124E-05	3.28287E-05
4	26.25	5.60605E-05	2.39533E-05	3.21072E-05
5	33.75	5.32835E-05	2.24213E-05	3.08622E-05
6	41.25	5.15130E-05	2.00381E-05	3.14749E-05
7	48.75	5.11569E-05	1.74012E-05	3.37557E-05
8	56.25	5.34003E-05	1.64979E-05	3.69024E-05
9	63.75	5.57600E-05	1.57493E-05	4.00107E-05
10	71.25	5.72209E-05	1.49132E-05	4.23077E-05
11	78.75	5.83840E-05	1.42058E-05	4.41782E-05
12	86.25	5.84419E-05	1.27258E-05	4.57161E-05
13	93.75	5.88133E-05	1.22119E-05	4.66014E-05
14	101.25	5.82650E-05	1.14273E-05	4.68377E-05
15	108.75	5.73448E-05	1.06630E-05	4.66818E-05
16	116.25	5.56966E-05	9.97167E-06	4.57249E-05
17	123.75	5.33830E-05	8.73020E-06	4.46528E-05
18	131.25	5.11155E-05	7.87211E-06	4.32434E-05
19	138.75	5.14730E-05	6.89561E-06	4.45774E-05
20	146.25	5.38834E-05	6.73631E-06	4.71471E-05
21	153.75	5.58478E-05	6.74200E-06	4.91058E-05
22	161.25	5.75257E-05	6.70552E-06	5.08202E-05
23	168.75	5.80993E-05	6.34164E-06	5.17577E-05
24	176.25	5.85249E-05	6.34491E-06	5.21800E-05
25	183.75	5.88895E-05	6.41937E-06	5.24701E-05
26	191.25	5.83086E-05	6.56268E-06	5.17459E-05
27	198.75	5.75266E-05	6.84244E-06	5.06842E-05
28	206.25	5.57866E-05	7.07222E-06	4.87144E-05
29	213.75	5.34934E-05	7.07356E-06	4.64198E-05
30	221.25	5.12683E-05	7.33599E-06	4.39323E-05
31	228.75	5.14502E-05	8.19525E-06	4.32550E-05
32	236.25	5.33826E-05	9.28769E-06	4.40949E-05
33	243.75	5.59690E-05	1.00811E-05	4.58879E-05
34	251.25	5.76212E-05	1.09779E-05	4.66433E-05
35	258.75	5.87274E-05	1.16812E-05	4.70462E-05
36	266.25	5.88202E-05	1.20870E-05	4.67332E-05
37	273.75	5.87723E-05	1.25753E-05	4.61970E-05
38	281.25	5.83227E-05	1.36421E-05	4.46806E-05
39	288.75	5.72042E-05	1.48489E-05	4.23553E-05
40	296.25	5.56483E-05	1.57576E-05	3.98907E-05
41	303.75	5.34180E-05	1.63237E-05	3.70943E-05
42	311.25	5.10647E-05	1.75624E-05	3.35023E-05
43	318.75	5.12330E-05	2.02729E-05	3.09601E-05
44	326.25	5.34987E-05	2.26872E-05	3.08115E-05
45	333.75	5.57631E-05	2.39852E-05	3.17779E-05
46	341.25	5.73879E-05	2.40583E-05	3.33296E-05
47	348.75	5.82628E-05	2.28185E-05	3.54443E-05
48	356.25	5.86905E-05	2.14112E-05	3.72793E-05

APPENDIX F

Method 1 cDVHs

The red data points represent the cDVH of the target volume, the orange data points represent the cDVH of the critical structure, and the green data points represent the cDVH of the normal tissue in the following figures. Furthermore, below the cDVHs are the maximum dose, minimum dose, and mean dose for the three structures.

F.1 Square Target Geometry

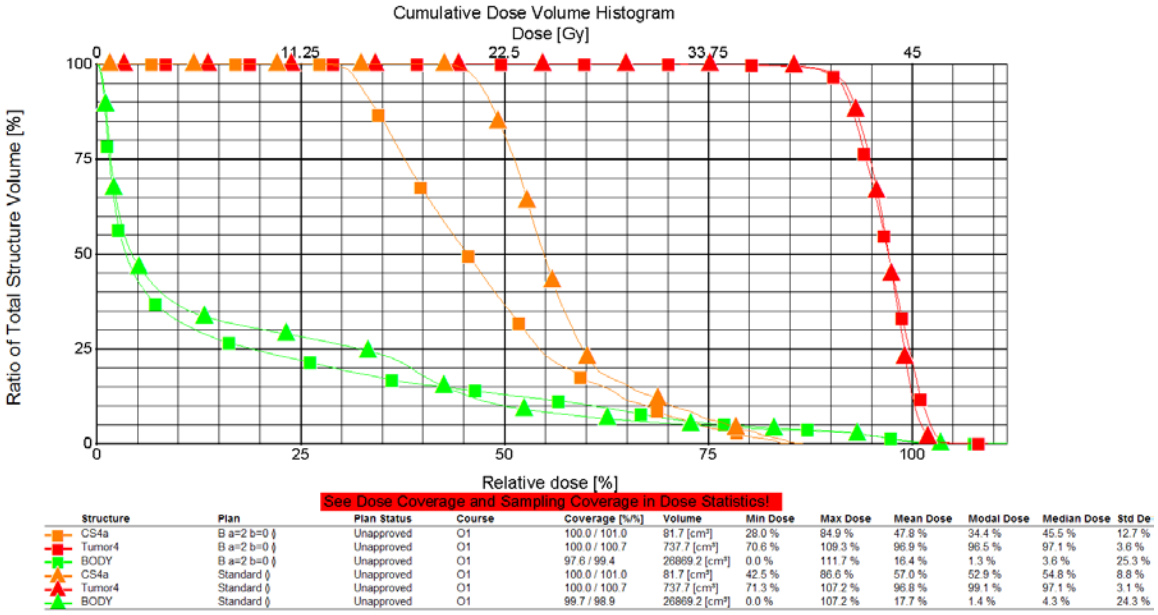

Structure	Plan	Plan Status	Course	Coverage [%/%]	Volume	Min Dose	Max Dose	Mean Dose	Modal Dose	Median Dose	Std De
CS4a	B a=2 b=0 ()	Unapproved	O1	100.0 / 101.0	81.7 [cm³]	28.0 %	84.9 %	47.8 %	34.4 %	45.5 %	12.7 %
Tumor4	B a=2 b=0 ()	Unapproved	O1	100.0 / 100.7	737.7 [cm³]	70.6 %	109.3 %	96.9 %	96.5 %	97.1 %	3.6 %
BODY	B a=2 b=0 ()	Unapproved	O1	97.6 / 99.4	26869.2 [cm³]	0.0 %	111.7 %	16.4 %	1.3 %	3.6 %	25.3 %
CS4a	Standard ()	Unapproved	O1	100.0 / 101.0	81.7 [cm³]	42.5 %	86.6 %	57.0 %	52.9 %	54.8 %	8.8 %
Tumor4	Standard ()	Unapproved	O1	100.0 / 100.7	737.7 [cm³]	71.3 %	107.2 %	96.8 %	99.1 %	97.1 %	3.1 %
BODY	Standard ()	Unapproved	O1	99.7 / 98.9	26869.2 [cm³]	0.0 %	107.2 %	17.7 %	1.4 %	4.3 %	24.3 %

Figure F.12: cDVH of equispaced IMRT plan vs. optimized IMRT plan using Method 1 algorithm with sela=2 and selb=0 for the square target geometry

The square data points represent the optimized IMRT plan and the triangle data points represent the equispaced IMRT plan.

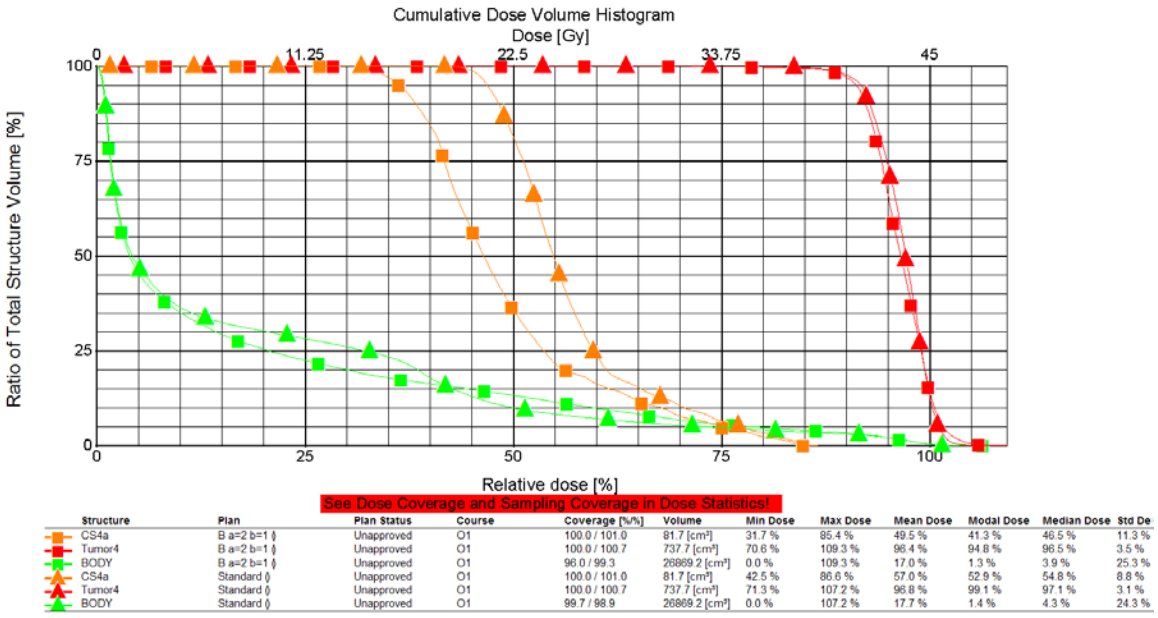

Structure	Plan	Plan Status	Course	Coverage [%/%]	Volume	Min Dose	Max Dose	Mean Dose	Modal Dose	Median Dose	Std De
CS4a	B a=2 b=1 ()	Unapproved	O1	100.0 / 101.0	81.7 [cm³]	31.7 %	85.4 %	49.5 %	41.3 %	46.5 %	11.3 %
Tumor4	B a=2 b=1 ()	Unapproved	O1	100.0 / 100.7	737.7 [cm³]	70.6 %	109.3 %	96.4 %	94.8 %	96.5 %	3.5 %
BODY	B a=2 b=1 ()	Unapproved	O1	96.0 / 99.3	26869.2 [cm³]	0.0 %	109.3 %	17.0 %	1.3 %	3.9 %	25.3 %
CS4a	Standard ()	Unapproved	O1	100.0 / 101.0	81.7 [cm³]	42.5 %	86.6 %	57.0 %	52.9 %	54.8 %	8.8 %
Tumor4	Standard ()	Unapproved	O1	100.0 / 100.7	737.7 [cm³]	71.3 %	107.2 %	96.8 %	99.1 %	97.1 %	3.1 %
BODY	Standard ()	Unapproved	O1	99.7 / 98.9	26869.2 [cm³]	0.0 %	107.2 %	17.7 %	1.4 %	4.3 %	24.3 %

Figure F.13: cDVH of equispaced IMRT plan vs. optimized IMRT plan using Method 1 algorithm with sela=2 and selb=1 for the square target geometry

The square data points represent the optimized IMRT plan and the triangle data points represent the equispaced IMRT plan.

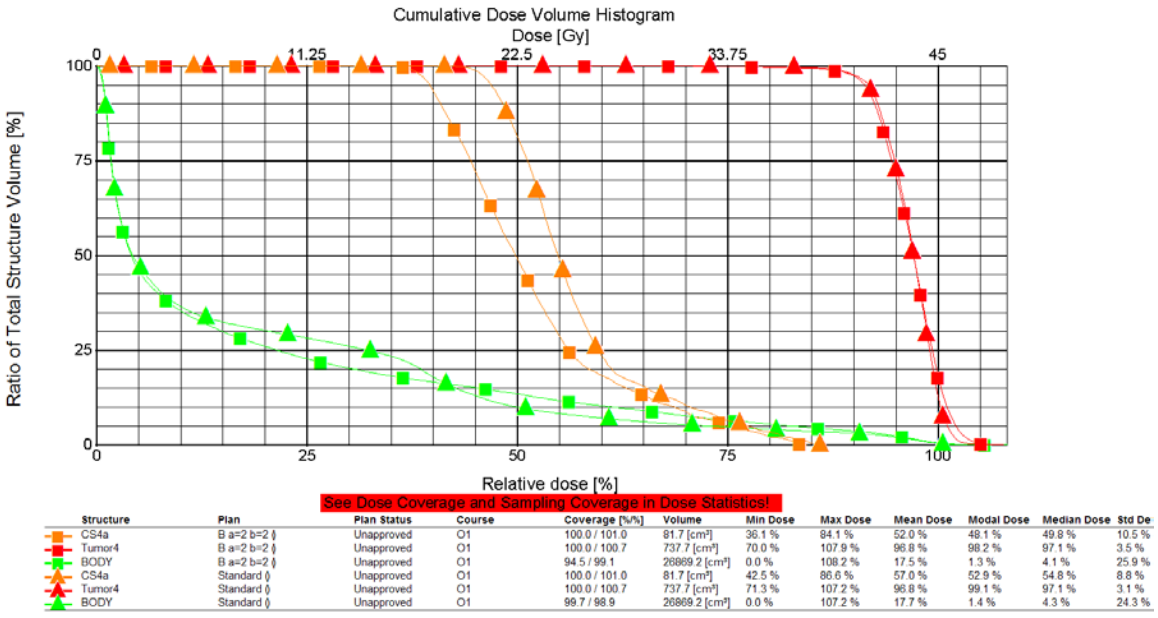

Structure	Plan	Plan Status	Course	Coverage [%/%]	Volume	Min Dose	Max Dose	Mean Dose	Modal Dose	Median Dose	Std De
CS4a	B a=2 b=2 ()	Unapproved	O1	100.0 / 101.0	81.7 [cm³]	36.1 %	84.1 %	52.0 %	48.1 %	49.8 %	10.5 %
Tumor4	B a=2 b=2 ()	Unapproved	O1	100.0 / 100.7	737.7 [cm³]	70.0 %	107.9 %	96.8 %	98.2 %	97.1 %	3.5 %
BODY	B a=2 b=2 ()	Unapproved	O1	94.5 / 99.1	26869.2 [cm³]	0.0 %	108.2 %	17.5 %	1.3 %	4.1 %	25.9 %
CS4a	Standard ()	Unapproved	O1	100.0 / 101.0	81.7 [cm³]	42.5 %	86.6 %	57.0 %	52.9 %	54.8 %	8.8 %
Tumor4	Standard ()	Unapproved	O1	100.0 / 100.7	737.7 [cm³]	71.3 %	107.2 %	96.8 %	99.1 %	97.1 %	3.1 %
BODY	Standard ()	Unapproved	O1	99.7 / 98.9	26869.2 [cm³]	0.0 %	107.2 %	17.7 %	1.4 %	4.3 %	24.3 %

Figure F.14: cDVH of equispaced IMRT plan vs. optimized IMRT plan using Method 1 algorithm with sela=2 and selb=2 for the square target geometry

The square data points represent the optimized IMRT plan and the triangle data points represent the equispaced IMRT plan.

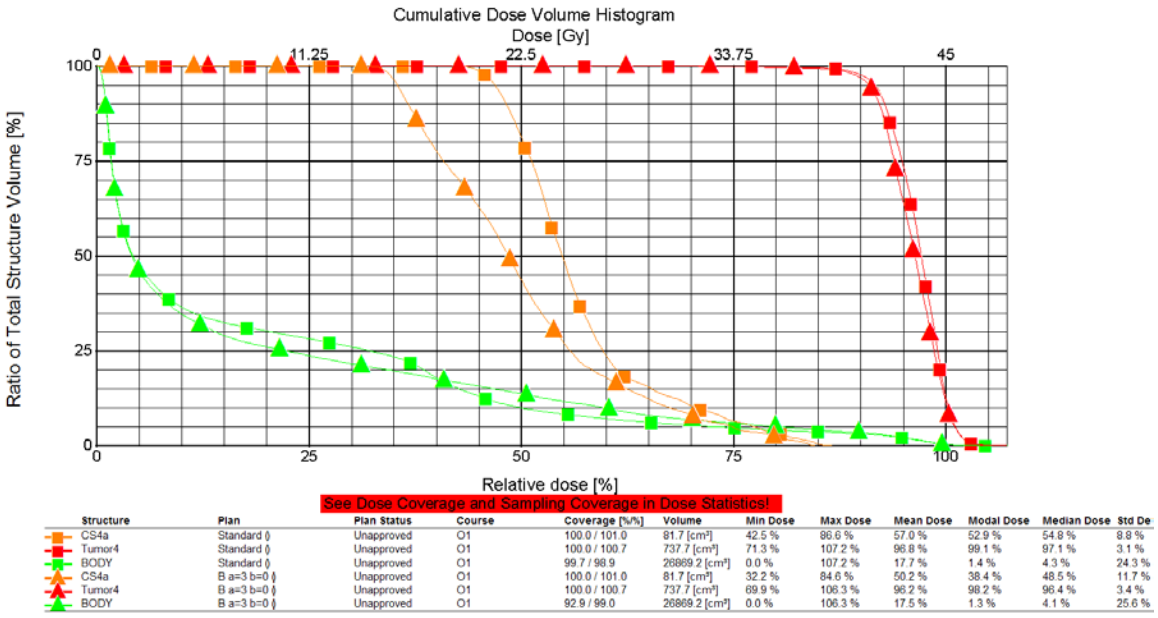

Structure	Plan	Plan Status	Course	Coverage [%/%]	Volume	Min Dose	Max Dose	Mean Dose	Modal Dose	Median Dose	Std De
CS4a	Standard ()	Unapproved	O1	100.0 / 101.0	81.7 [cm³]	42.5 %	86.6 %	57.0 %	52.9 %	54.8 %	8.8 %
Tumor4	Standard ()	Unapproved	O1	100.0 / 100.7	737.7 [cm³]	71.3 %	107.2 %	96.8 %	99.1 %	97.1 %	3.1 %
BODY	Standard ()	Unapproved	O1	99.7 / 98.9	26869.2 [cm³]	0.0 %	107.2 %	17.7 %	1.4 %	4.3 %	24.3 %
CS4a	B a=3 b=0 ()	Unapproved	O1	100.0 / 101.0	81.7 [cm³]	32.2 %	84.6 %	50.2 %	38.4 %	48.5 %	11.7 %
Tumor4	B a=3 b=0 ()	Unapproved	O1	100.0 / 100.7	737.7 [cm³]	69.9 %	108.3 %	96.2 %	98.2 %	96.4 %	3.4 %
BODY	B a=3 b=0 ()	Unapproved	O1	92.9 / 99.0	26869.2 [cm³]	0.0 %	108.3 %	17.5 %	1.3 %	4.1 %	25.6 %

Figure F.15: cDVH of equispaced IMRT plan vs. optimized IMRT plan using Method 1 algorithm with sela=3 and selb=0 for the square target geometry

The triangle data points represent the optimized IMRT plan and the square data points represent the equispaced IMRT plan.

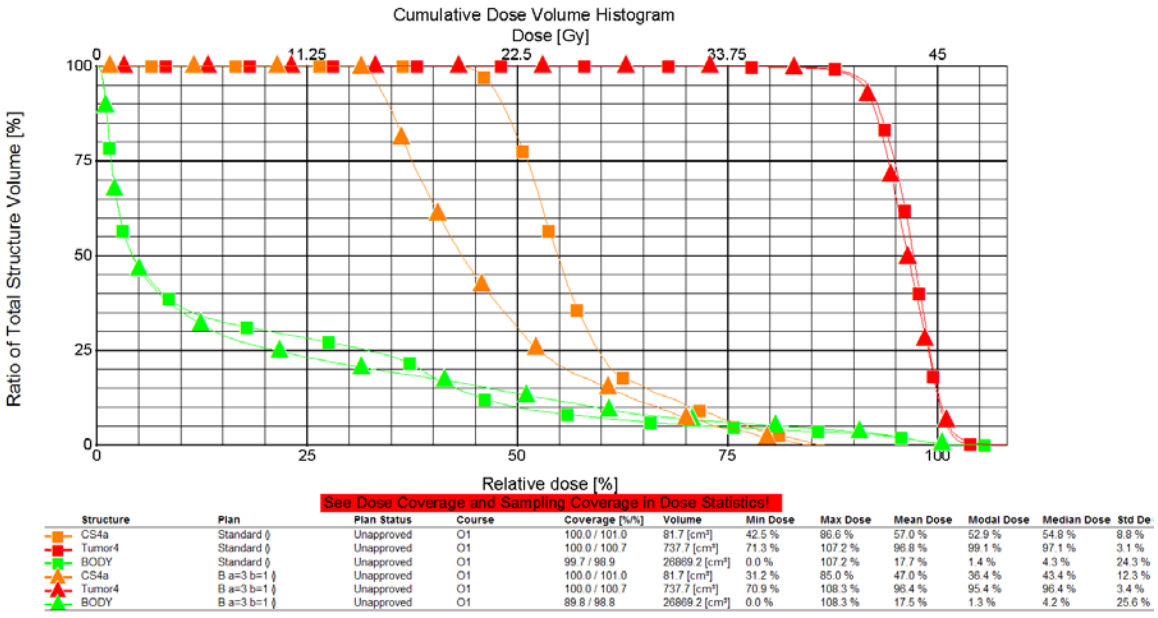

Structure	Plan	Plan Status	Course	Coverage [%/%]	Volume	Min Dose	Max Dose	Mean Dose	Modal Dose	Median Dose	Std De
CS4a	Standard ()	Unapproved	O1	100.0 / 101.0	81.7 [cm³]	42.5 %	86.6 %	57.0 %	52.9 %	54.8 %	8.8 %
Tumor4	Standard ()	Unapproved	O1	100.0 / 100.7	737.7 [cm³]	71.3 %	107.2 %	96.8 %	99.1 %	97.1 %	3.1 %
BODY	Standard ()	Unapproved	O1	99.7 / 98.9	26869.2 [cm³]	0.0 %	107.2 %	17.7 %	1.4 %	4.3 %	24.3 %
CS4a	B a=3 b=1 ()	Unapproved	O1	100.0 / 101.0	81.7 [cm³]	31.2 %	85.0 %	47.0 %	36.4 %	43.4 %	12.3 %
Tumor4	B a=3 b=1 ()	Unapproved	O1	100.0 / 100.7	737.7 [cm³]	70.9 %	108.3 %	96.4 %	95.4 %	96.4 %	3.4 %
BODY	B a=3 b=1 ()	Unapproved	O1	89.8 / 98.8	26869.2 [cm³]	0.0 %	108.3 %	17.5 %	1.3 %	4.2 %	25.6 %

Figure F.16: cDVH of equispaced IMRT plan vs. optimized IMRT plan using Method 1 algorithm with sela=3 and selb=1 for the square target geometry

The triangle data points represent the optimized IMRT plan and the square data points represent the equispaced IMRT plan.

F.2 L-Shaped Target Geometry

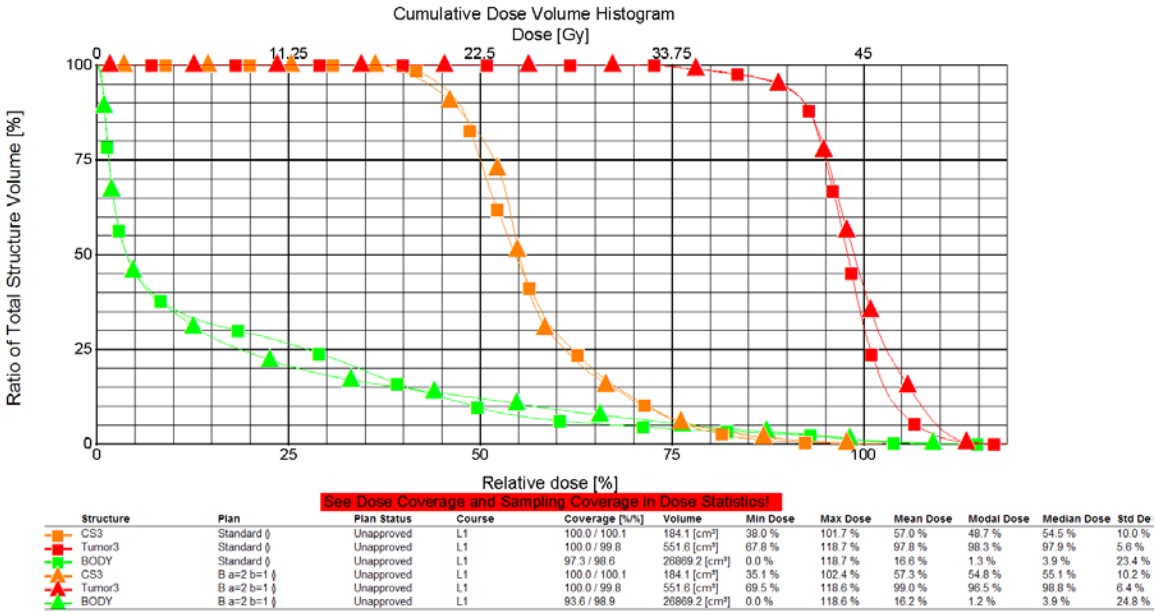

Structure	Plan	Plan Status	Course	Coverage [%/%]	Volume	Min Dose	Max Dose	Mean Dose	Modal Dose	Median Dose	Std De
CS3	Standard ()	Unapproved	L1	100.0 / 100.1	184.1 [cm³]	38.0 %	101.7 %	57.0 %	48.7 %	54.5 %	10.0 %
Tumor3	Standard ()	Unapproved	L1	100.0 / 99.8	551.6 [cm³]	67.8 %	118.7 %	97.8 %	98.3 %	97.9 %	5.6 %
BODY	Standard ()	Unapproved	L1	97.3 / 98.6	26869.2 [cm³]	0.0 %	118.7 %	16.6 %	1.3 %	3.9 %	23.4 %
CS3	B a=2 b=1 ()	Unapproved	L1	100.0 / 100.1	184.1 [cm³]	35.1 %	102.4 %	57.3 %	54.8 %	55.1 %	10.2 %
Tumor3	B a=2 b=1 ()	Unapproved	L1	100.0 / 99.8	551.6 [cm³]	69.5 %	118.6 %	99.0 %	96.5 %	98.8 %	6.4 %
BODY	B a=2 b=1 ()	Unapproved	L1	93.6 / 98.9	26869.2 [cm³]	0.0 %	118.6 %	16.2 %	1.2 %	3.9 %	24.8 %

Figure F.17: cDVH of equispaced IMRT plan vs. optimized IMRT plan using Method 1 algorithm with sela=2 and selb=1 for the L-shaped target geometry

The triangle data points represent the optimized IMRT plan and the square data points represent the equispaced IMRT plan.

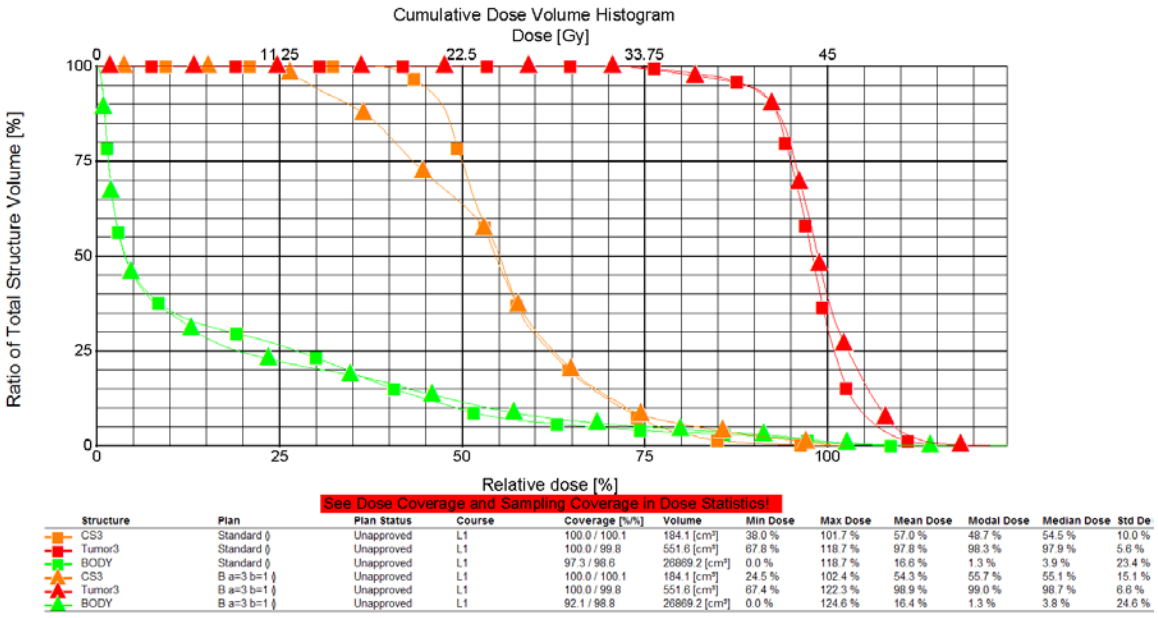

Figure F.18: cDVH of equispaced IMRT plan vs. optimized IMRT plan using Method 1 algorithm with sela=3 and selb=1 for the L-shaped target geometry

The triangle data points represent the optimized IMRT plan and the square data points represent the equispaced IMRT plan.

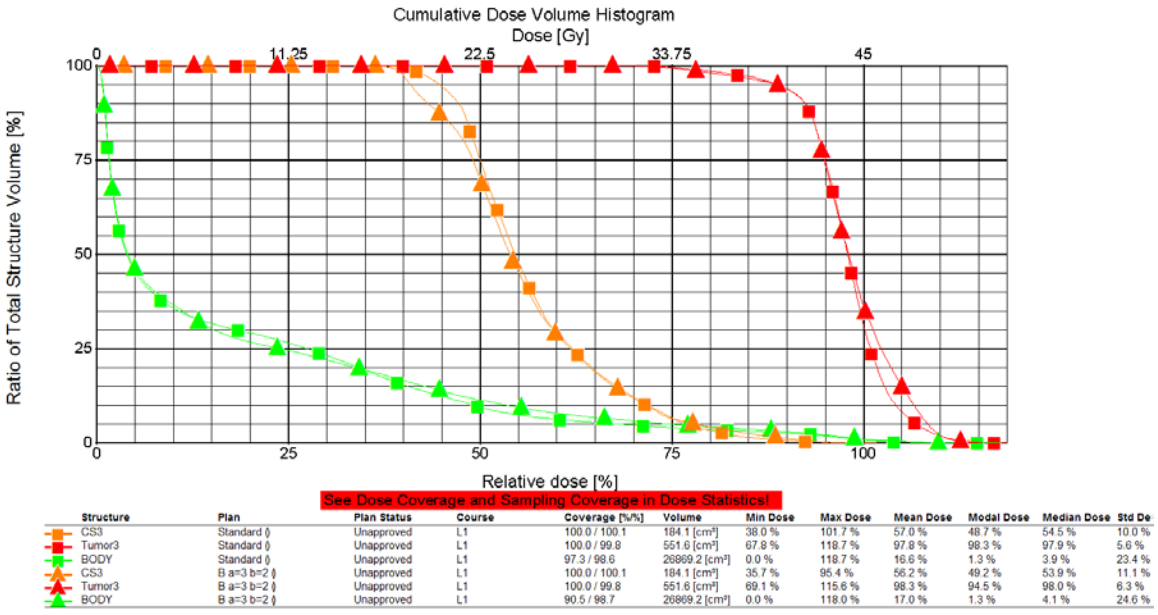

Figure F.19: cDVH of equispaced IMRT plan vs. optimized IMRT plan using Method 1 algorithm with sela=3 and selb=2 for the L-shaped target geometry

The triangle data points represent the optimized IMRT plan and the square data points represent the equispaced IMRT plan.

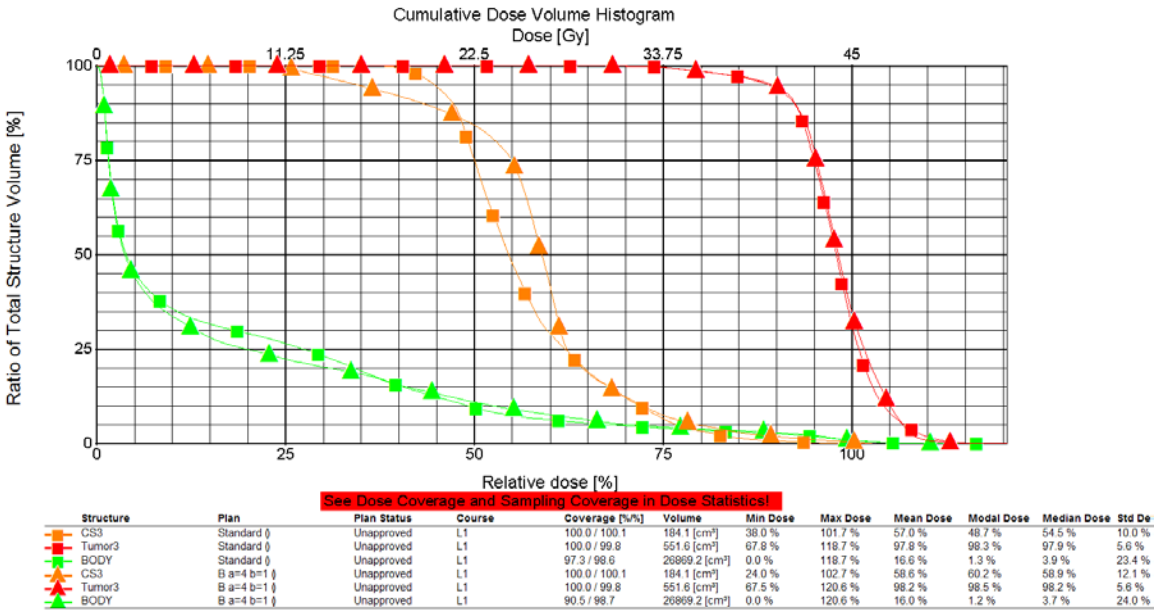

Structure	Plan	Plan Status	Course	Coverage [%/%]	Volume	Min Dose	Max Dose	Mean Dose	Modal Dose	Median Dose	Std De
CS3	Standard ()	Unapproved	L1	100.0 / 100.1	184.1 [cm³]	38.0 %	101.7 %	57.0 %	48.7 %	54.5 %	10.0 %
Tumor3	Standard ()	Unapproved	L1	100.0 / 99.8	551.6 [cm³]	67.8 %	118.7 %	97.8 %	98.3 %	97.9 %	5.6 %
BODY	Standard ()	Unapproved	L1	97.3 / 98.6	26869.2 [cm³]	0.0 %	118.7 %	16.6 %	1.3 %	3.9 %	23.4 %
CS3	B a=4 b=1 ()	Unapproved	L1	100.0 / 100.1	184.1 [cm³]	24.0 %	102.7 %	58.6 %	60.2 %	58.9 %	12.1 %
Tumor3	B a=4 b=1 ()	Unapproved	L1	100.0 / 99.8	551.6 [cm³]	67.5 %	120.6 %	98.2 %	98.5 %	98.2 %	5.6 %
BODY	B a=4 b=1 ()	Unapproved	L1	90.5 / 98.7	26869.2 [cm³]	0.0 %	120.6 %	16.0 %	1.2 %	3.7 %	24.0 %

Figure F.20: cDVH of equispaced IMRT plan vs. optimized IMRT plan using Method 1 algorithm with sela=4 and selb=1 for the L-shaped target geometry

The triangle data points represent the optimized IMRT plan and the square data points represent the equispaced IMRT plan.

F.3 U-Shaped Target Geometry

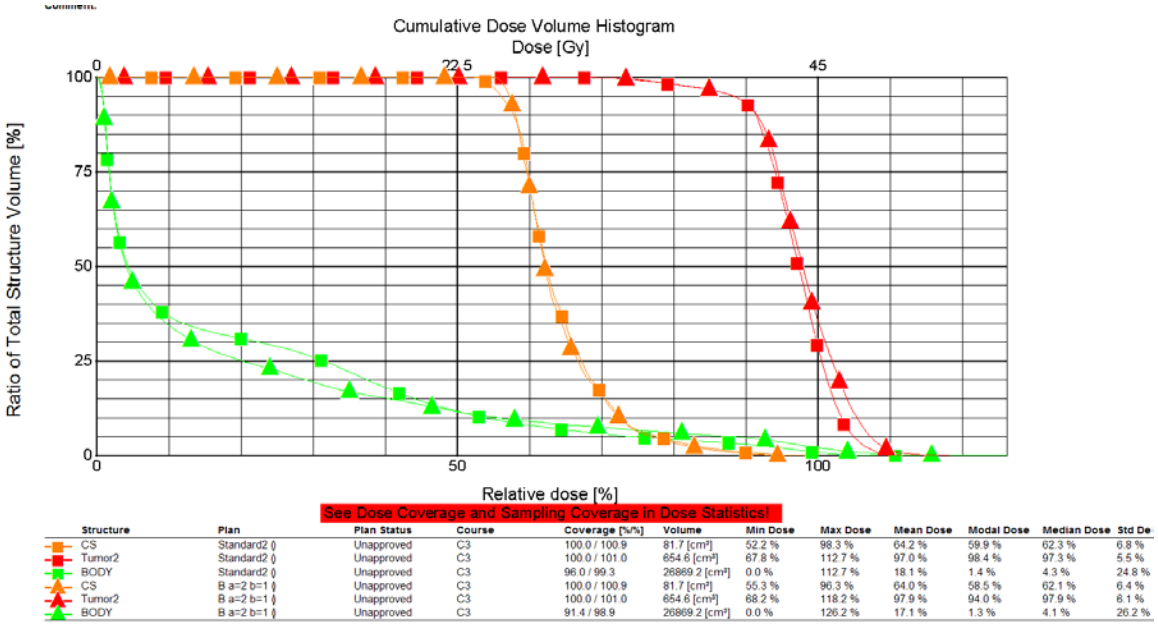

Structure	Plan	Plan Status	Course	Coverage [%/%]	Volume	Min Dose	Max Dose	Mean Dose	Modal Dose	Median Dose	Std De
CS	Standard2 ()	Unapproved	C3	100.0 / 100.9	81.7 [cm³]	52.2 %	98.3 %	64.2 %	59.9 %	62.3 %	6.8 %
Tumor2	Standard2 ()	Unapproved	C3	100.0 / 101.0	654.6 [cm³]	67.8 %	112.7 %	97.0 %	98.4 %	97.3 %	5.5 %
BODY	Standard2 ()	Unapproved	C3	96.0 / 99.3	26869.2 [cm³]	0.0 %	112.7 %	18.1 %	1.4 %	4.3 %	24.8 %
CS	B a=2 b=1 ()	Unapproved	C3	100.0 / 100.9	81.7 [cm³]	55.3 %	96.3 %	64.0 %	58.5 %	62.1 %	6.4 %
Tumor2	B a=2 b=1 ()	Unapproved	C3	100.0 / 101.0	654.6 [cm³]	68.2 %	118.2 %	97.9 %	94.0 %	97.9 %	6.1 %
BODY	B a=2 b=1 ()	Unapproved	C3	91.4 / 98.9	26869.2 [cm³]	0.0 %	126.2 %	17.1 %	1.3 %	4.1 %	26.2 %

Figure F.21: cDVH of equispaced IMRT plan vs. optimized IMRT plan using Method 1 algorithm with sela=2 and selb=1 for the U-shaped target geometry

The triangle data points represent the optimized IMRT plan and the square data points represent the equispaced IMRT plan.

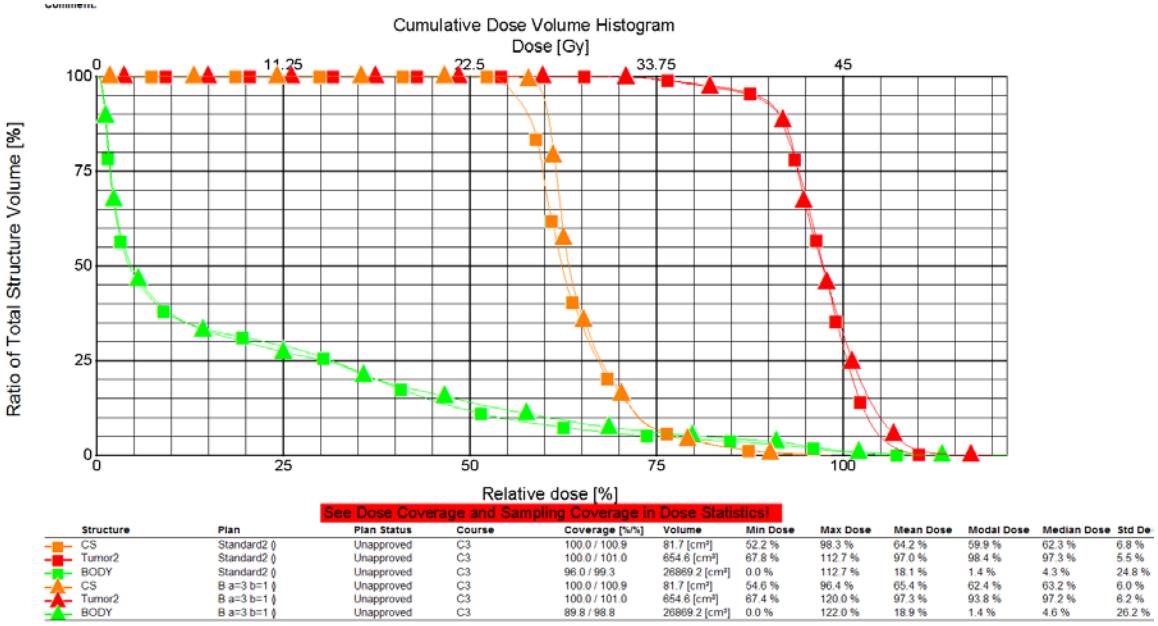

Figure F.22: cDVH of equispaced IMRT plan vs. optimized IMRT plan using Method 1 algorithm with sela=3 and selb=1 for the U-shaped target geometry

The triangle data points represent the optimized IMRT plan and the square data points represent the equispaced IMRT plan.

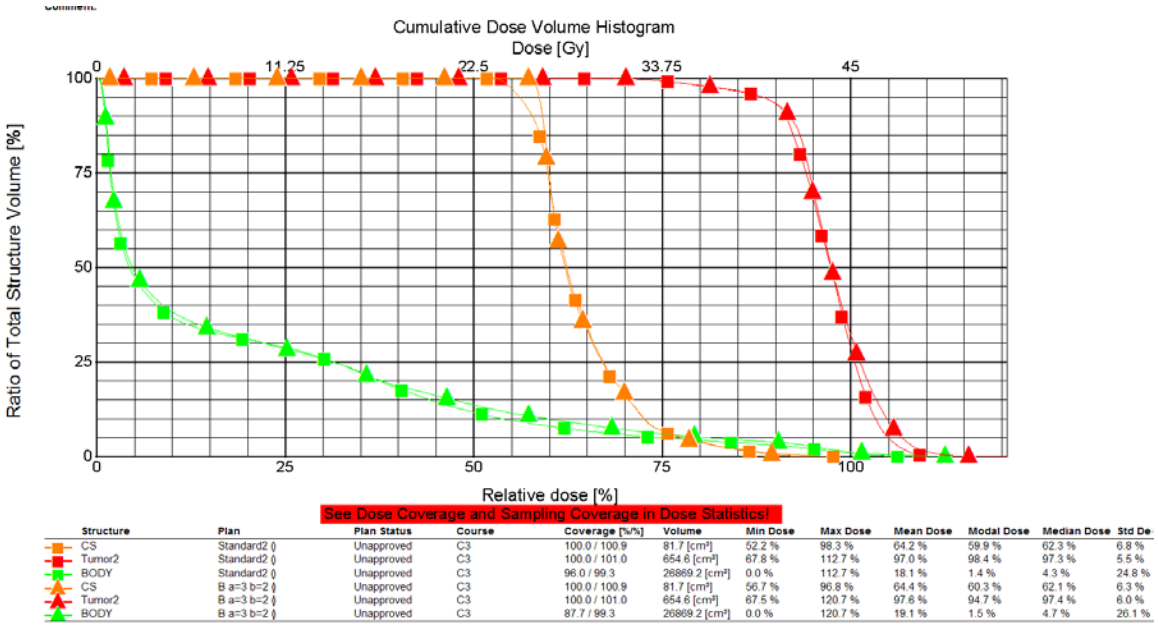

Figure F.23: cDVH of equispaced IMRT plan vs. optimized IMRT plan using Method 1 algorithm with sela=3 and selb=2 for the U-shaped target geometry

The triangle data points represent the optimized IMRT plan and the square data points represent the equispaced IMRT plan.

APPENDIX G

Method 2 cDVHs

The red data points represent the cDVH of the target volume, the orange data points represent the cDVH of the critical structure, and the green data points represent the cDVH of the normal tissue in the following figures. Furthermore, below the cDVHs are the maximum dose, minimum dose, and mean dose for the three structures.

G.1 Square Target Geometry

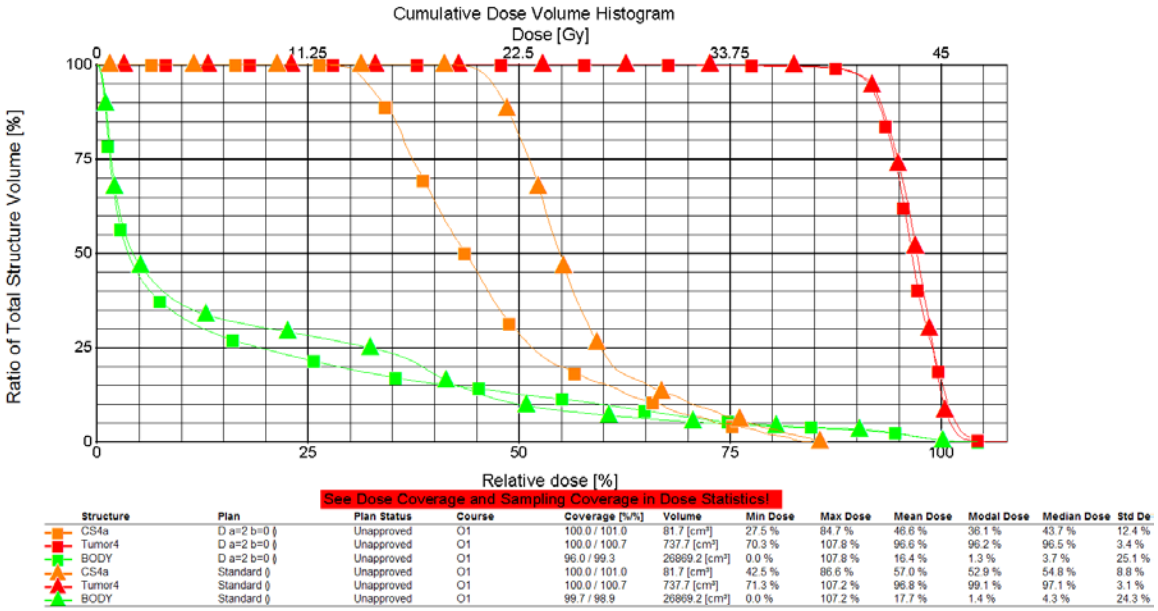

Structure	Plan	Plan Status	Course	Coverage [%/%]	Volume	Min Dose	Max Dose	Mean Dose	Modal Dose	Median Dose	Std De
CS4a	D a=2 b=0 ()	Unapproved	O1	100.0 / 101.0	81.7 [cm³]	27.5 %	84.7 %	46.6 %	36.1 %	43.7 %	12.4 %
Tumor4	D a=2 b=0 ()	Unapproved	O1	100.0 / 100.7	737.7 [cm³]	70.3 %	107.8 %	96.6 %	96.2 %	96.5 %	3.4 %
BODY	D a=2 b=0 ()	Unapproved	O1	96.0 / 99.3	26869.2 [cm³]	0.0 %	107.8 %	16.4 %	1.3 %	3.7 %	25.1 %
CS4a	Standard ()	Unapproved	O1	100.0 / 101.0	81.7 [cm³]	42.5 %	86.6 %	57.0 %	52.9 %	54.8 %	8.8 %
Tumor4	Standard ()	Unapproved	O1	100.0 / 100.7	737.7 [cm³]	71.3 %	107.2 %	96.8 %	99.1 %	97.1 %	3.1 %
BODY	Standard ()	Unapproved	O1	99.7 / 98.9	26869.2 [cm³]	0.0 %	107.2 %	17.7 %	1.4 %	4.3 %	24.3 %

Figure G.24: cDVH of equispaced IMRT plan vs. optimized IMRT plan using Method 2 algorithm with sela=2 and selb=0 for the square target geometry

The square data points represent the optimized IMRT plan and the triangle data points represent the equispaced IMRT plan.

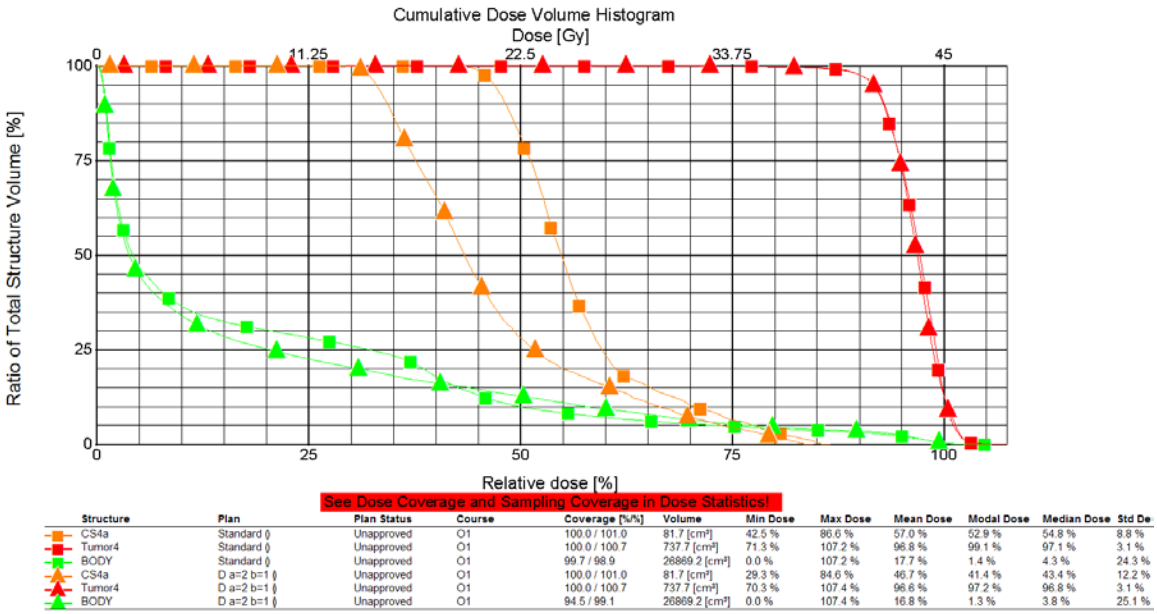

Structure	Plan	Plan Status	Course	Coverage [%/%]	Volume	Min Dose	Max Dose	Mean Dose	Modal Dose	Median Dose	Std De
CS4a	Standard ()	Unapproved	O1	100.0 / 101.0	81.7 [cm³]	42.5 %	86.6 %	57.0 %	52.9 %	54.8 %	8.8 %
Tumor4	Standard ()	Unapproved	O1	100.0 / 100.7	737.7 [cm³]	71.3 %	107.2 %	96.8 %	99.1 %	97.1 %	3.1 %
BODY	Standard ()	Unapproved	O1	99.7 / 98.9	26869.2 [cm³]	0.0 %	107.2 %	17.7 %	1.4 %	4.3 %	24.3 %
CS4a	D a=2 b=1 ()	Unapproved	O1	100.0 / 101.0	81.7 [cm³]	29.3 %	84.6 %	46.7 %	41.4 %	43.4 %	12.2 %
Tumor4	D a=2 b=1 ()	Unapproved	O1	100.0 / 100.7	737.7 [cm³]	70.3 %	107.4 %	96.6 %	97.2 %	96.8 %	3.1 %
BODY	D a=2 b=1 ()	Unapproved	O1	94.5 / 99.1	26869.2 [cm³]	0.0 %	107.4 %	16.8 %	1.3 %	3.8 %	25.1 %

Figure G.25: cDVH of equispaced IMRT plan vs. optimized IMRT plan using Method 2 algorithm with sela=2 and selb=1 for the square target geometry

The triangle data points represent the optimized IMRT plan and the square data points represent the equispaced IMRT plan.

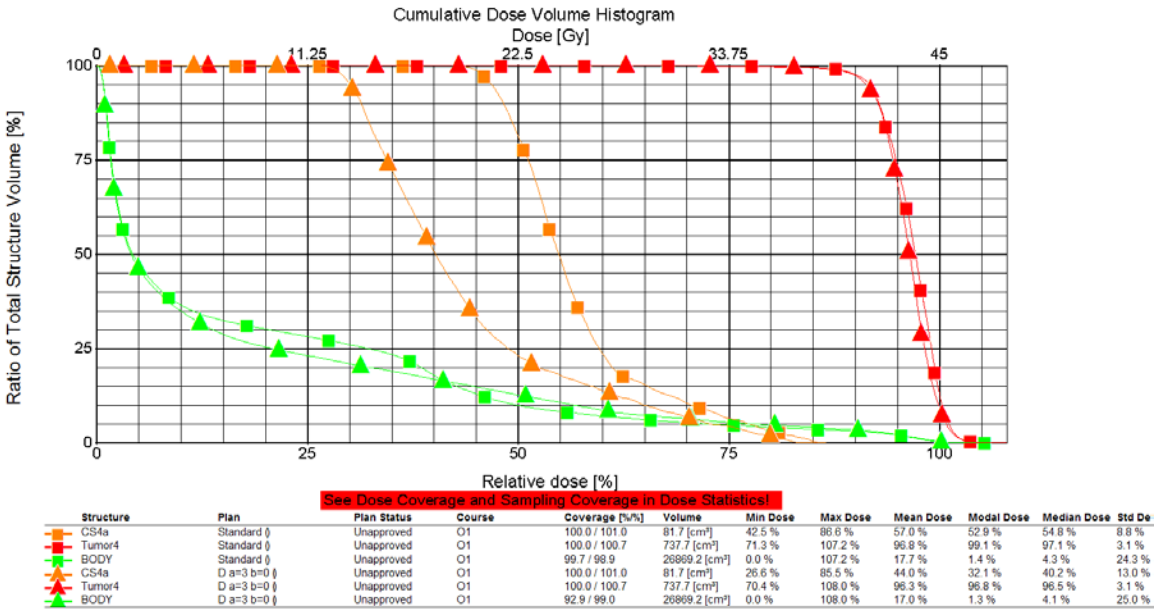

Structure	Plan	Plan Status	Course	Coverage [%/%]	Volume	Min Dose	Max Dose	Mean Dose	Modal Dose	Median Dose	Std De
CS4a	Standard ()	Unapproved	O1	100.0 / 101.0	81.7 [cm³]	42.5 %	86.6 %	57.0 %	52.9 %	54.8 %	8.8 %
Tumor4	Standard ()	Unapproved	O1	100.0 / 100.7	737.7 [cm³]	71.3 %	107.2 %	96.8 %	99.1 %	97.1 %	3.1 %
BODY	Standard ()	Unapproved	O1	99.7 / 98.9	26869.2 [cm³]	0.0 %	107.2 %	17.7 %	1.4 %	4.3 %	24.3 %
CS4a	D a=3 b=0 ()	Unapproved	O1	100.0 / 101.0	81.7 [cm³]	26.6 %	85.5 %	44.0 %	32.1 %	40.2 %	13.0 %
Tumor4	D a=3 b=0 ()	Unapproved	O1	100.0 / 100.7	737.7 [cm³]	70.4 %	108.0 %	96.3 %	96.8 %	96.5 %	3.1 %
BODY	D a=3 b=0 ()	Unapproved	O1	92.9 / 99.0	26869.2 [cm³]	0.0 %	108.0 %	17.0 %	1.3 %	4.1 %	25.0 %

Figure G.26: cDVH of equispaced IMRT plan vs. optimized IMRT plan using Method 2 algorithm with sela=3 and selb=0 for the square target geometry

The triangle data points represent the optimized IMRT plan and the square data points represent the equispaced IMRT plan. In addition, the same beam angle arrangement is used for sela=3 and selb=1.

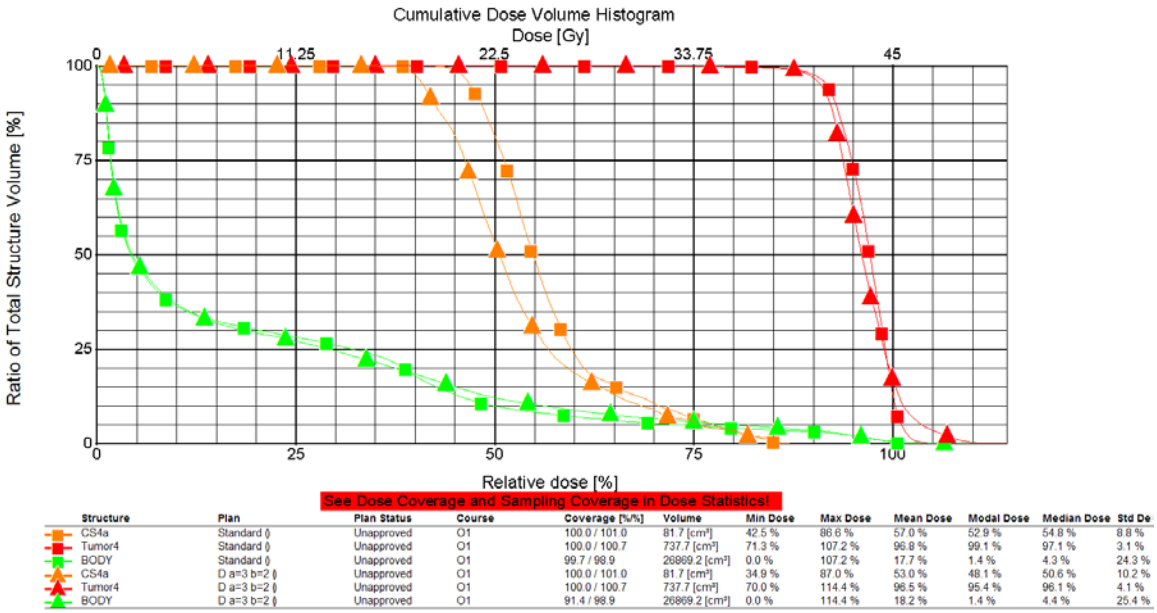

Structure	Plan	Plan Status	Course	Coverage [%/%]	Volume	Min Dose	Max Dose	Mean Dose	Modal Dose	Median Dose	Std De
CS4a	Standard ()	Unapproved	O1	100.0 / 101.0	81.7 [cm³]	42.5 %	86.6 %	57.0 %	52.9 %	54.8 %	8.8 %
Tumor4	Standard ()	Unapproved	O1	100.0 / 100.7	737.7 [cm³]	71.3 %	107.2 %	96.8 %	99.1 %	97.1 %	3.1 %
BODY	Standard ()	Unapproved	O1	99.7 / 98.9	26869.2 [cm³]	0.0 %	107.2 %	17.7 %	1.4 %	4.3 %	24.3 %
CS4a	D a=3 b=2 ()	Unapproved	O1	100.0 / 101.0	81.7 [cm³]	34.9 %	87.0 %	53.0 %	48.1 %	50.6 %	10.2 %
Tumor4	D a=3 b=2 ()	Unapproved	O1	100.0 / 100.7	737.7 [cm³]	70.0 %	114.4 %	96.5 %	95.4 %	96.1 %	4.1 %
BODY	D a=3 b=2 ()	Unapproved	O1	91.4 / 98.9	26869.2 [cm³]	0.0 %	114.4 %	18.2 %	1.4 %	4.4 %	25.4 %

Figure G.27: cDVH of equispaced IMRT plan vs. optimized IMRT plan using Method 2 algorithm with sela=3 and selb=2 for the square target geometry

The triangle data points represent the optimized IMRT plan and the square data points represent the equispaced IMRT plan.

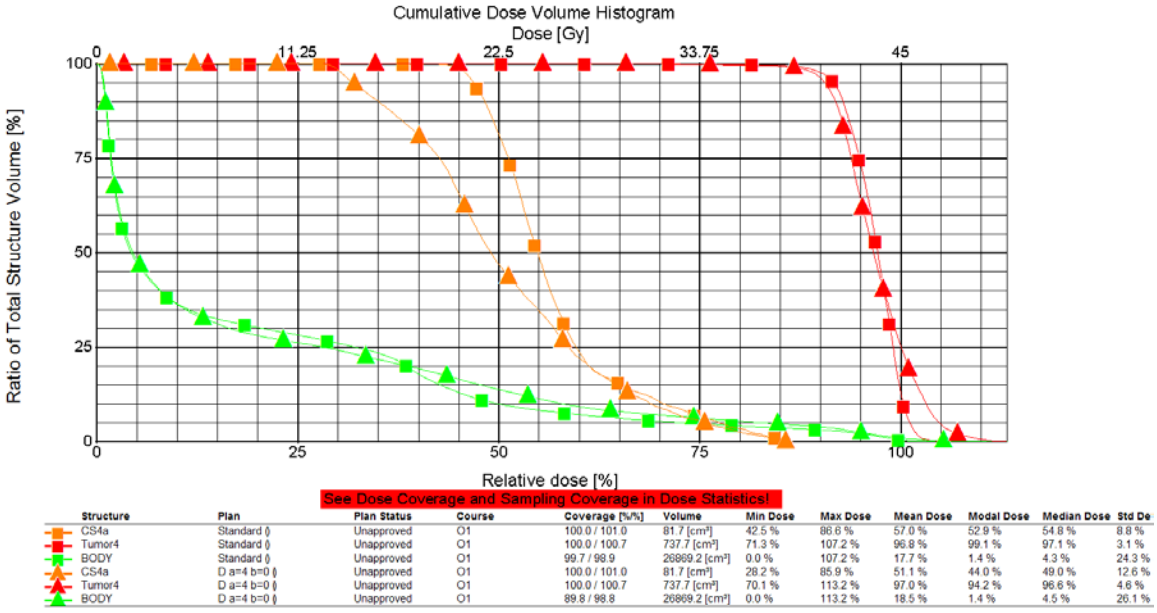

Structure	Plan	Plan Status	Course	Coverage [%/%]	Volume	Min Dose	Max Dose	Mean Dose	Modal Dose	Median Dose	Std De
CS4a	Standard ()	Unapproved	O1	100.0 / 101.0	81.7 [cm³]	42.5 %	86.6 %	57.0 %	52.9 %	54.8 %	8.8 %
Tumor4	Standard ()	Unapproved	O1	100.0 / 100.7	737.7 [cm³]	71.3 %	107.2 %	96.8 %	99.1 %	97.1 %	3.1 %
BODY	Standard ()	Unapproved	O1	99.7 / 98.9	26869.2 [cm³]	0.0 %	107.2 %	17.7 %	1.4 %	4.3 %	24.3 %
CS4a	D a=4 b=0 ()	Unapproved	O1	100.0 / 101.0	81.7 [cm³]	28.2 %	85.9 %	51.1 %	44.0 %	49.0 %	12.6 %
Tumor4	D a=4 b=0 ()	Unapproved	O1	100.0 / 100.7	737.7 [cm³]	70.1 %	113.2 %	97.0 %	94.2 %	96.6 %	4.6 %
BODY	D a=4 b=0 ()	Unapproved	O1	89.8 / 98.8	26869.2 [cm³]	0.0 %	113.2 %	18.5 %	1.4 %	4.5 %	26.1 %

Figure G.28: cDVH of equispaced IMRT plan vs. optimized IMRT plan using Method 2 algorithm with sela=4 and selb=0 for the square target geometry

The triangle data points represent the optimized IMRT plan and the square data points represent the equispaced IMRT plan.

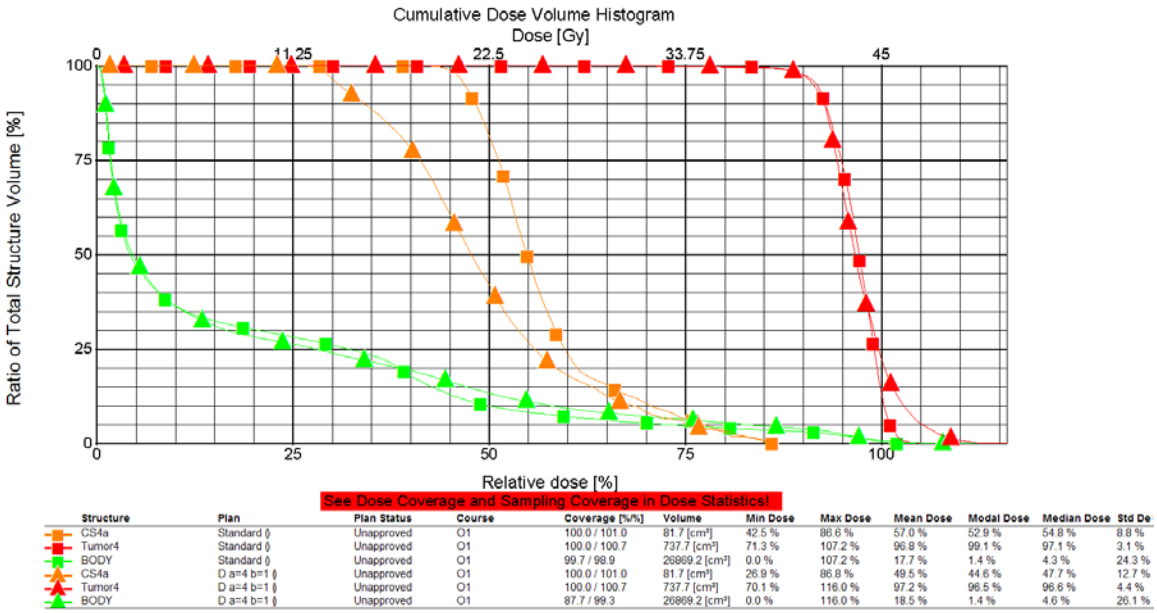

Structure	Plan	Plan Status	Course	Coverage [%/%]	Volume	Min Dose	Max Dose	Mean Dose	Modal Dose	Median Dose	Std De
CS4a	Standard ()	Unapproved	O1	100.0 / 101.0	81.7 [cm³]	42.5 %	86.6 %	57.0 %	52.9 %	54.8 %	8.8 %
Tumor4	Standard ()	Unapproved	O1	100.0 / 100.7	737.7 [cm³]	71.3 %	107.2 %	96.8 %	99.1 %	97.1 %	3.1 %
BODY	Standard ()	Unapproved	O1	99.7 / 98.9	26869.2 [cm³]	0.0 %	107.2 %	17.7 %	1.4 %	4.3 %	24.3 %
CS4a	D a=4 b=1 ()	Unapproved	O1	100.0 / 101.0	81.7 [cm³]	26.9 %	86.8 %	49.5 %	44.6 %	47.7 %	12.7 %
Tumor4	D a=4 b=1 ()	Unapproved	O1	100.0 / 100.7	737.7 [cm³]	70.1 %	116.0 %	97.2 %	96.5 %	96.6 %	4.4 %
BODY	D a=4 b=1 ()	Unapproved	O1	87.7 / 99.3	26869.2 [cm³]	0.0 %	116.0 %	18.5 %	1.4 %	4.6 %	26.1 %

Figure G.29: cDVH of equispaced IMRT plan vs. optimized IMRT plan using Method 2 algorithm with sela=4 and selb=1 for the square target geometry

The triangle data points represent the optimized IMRT plan and the square data points represent the equispaced IMRT plan.

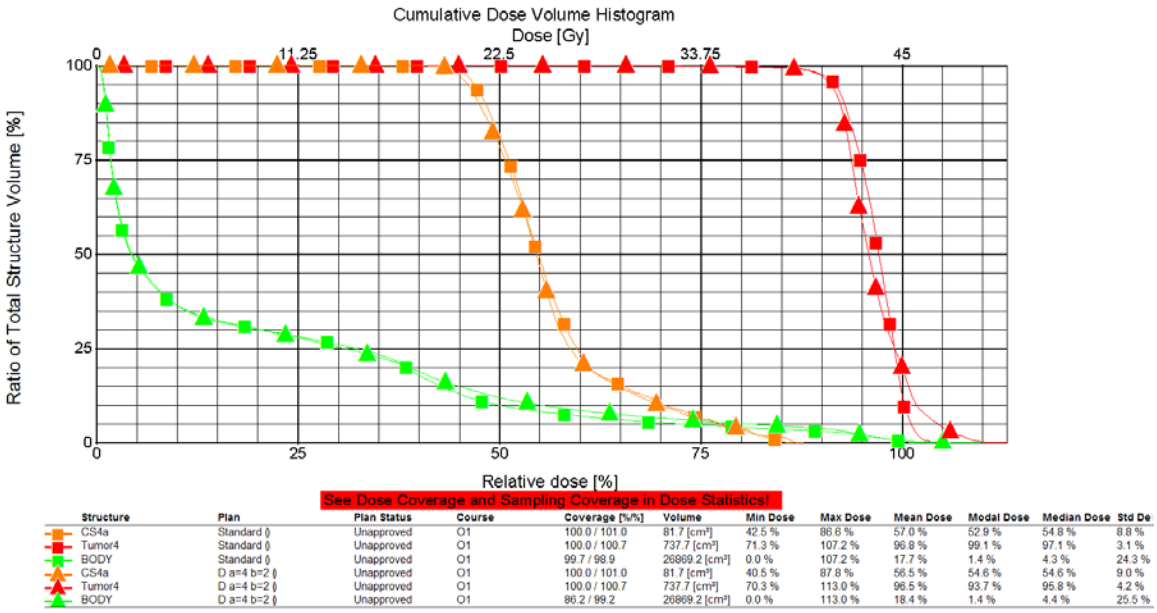

Structure	Plan	Plan Status	Course	Coverage [%/%]	Volume	Min Dose	Max Dose	Mean Dose	Modal Dose	Median Dose	Std De
CS4a	Standard ()	Unapproved	O1	100.0 / 101.0	81.7 [cm³]	42.5 %	86.6 %	57.0 %	52.9 %	54.8 %	8.8 %
Tumor4	Standard ()	Unapproved	O1	100.0 / 100.7	737.7 [cm³]	71.3 %	107.2 %	96.8 %	99.1 %	97.1 %	3.1 %
BODY	Standard ()	Unapproved	O1	99.7 / 98.9	26869.2 [cm³]	0.0 %	107.2 %	17.7 %	1.4 %	4.3 %	24.3 %
CS4a	D a=4 b=2 ()	Unapproved	O1	100.0 / 101.0	81.7 [cm³]	40.5 %	87.8 %	56.5 %	54.6 %	54.6 %	9.0 %
Tumor4	D a=4 b=2 ()	Unapproved	O1	100.0 / 100.7	737.7 [cm³]	70.3 %	113.0 %	96.5 %	93.7 %	95.8 %	4.2 %
BODY	D a=4 b=2 ()	Unapproved	O1	86.2 / 99.2	26869.2 [cm³]	0.0 %	113.0 %	18.4 %	1.4 %	4.4 %	25.5 %

Figure G.30: cDVH of equispaced IMRT plan vs. optimized IMRT plan using Method 2 algorithm with sela=4 and selb=2 for the square target geometry

The triangle data points represent the optimized IMRT plan and the square data points represent the equispaced IMRT plan.

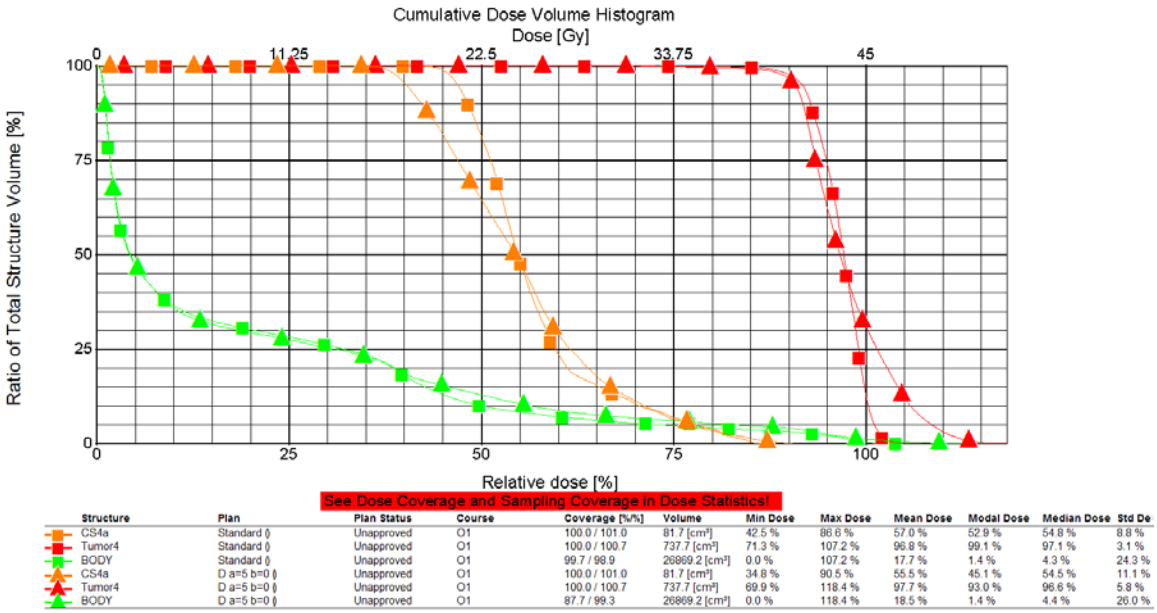

Structure	Plan	Plan Status	Course	Coverage [%/%]	Volume	Min Dose	Max Dose	Mean Dose	Modal Dose	Median Dose	Std De
CS4a	Standard ()	Unapproved	O1	100.0 / 101.0	81.7 [cm³]	42.5 %	86.6 %	57.0 %	52.9 %	54.8 %	8.8 %
Tumor4	Standard ()	Unapproved	O1	100.0 / 100.7	737.7 [cm³]	71.3 %	107.2 %	96.8 %	99.1 %	97.1 %	3.1 %
BODY	Standard ()	Unapproved	O1	99.7 / 98.9	26869.2 [cm³]	0.0 %	107.2 %	17.7 %	1.4 %	4.3 %	24.3 %
CS4a	D a=5 b=0 ()	Unapproved	O1	100.0 / 101.0	81.7 [cm³]	34.8 %	90.5 %	55.5 %	45.1 %	54.5 %	11.1 %
Tumor4	D a=5 b=0 ()	Unapproved	O1	100.0 / 100.7	737.7 [cm³]	69.9 %	118.4 %	97.7 %	93.0 %	96.6 %	5.8 %
BODY	D a=5 b=0 ()	Unapproved	O1	87.7 / 99.3	26869.2 [cm³]	0.0 %	118.4 %	18.5 %	1.4 %	4.4 %	26.0 %

Figure G.31: cDVH of equispaced IMRT plan vs. optimized IMRT plan using Method 2 algorithm with sela=5 and selb=0 for the square target geometry

The triangle data points represent the optimized IMRT plan and the square data points represent the equispaced IMRT plan.

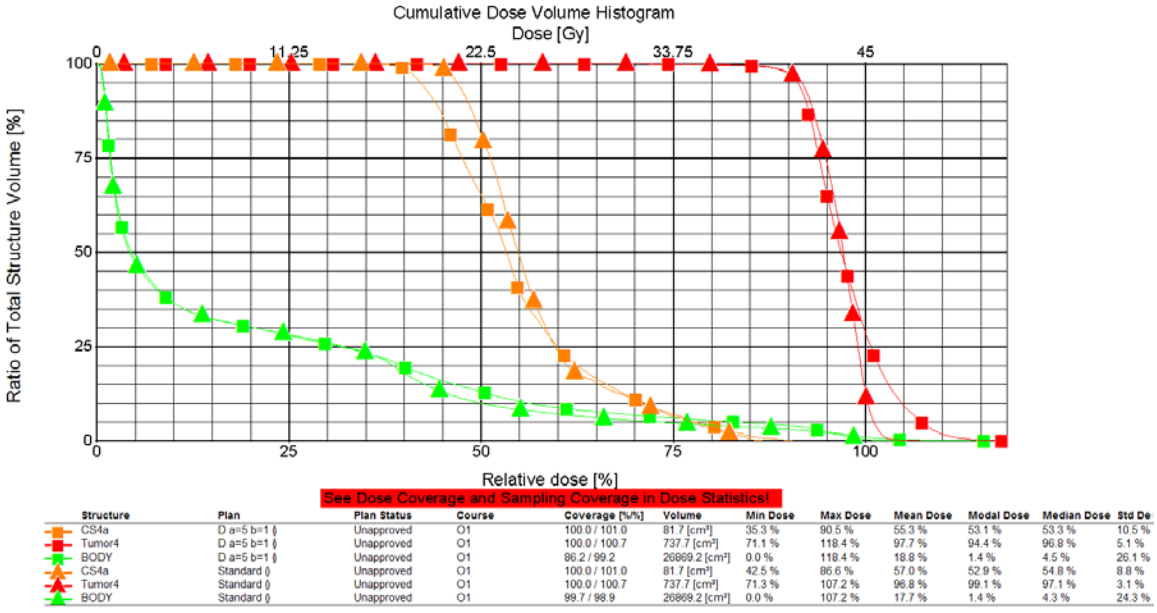

Structure	Plan	Plan Status	Course	Coverage [%/%]	Volume	Min Dose	Max Dose	Mean Dose	Modal Dose	Median Dose	Std De
CS4a	D a=5 b=1 ()	Unapproved	O1	100.0 / 101.0	81.7 [cm³]	35.3 %	90.5 %	55.3 %	53.1 %	53.3 %	10.5 %
Tumor4	D a=5 b=1 ()	Unapproved	O1	100.0 / 100.7	737.7 [cm³]	71.1 %	118.4 %	97.7 %	94.4 %	96.8 %	5.1 %
BODY	D a=5 b=1 ()	Unapproved	O1	86.2 / 99.2	26869.2 [cm³]	0.0 %	118.4 %	18.8 %	1.4 %	4.5 %	26.1 %
CS4a	Standard ()	Unapproved	O1	100.0 / 101.0	81.7 [cm³]	42.5 %	86.6 %	57.0 %	52.9 %	54.8 %	8.8 %
Tumor4	Standard ()	Unapproved	O1	100.0 / 100.7	737.7 [cm³]	71.3 %	107.2 %	96.8 %	99.1 %	97.1 %	3.1 %
BODY	Standard ()	Unapproved	O1	99.7 / 98.9	26869.2 [cm³]	0.0 %	107.2 %	17.7 %	1.4 %	4.3 %	24.3 %

Figure G.32: cDVH of equispaced IMRT plan vs. optimized IMRT plan using Method 2 algorithm with sela=5 and selb=1 for the square target geometry

The square data points represent the optimized IMRT plan and the triangle data points represent the equispaced IMRT plan. In addition, the same beam angle arrangement is used for sela=3 and selb=2.

G.2 L-Shaped Target Geometry

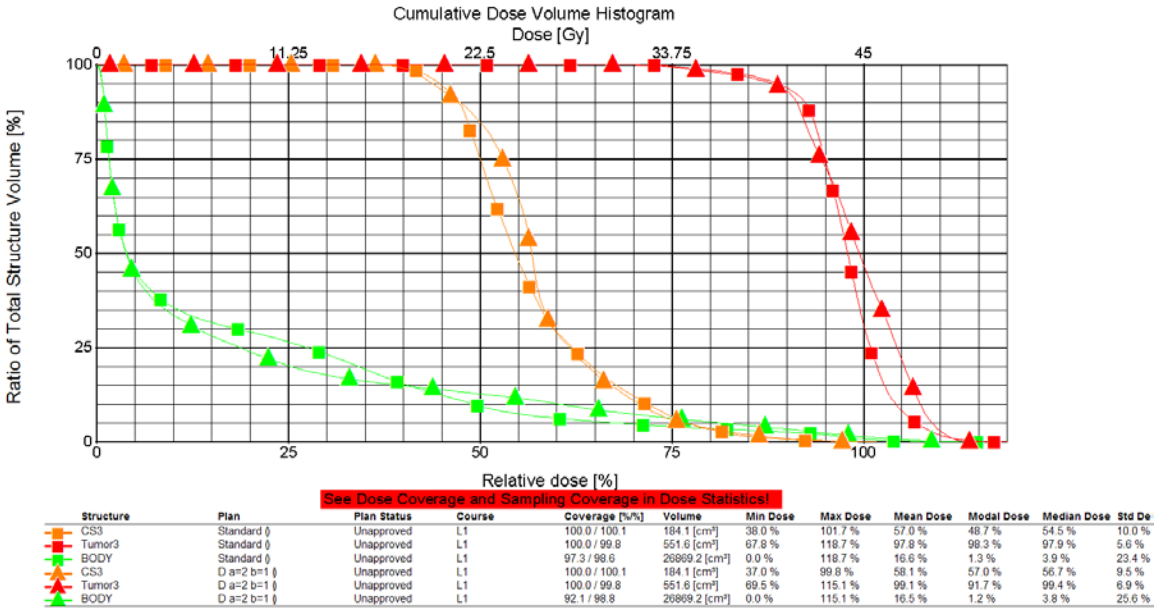

Figure G.33: cDVH of equispaced IMRT plan vs. optimized IMRT plan using Method 2 algorithm with sela=2 and selb=1 for the L-shaped target geometry

The triangle data points represent the optimized IMRT plan and the square data points represent the equispaced IMRT plan. In addition, the same beam angle arrangement is used for sela=2 and selb=2.

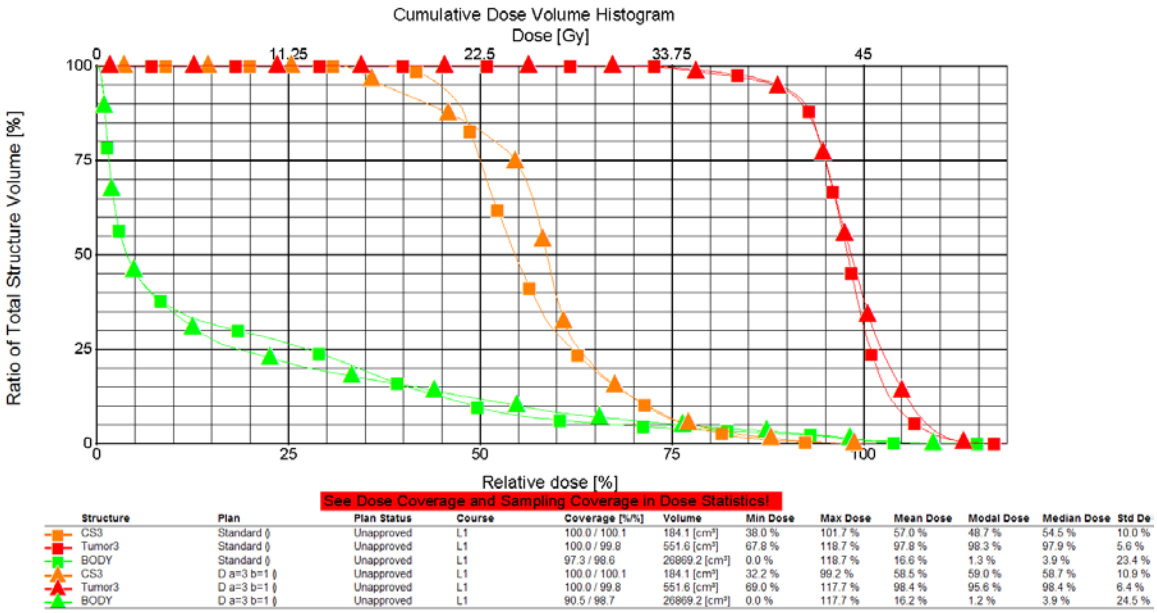

Structure	Plan	Plan Status	Course	Coverage [%/%]	Volume	Min Dose	Max Dose	Mean Dose	Modal Dose	Median Dose	Std De
CS3	Standard ()	Unapproved	L1	100.0 / 100.1	184.1 [cm³]	38.0 %	101.7 %	57.0 %	48.7 %	54.5 %	10.0 %
Tumor3	Standard ()	Unapproved	L1	100.0 / 99.8	551.6 [cm³]	67.8 %	118.7 %	97.8 %	98.3 %	97.9 %	5.6 %
BODY	Standard ()	Unapproved	L1	97.3 / 98.6	26869.2 [cm³]	0.0 %	118.7 %	16.6 %	1.3 %	3.9 %	23.4 %
CS3	D a=3 b=1 ()	Unapproved	L1	100.0 / 100.1	184.1 [cm³]	32.2 %	99.2 %	58.5 %	59.0 %	58.7 %	10.9 %
Tumor3	D a=3 b=1 ()	Unapproved	L1	100.0 / 99.8	551.6 [cm³]	69.0 %	117.7 %	98.4 %	95.6 %	98.4 %	6.4 %
BODY	D a=3 b=1 ()	Unapproved	L1	90.5 / 98.7	26869.2 [cm³]	0.0 %	117.7 %	16.2 %	1.2 %	3.9 %	24.5 %

Figure G.34: cDVH of equispaced IMRT plan vs. optimized IMRT plan using Method 2 algorithm with sela=3 and selb=1 for the L-shaped target geometry

The triangle data points represent the optimized IMRT plan and the square data points represent the equispaced IMRT plan.

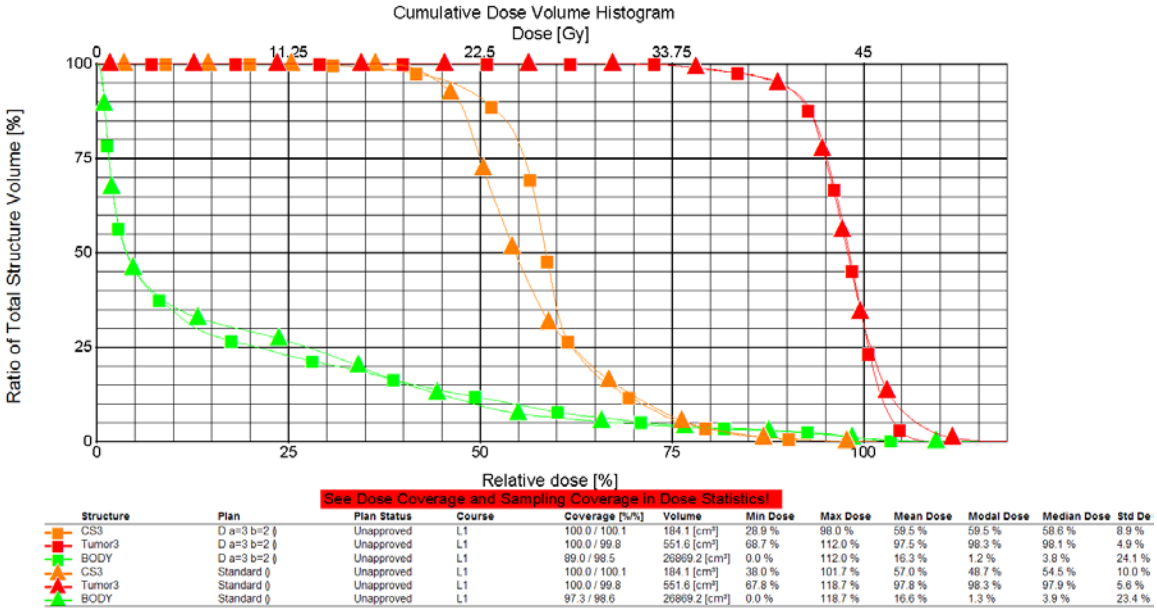

Structure	Plan	Plan Status	Course	Coverage [%/%]	Volume	Min Dose	Max Dose	Mean Dose	Modal Dose	Median Dose	Std De
CS3	D a=3 b=2 ()	Unapproved	L1	100.0 / 100.1	184.1 [cm³]	28.9 %	98.0 %	59.5 %	59.5 %	58.6 %	8.9 %
Tumor3	D a=3 b=2 ()	Unapproved	L1	100.0 / 99.8	551.6 [cm³]	68.7 %	112.0 %	97.5 %	98.3 %	98.1 %	4.9 %
BODY	D a=3 b=2 ()	Unapproved	L1	99.0 / 98.5	26869.2 [cm³]	0.0 %	112.0 %	16.3 %	1.2 %	3.8 %	24.1 %
CS3	Standard ()	Unapproved	L1	100.0 / 100.1	184.1 [cm³]	38.0 %	101.7 %	57.0 %	48.7 %	54.5 %	10.0 %
Tumor3	Standard ()	Unapproved	L1	100.0 / 99.8	551.6 [cm³]	67.8 %	118.7 %	97.8 %	98.3 %	97.9 %	5.6 %
BODY	Standard ()	Unapproved	L1	97.3 / 98.6	26869.2 [cm³]	0.0 %	118.7 %	16.6 %	1.3 %	3.9 %	23.4 %

Figure G.35: cDVH of equispaced IMRT plan vs. optimized IMRT plan using Method 2 algorithm with sela=3 and selb=2 for the L-shaped target geometry

The square data points represent the optimized IMRT plan and the triangle data points represent the equispaced IMRT plan.

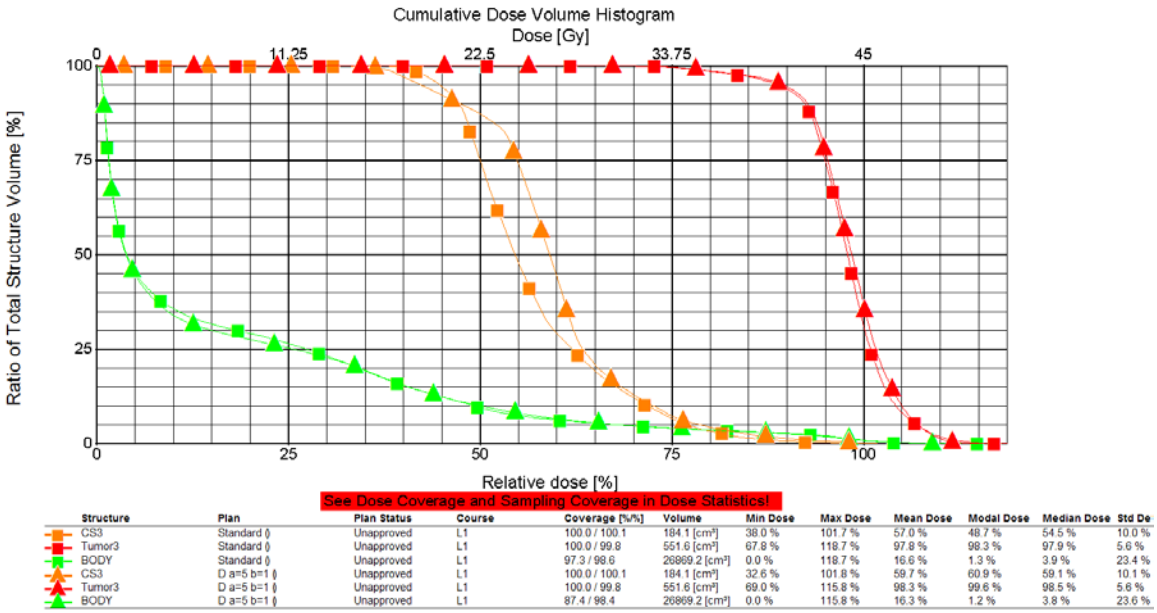

Structure	Plan	Plan Status	Course	Coverage [%/%]	Volume	Min Dose	Max Dose	Mean Dose	Modal Dose	Median Dose	Std De
CS3	Standard ()	Unapproved	L1	100.0 / 100.1	184.1 [cm³]	38.0 %	101.7 %	57.0 %	48.7 %	54.5 %	10.0 %
Tumor3	Standard ()	Unapproved	L1	100.0 / 99.8	551.6 [cm³]	67.8 %	118.7 %	97.8 %	98.3 %	97.9 %	5.6 %
BODY	Standard ()	Unapproved	L1	97.3 / 98.6	26869.2 [cm³]	0.0 %	118.7 %	16.6 %	1.3 %	3.9 %	23.4 %
CS3	D a=5 b=1 ()	Unapproved	L1	100.0 / 100.1	184.1 [cm³]	32.6 %	101.8 %	59.7 %	60.9 %	59.1 %	10.1 %
Tumor3	D a=5 b=1 ()	Unapproved	L1	100.0 / 99.8	551.6 [cm³]	69.0 %	115.8 %	98.3 %	99.6 %	98.5 %	5.6 %
BODY	D a=5 b=1 ()	Unapproved	L1	87.4 / 98.4	26869.2 [cm³]	0.0 %	115.8 %	16.3 %	1.2 %	3.8 %	23.6 %

Figure G.36: cDVH of equispaced IMRT plan vs. optimized IMRT plan using Method 2 algorithm with sela=5 and selb=1 for the L-shaped target geometry

The triangle data points represent the optimized IMRT plan and the square data points represent the equispaced IMRT plan.

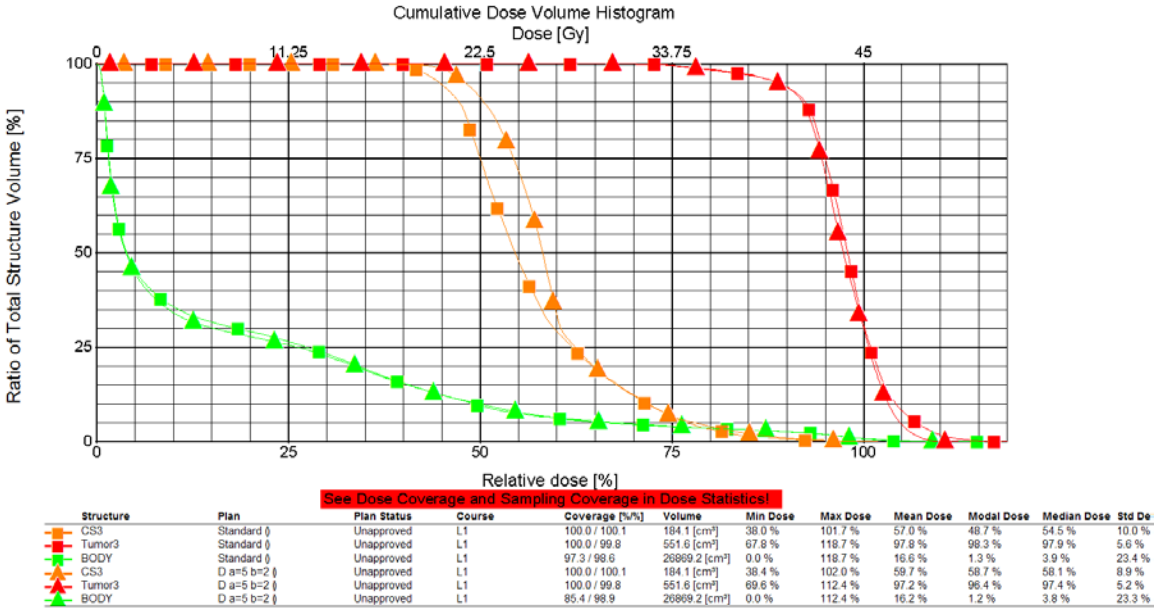

Structure	Plan	Plan Status	Course	Coverage [%/%]	Volume	Min Dose	Max Dose	Mean Dose	Modal Dose	Median Dose	Std De
CS3	Standard ()	Unapproved	L1	100.0 / 100.1	184.1 [cm³]	38.0 %	101.7 %	57.0 %	48.7 %	54.5 %	10.0 %
Tumor3	Standard ()	Unapproved	L1	100.0 / 99.8	551.6 [cm³]	67.8 %	118.7 %	97.8 %	98.3 %	97.9 %	5.6 %
BODY	Standard ()	Unapproved	L1	97.3 / 98.6	26869.2 [cm³]	0.0 %	118.7 %	16.6 %	1.3 %	3.9 %	23.4 %
CS3	D a=5 b=2 ()	Unapproved	L1	100.0 / 100.1	184.1 [cm³]	38.4 %	102.0 %	59.7 %	58.7 %	58.1 %	8.9 %
Tumor3	D a=5 b=2 ()	Unapproved	L1	100.0 / 99.8	551.6 [cm³]	69.6 %	112.4 %	97.2 %	96.4 %	97.4 %	5.2 %
BODY	D a=5 b=2 ()	Unapproved	L1	85.4 / 98.9	26869.2 [cm³]	0.0 %	112.4 %	16.2 %	1.2 %	3.8 %	23.3 %

Figure G.37: cDVH of equispaced IMRT plan vs. optimized IMRT plan using Method 2 algorithm with sela=5 and selb=2 for the L-shaped target geometry

The triangle data points represent the optimized IMRT plan and the square data points represent the equispaced IMRT plan.

G.3 U-Shaped Target Geometry

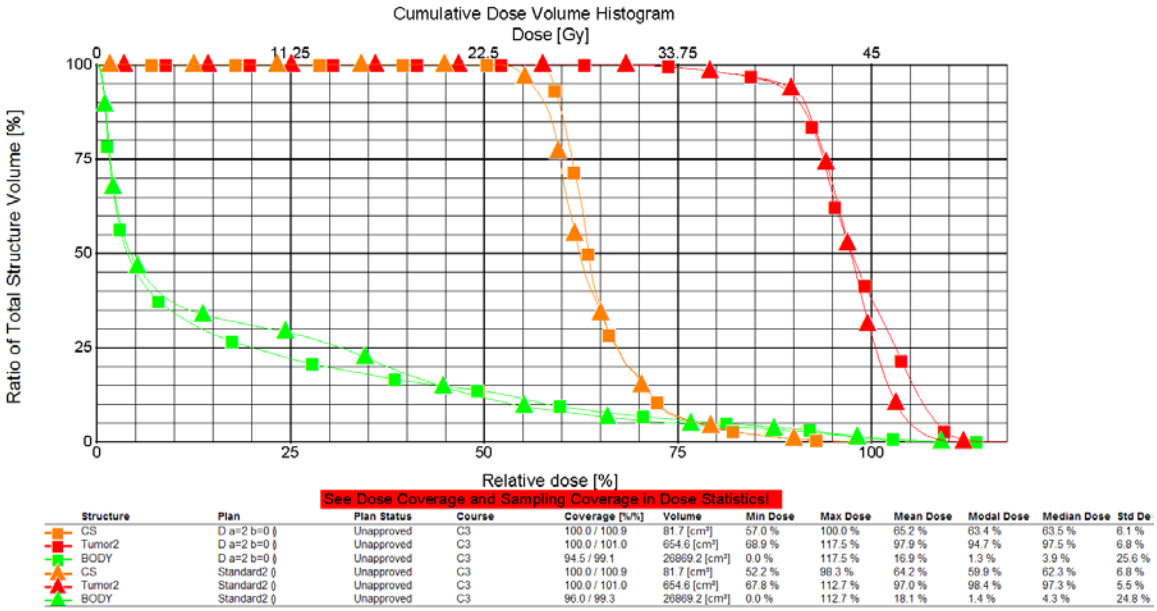

Structure	Plan	Plan Status	Course	Coverage [%/%]	Volume	Min Dose	Max Dose	Mean Dose	Modal Dose	Median Dose	Std De
CS	D a=2 b=0 ()	Unapproved	C3	100.0 / 100.9	81.7 [cm³]	57.0 %	100.0 %	65.2 %	63.4 %	63.5 %	6.1 %
Tumor2	D a=2 b=0 ()	Unapproved	C3	100.0 / 101.0	654.6 [cm³]	68.9 %	117.5 %	97.9 %	94.7 %	97.5 %	6.8 %
BODY	D a=2 b=0 ()	Unapproved	C3	94.5 / 99.1	26869.2 [cm³]	0.0 %	117.5 %	16.9 %	1.3 %	3.9 %	25.6 %
CS	Standard2 ()	Unapproved	C3	100.0 / 100.9	81.7 [cm³]	52.2 %	98.3 %	64.2 %	59.9 %	62.3 %	6.8 %
Tumor2	Standard2 ()	Unapproved	C3	100.0 / 101.0	654.6 [cm³]	67.8 %	112.7 %	97.0 %	98.4 %	97.3 %	5.5 %
BODY	Standard2 ()	Unapproved	C3	96.0 / 99.3	26869.2 [cm³]	0.0 %	112.7 %	18.1 %	1.4 %	4.3 %	24.8 %

Figure G.38: cDVH of equispaced IMRT plan vs. optimized IMRT plan using Method 2 algorithm with sela=2 and selb=0 for the U-shaped target geometry

The square data points represent the optimized IMRT plan and the triangle data points represent the equispaced IMRT plan.

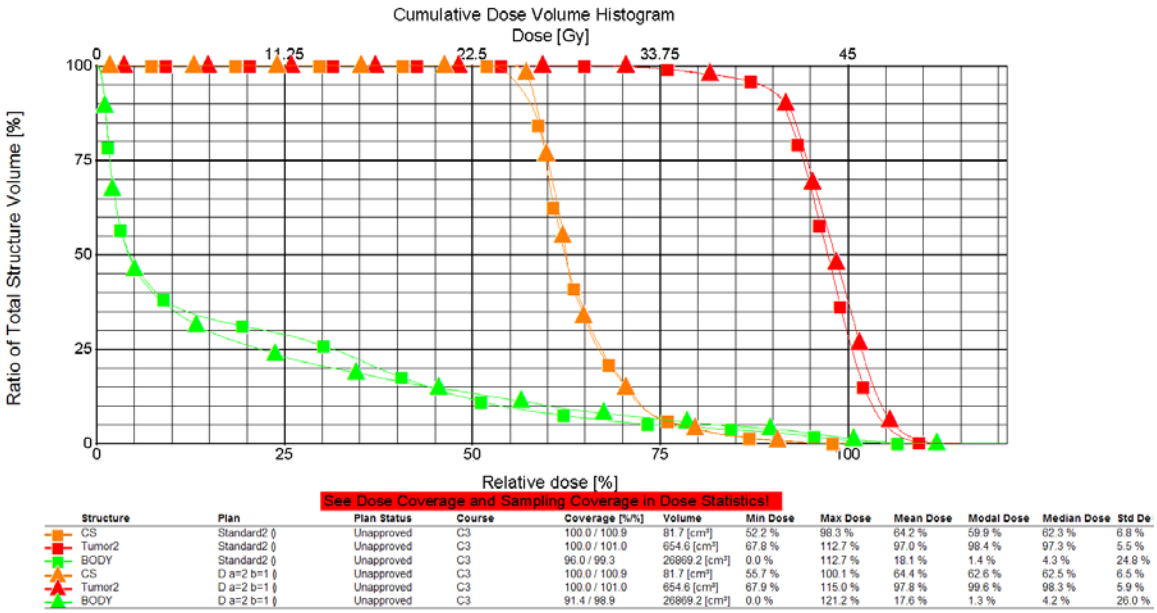

Structure	Plan	Plan Status	Course	Coverage [%/%]	Volume	Min Dose	Max Dose	Mean Dose	Modal Dose	Median Dose	Std De
CS	Standard2 ()	Unapproved	C3	100.0 / 100.9	81.7 [cm³]	52.2 %	98.3 %	64.2 %	59.9 %	62.3 %	6.8 %
Tumor2	Standard2 ()	Unapproved	C3	100.0 / 101.0	654.6 [cm³]	67.8 %	112.7 %	97.0 %	98.4 %	97.3 %	5.5 %
BODY	Standard2 ()	Unapproved	C3	96.0 / 99.3	26869.2 [cm³]	0.0 %	112.7 %	18.1 %	1.4 %	4.3 %	24.8 %
CS	D a=2 b=1 ()	Unapproved	C3	100.0 / 100.9	81.7 [cm³]	55.7 %	100.1 %	64.4 %	62.6 %	62.5 %	6.5 %
Tumor2	D a=2 b=1 ()	Unapproved	C3	100.0 / 101.0	654.6 [cm³]	67.9 %	115.0 %	97.8 %	99.6 %	98.3 %	5.9 %
BODY	D a=2 b=1 ()	Unapproved	C3	91.4 / 98.9	26869.2 [cm³]	0.0 %	121.2 %	17.6 %	1.3 %	4.2 %	26.0 %

Figure G.39: cDVH of equispaced IMRT plan vs. optimized IMRT plan using Method 2 algorithm with sela=2 and selb=1 for the U-shaped target geometry

The triangle data points represent the optimized IMRT plan and the square data points represent the equispaced IMRT plan.

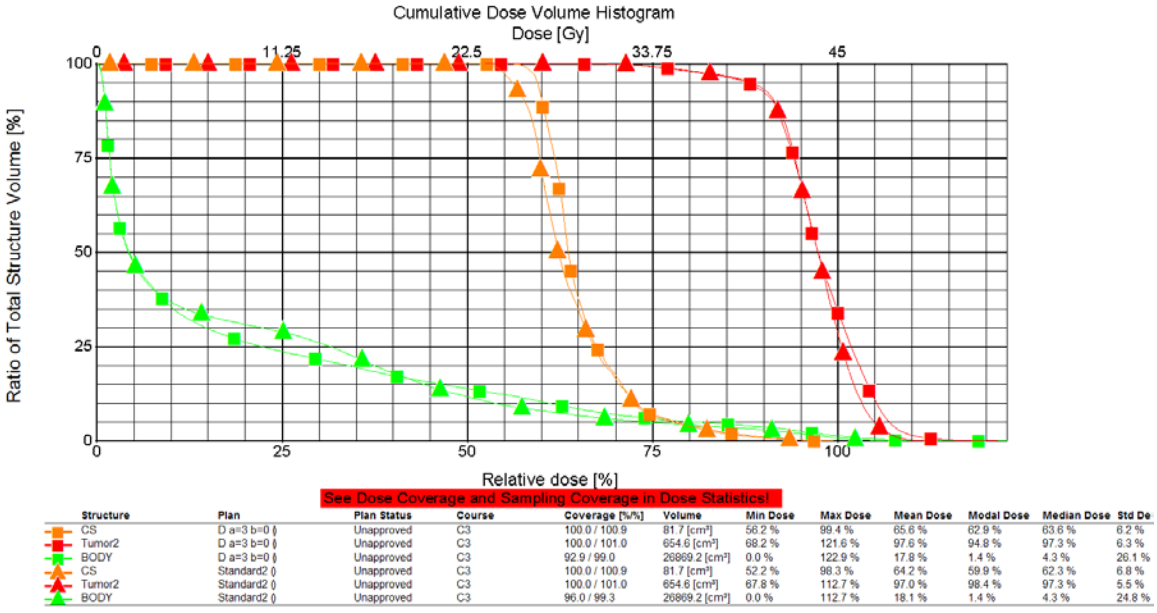

Structure	Plan	Plan Status	Course	Coverage [%/%]	Volume	Min Dose	Max Dose	Mean Dose	Modal Dose	Median Dose	Std De
CS	D a=3 b=0 ()	Unapproved	C3	100.0 / 100.9	81.7 [cm³]	56.2 %	99.4 %	65.6 %	62.9 %	63.6 %	6.2 %
Tumor2	D a=3 b=0 ()	Unapproved	C3	100.0 / 101.0	654.6 [cm³]	68.2 %	121.6 %	97.6 %	94.8 %	97.3 %	6.3 %
BODY	D a=3 b=0 ()	Unapproved	C3	92.9 / 99.0	26869.2 [cm³]	0.0 %	122.9 %	17.8 %	1.4 %	4.3 %	26.1 %
CS	Standard2 ()	Unapproved	C3	100.0 / 100.9	81.7 [cm³]	52.2 %	98.3 %	64.2 %	59.9 %	62.3 %	6.8 %
Tumor2	Standard2 ()	Unapproved	C3	100.0 / 101.0	654.6 [cm³]	67.8 %	112.7 %	97.0 %	98.4 %	97.3 %	5.5 %
BODY	Standard2 ()	Unapproved	C3	96.0 / 99.3	26869.2 [cm³]	0.0 %	112.7 %	18.1 %	1.4 %	4.3 %	24.8 %

Figure G.40: cDVH of equispaced IMRT plan vs. optimized IMRT plan using Method 2 algorithm with sela=3 and selb=0 for the U-shaped target geometry

The square data points represent the optimized IMRT plan and the triangle data points represent the equispaced IMRT plan. In addition, the same beam angle arrangement is used for sela=3 and selb=1.

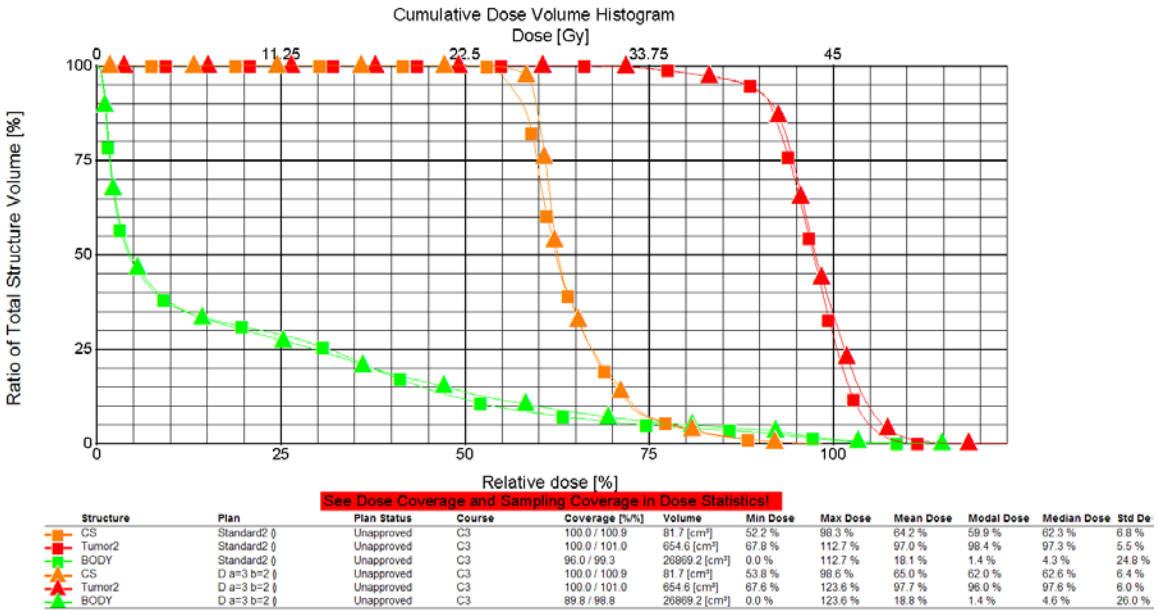

Structure	Plan	Plan Status	Course	Coverage [%/%]	Volume	Min Dose	Max Dose	Mean Dose	Modal Dose	Median Dose	Std De
CS	Standard2 ()	Unapproved	C3	100.0 / 100.9	81.7 [cm³]	52.2 %	98.3 %	64.2 %	59.9 %	62.3 %	6.8 %
Tumor2	Standard2 ()	Unapproved	C3	100.0 / 101.0	654.6 [cm³]	67.8 %	112.7 %	97.0 %	98.4 %	97.3 %	5.5 %
BODY	Standard2 ()	Unapproved	C3	96.0 / 99.3	26869.2 [cm³]	0.0 %	112.7 %	18.1 %	1.4 %	4.3 %	24.8 %
CS	D a=3 b=2 ()	Unapproved	C3	100.0 / 100.9	81.7 [cm³]	53.8 %	98.6 %	65.0 %	62.0 %	62.6 %	6.4 %
Tumor2	D a=3 b=2 ()	Unapproved	C3	100.0 / 101.0	654.6 [cm³]	67.6 %	123.6 %	97.7 %	96.0 %	97.6 %	6.0 %
BODY	D a=3 b=2 ()	Unapproved	C3	89.8 / 98.8	26869.2 [cm³]	0.0 %	123.6 %	18.8 %	1.4 %	4.6 %	26.0 %

Figure G.41: cDVH of equispaced IMRT plan vs. optimized IMRT plan using Method 2 algorithm with sela=3 and selb=2 for the U-shaped target geometry

The triangle data points represent the optimized IMRT plan and the square data points represent the equispaced IMRT plan.

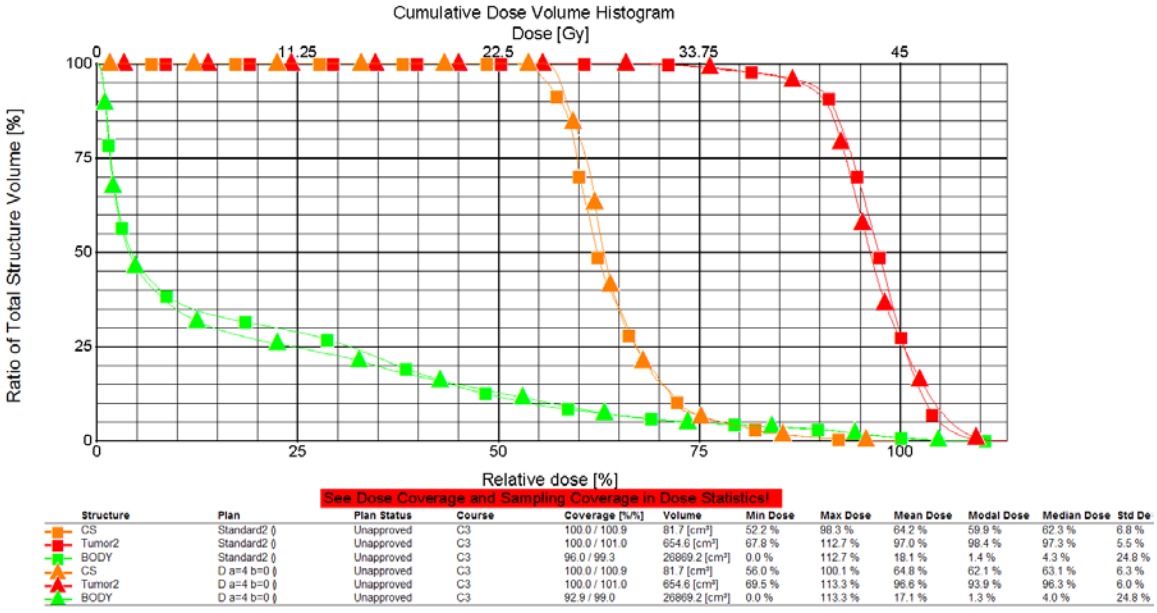

Structure	Plan	Plan Status	Course	Coverage [%/%]	Volume	Min Dose	Max Dose	Mean Dose	Modal Dose	Median Dose	Std De
CS	Standard2 ()	Unapproved	C3	100.0 / 100.9	81.7 [cm³]	52.2 %	98.3 %	64.2 %	59.9 %	62.3 %	6.8 %
Tumor2	Standard2 ()	Unapproved	C3	100.0 / 101.0	654.6 [cm³]	67.8 %	112.7 %	97.0 %	98.4 %	97.3 %	5.5 %
BODY	Standard2 ()	Unapproved	C3	96.0 / 99.3	26869.2 [cm³]	0.0 %	112.7 %	18.1 %	1.4 %	4.3 %	24.8 %
CS	D a=4 b=0 ()	Unapproved	C3	100.0 / 100.9	81.7 [cm³]	56.0 %	100.1 %	64.8 %	62.1 %	63.1 %	6.3 %
Tumor2	D a=4 b=0 ()	Unapproved	C3	100.0 / 101.0	654.6 [cm³]	69.5 %	113.3 %	96.6 %	93.9 %	96.3 %	6.0 %
BODY	D a=4 b=0 ()	Unapproved	C3	92.9 / 99.0	26869.2 [cm³]	0.0 %	113.3 %	17.1 %	1.3 %	4.0 %	24.8 %

Figure G.42: cDVH of equispaced IMRT plan vs. optimized IMRT plan using Method 2 algorithm with sela=4 and selb=0 for the U-shaped target geometry

The triangle data points represent the optimized IMRT plan and the square data points represent the equispaced IMRT plan.

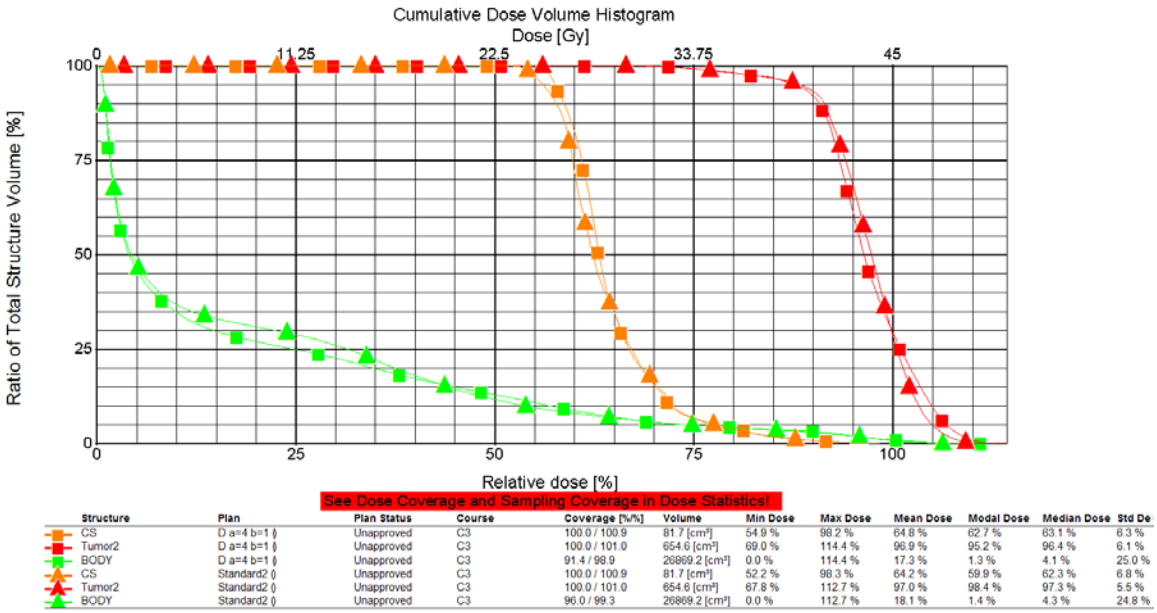

Structure	Plan	Plan Status	Course	Coverage [%/%]	Volume	Min Dose	Max Dose	Mean Dose	Modal Dose	Median Dose	Std De
CS	D a=4 b=1 ()	Unapproved	C3	100.0 / 100.9	81.7 [cm³]	54.9 %	98.2 %	64.8 %	62.7 %	63.1 %	6.3 %
Tumor2	D a=4 b=1 ()	Unapproved	C3	100.0 / 101.0	654.6 [cm³]	69.0 %	114.4 %	96.9 %	95.2 %	96.4 %	6.1 %
BODY	D a=4 b=1 ()	Unapproved	C3	91.4 / 98.9	26869.2 [cm³]	0.0 %	114.4 %	17.3 %	1.3 %	4.1 %	25.0 %
CS	Standard2 ()	Unapproved	C3	100.0 / 100.9	81.7 [cm³]	52.2 %	98.3 %	64.2 %	59.9 %	62.3 %	6.8 %
Tumor2	Standard2 ()	Unapproved	C3	100.0 / 101.0	654.6 [cm³]	67.8 %	112.7 %	97.0 %	98.4 %	97.3 %	5.5 %
BODY	Standard2 ()	Unapproved	C3	96.0 / 99.3	26869.2 [cm³]	0.0 %	112.7 %	18.1 %	1.4 %	4.3 %	24.8 %

Figure G.43: cDVH of equispaced IMRT plan vs. optimized IMRT plan using Method 2 algorithm with sela=4 and selb=1 for the U-shaped target geometry

The square data points represent the optimized IMRT plan and the triangle data points represent the equispaced IMRT plan.

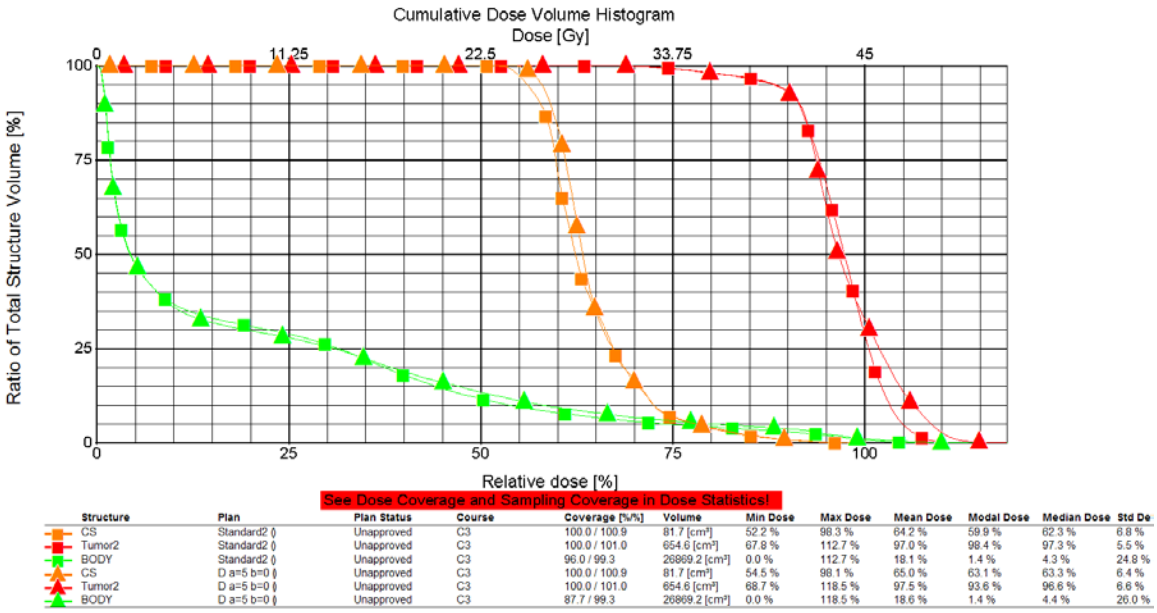

Structure	Plan	Plan Status	Course	Coverage [%/%]	Volume	Min Dose	Max Dose	Mean Dose	Modal Dose	Median Dose	Std De
CS	Standard2 ()	Unapproved	C3	100.0 / 100.9	81.7 [cm³]	52.2 %	98.3 %	64.2 %	59.9 %	62.3 %	6.8 %
Tumor2	Standard2 ()	Unapproved	C3	100.0 / 101.0	654.6 [cm³]	67.8 %	112.7 %	97.0 %	98.4 %	97.3 %	5.5 %
BODY	Standard2 ()	Unapproved	C3	96.0 / 99.3	26869.2 [cm³]	0.0 %	112.7 %	18.1 %	1.4 %	4.3 %	24.8 %
CS	D a=5 b=0 ()	Unapproved	C3	100.0 / 100.9	81.7 [cm³]	54.5 %	98.1 %	65.0 %	63.1 %	63.3 %	6.4 %
Tumor2	D a=5 b=0 ()	Unapproved	C3	100.0 / 101.0	654.6 [cm³]	68.7 %	118.5 %	97.5 %	93.6 %	96.6 %	6.6 %
BODY	D a=5 b=0 ()	Unapproved	C3	87.7 / 99.3	26869.2 [cm³]	0.0 %	118.5 %	18.6 %	1.4 %	4.4 %	26.0 %

Figure G.44: cDVH of equispaced IMRT plan vs. optimized IMRT plan using Method 2 algorithm with sela=5 and selb=0 for the U-shaped target geometry

The triangle data points represent the optimized IMRT plan and the square data points represent the equispaced IMRT plan.

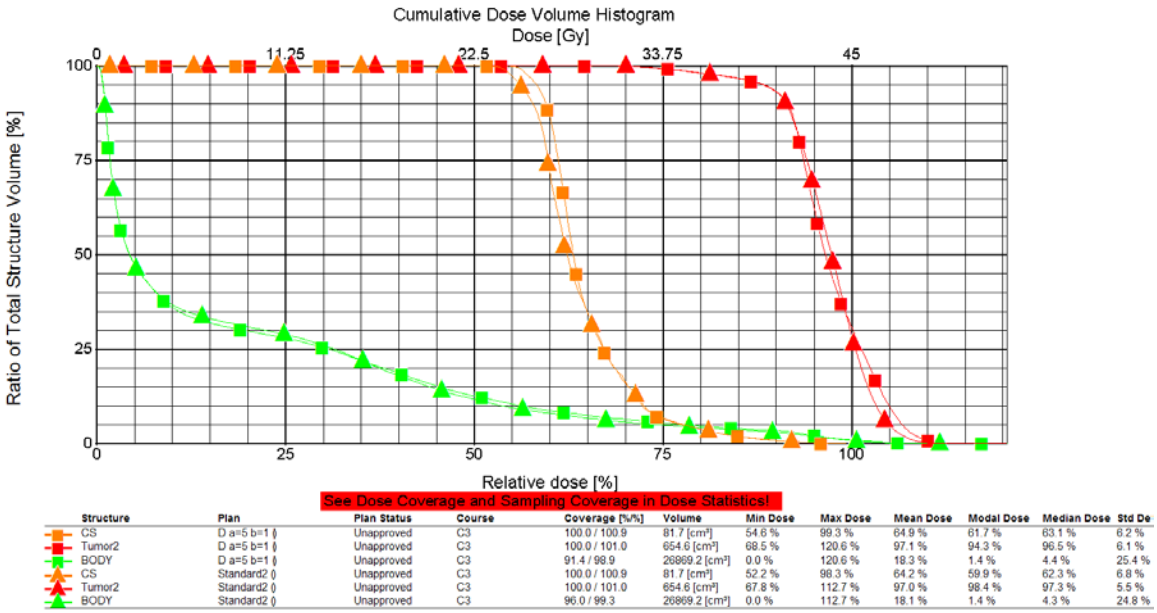

Structure	Plan	Plan Status	Course	Coverage [%/%]	Volume	Min Dose	Max Dose	Mean Dose	Modal Dose	Median Dose	Std De
CS	D a=5 b=1 ()	Unapproved	C3	100.0 / 100.9	81.7 [cm³]	54.6 %	99.3 %	64.9 %	61.7 %	63.1 %	6.2 %
Tumor2	D a=5 b=1 ()	Unapproved	C3	100.0 / 101.0	654.6 [cm³]	68.5 %	120.6 %	97.1 %	94.3 %	96.5 %	6.1 %
BODY	D a=5 b=1 ()	Unapproved	C3	91.4 / 98.9	26869.2 [cm³]	0.0 %	120.6 %	18.3 %	1.4 %	4.4 %	25.4 %
CS	Standard2 ()	Unapproved	C3	100.0 / 100.9	81.7 [cm³]	52.2 %	98.3 %	64.2 %	59.9 %	62.3 %	6.8 %
Tumor2	Standard2 ()	Unapproved	C3	100.0 / 101.0	654.6 [cm³]	67.8 %	112.7 %	97.0 %	98.4 %	97.3 %	5.5 %
BODY	Standard2 ()	Unapproved	C3	96.0 / 99.3	26869.2 [cm³]	0.0 %	112.7 %	18.1 %	1.4 %	4.3 %	24.8 %

Figure G.45: cDVH of equispaced IMRT plan vs. optimized IMRT plan using Method 2 algorithm with sela=5 and selb=1 for the U-shaped target geometry

The square data points represent the optimized IMRT plan and the triangle data points represent the equispaced IMRT plan.

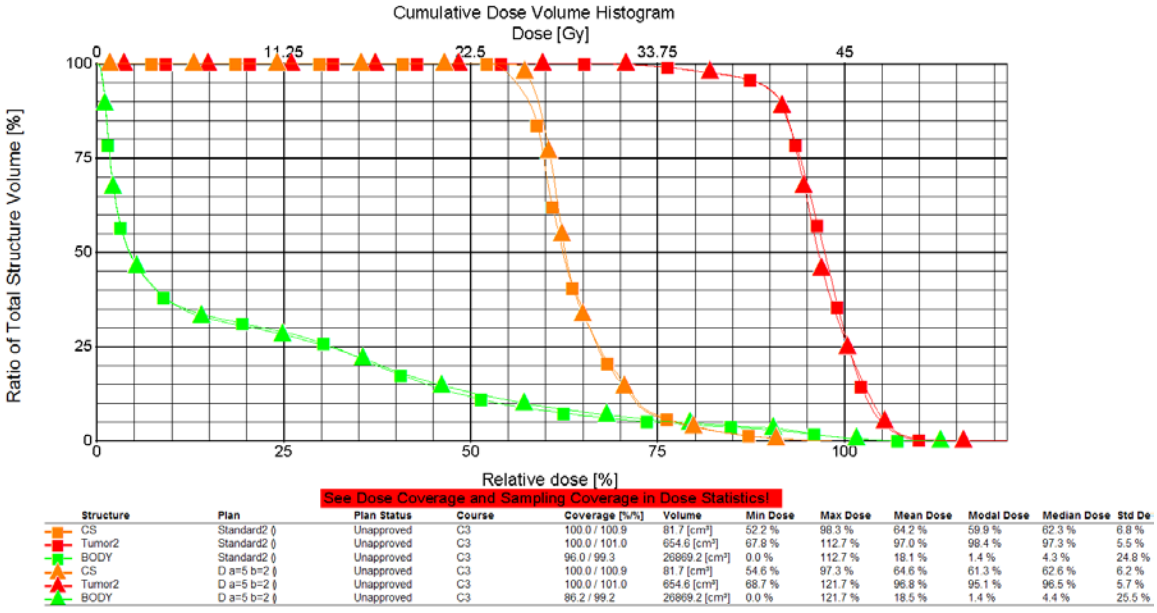

Structure	Plan	Plan Status	Course	Coverage [%/%]	Volume	Min Dose	Max Dose	Mean Dose	Modal Dose	Median Dose	Std De
CS	Standard2 ()	Unapproved	C3	100.0 / 100.9	81.7 [cm³]	52.2 %	98.3 %	64.2 %	59.9 %	62.3 %	6.8 %
Tumor2	Standard2 ()	Unapproved	C3	100.0 / 101.0	654.6 [cm³]	67.8 %	112.7 %	97.0 %	98.4 %	97.3 %	5.5 %
BODY	Standard2 ()	Unapproved	C3	96.0 / 99.3	26869.2 [cm³]	0.0 %	112.7 %	18.1 %	1.4 %	4.3 %	24.8 %
CS	D a=5 b=2 ()	Unapproved	C3	100.0 / 100.9	81.7 [cm³]	54.6 %	97.3 %	64.6 %	61.3 %	62.6 %	6.2 %
Tumor2	D a=5 b=2 ()	Unapproved	C3	100.0 / 101.0	654.6 [cm³]	68.7 %	121.7 %	96.8 %	95.1 %	96.5 %	5.7 %
BODY	D a=5 b=2 ()	Unapproved	C3	86.2 / 99.2	26869.2 [cm³]	0.0 %	121.7 %	18.5 %	1.4 %	4.4 %	25.5 %

Figure G.46: cDVH of equispaced IMRT plan vs. optimized IMRT plan using Method 2 algorithm with sela=5 and selb=2 for the U-shaped target geometry

The triangle data points represent the optimized IMRT plan and the square data points represent the equispaced IMRT plan.

APPENDIX H

Method 2 cDVHs with Rotated MCNP Simulation Data

The red data points represent the cDVH of the target volume, the orange data points represent the cDVH of the critical structure, and the green data points represent the cDVH of the normal tissue in the following figures.

H.1 Square Target Geometry

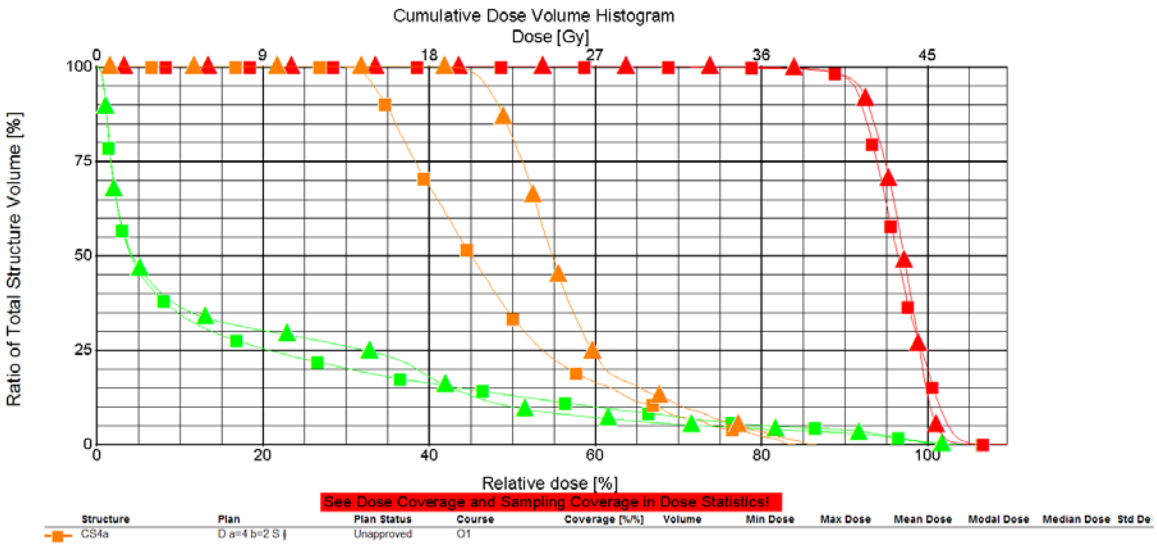

Figure H.47: cDVH of equispaced IMRT plan vs. optimized IMRT plan using Method 2 algorithm with rotated MCNP simulation data, and sela=4 and selb=2 for the square target geometry

The square data points represent the optimized IMRT plan and the triangle data points represent the equispaced IMRT plan.

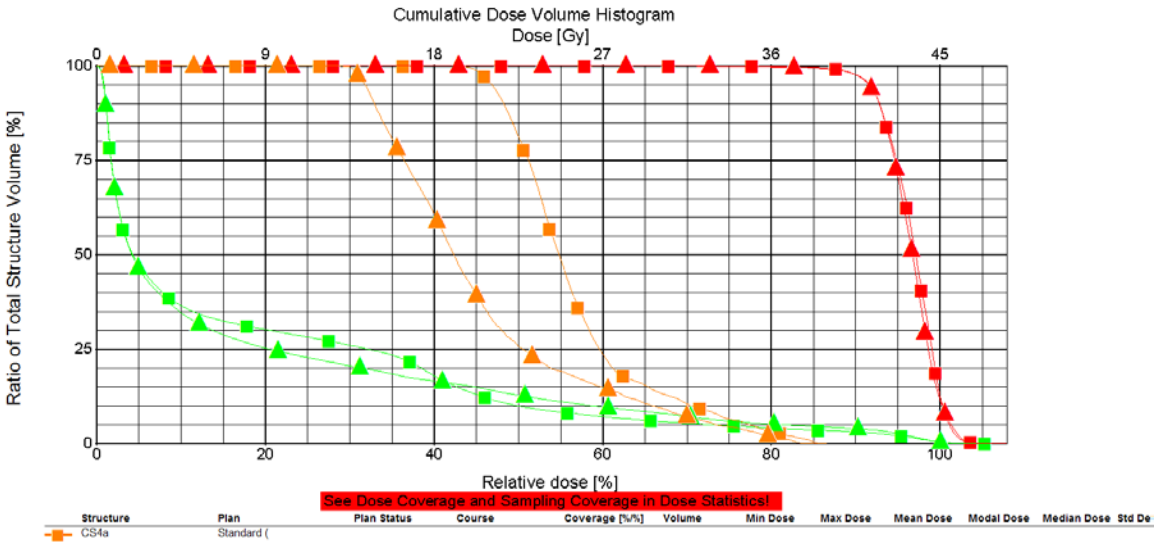

Figure H.48: cDVH of equispaced IMRT plan vs. optimized IMRT plan using Method 2 algorithm with rotated MCNP simulation data, and sela=4 and selb=3 for the square target geometry

The triangle data points represent the optimized IMRT plan and the square data points represent the equispaced IMRT plan.

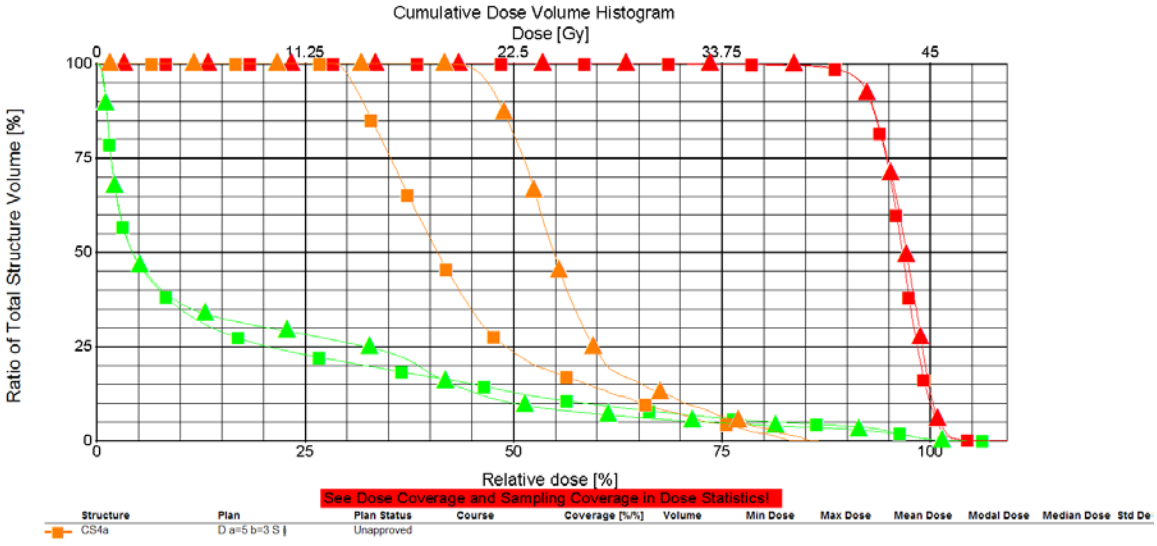

Figure H.49: cDVH of equispaced IMRT plan vs. optimized IMRT plan using Method 2 algorithm with rotated MCNP simulation data, and sela=5 and selb=3 for the square target geometry

The square data points represent the optimized IMRT plan and the triangle data points represent the equispaced IMRT plan.

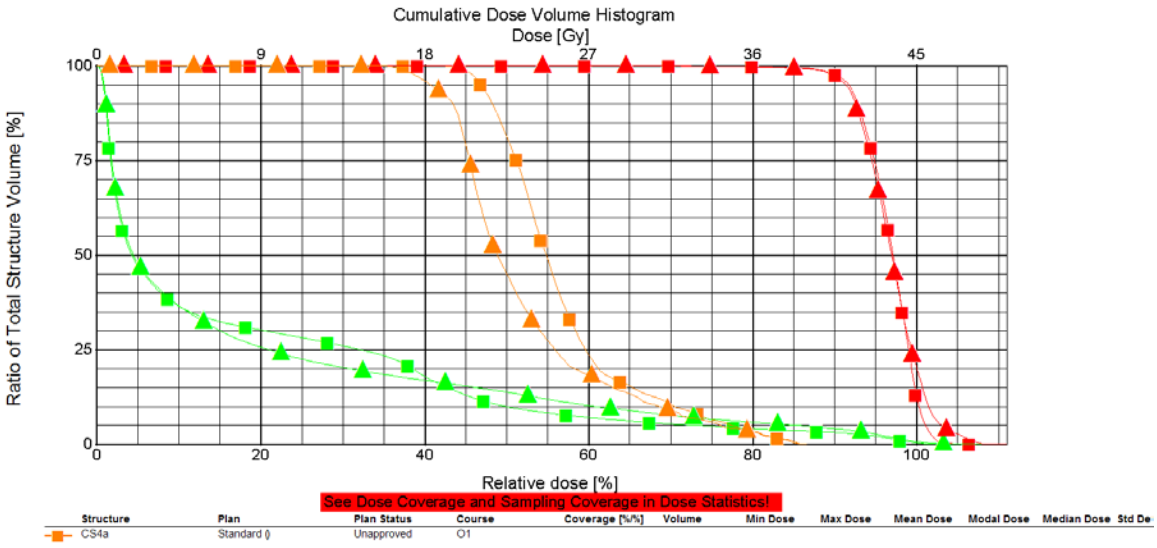

Figure H.50: cDVH of equispaced IMRT plan vs. optimized IMRT plan using Method 2 algorithm with rotated MCNP simulation data, and sela=5 and selb=4 for the square target geometry

The triangle data points represent the optimized IMRT plan and the square data points represent the equispaced IMRT plan.

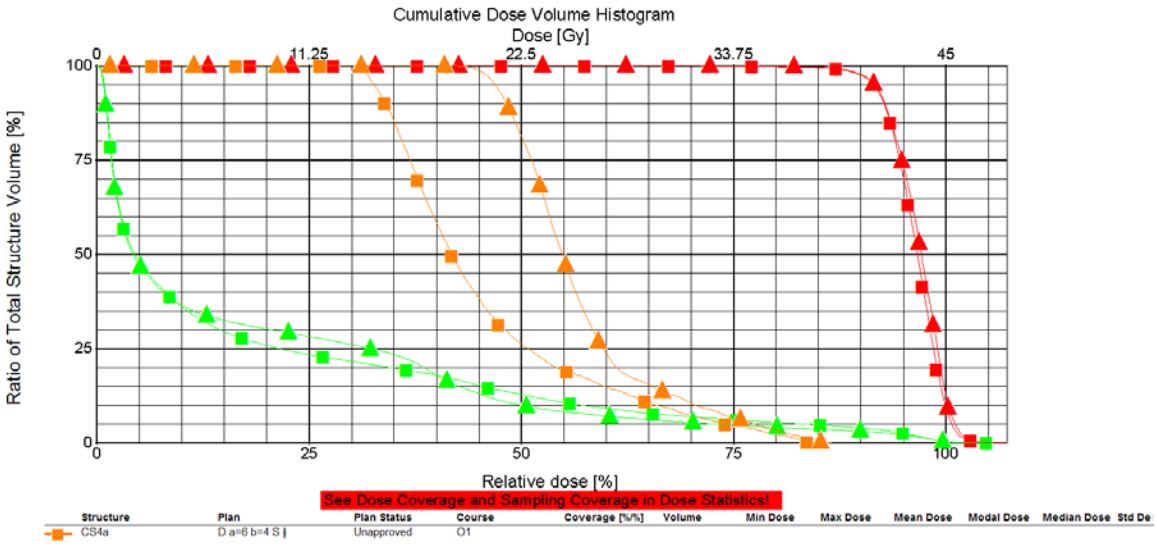

Figure H.51: cDVH of equispaced IMRT plan vs. optimized IMRT plan using Method 2 algorithm with rotated MCNP simulation data, and sela=6 and selb=4 for the square target geometry

The square data points represent the optimized IMRT plan and the triangle data points represent the equispaced IMRT plan.

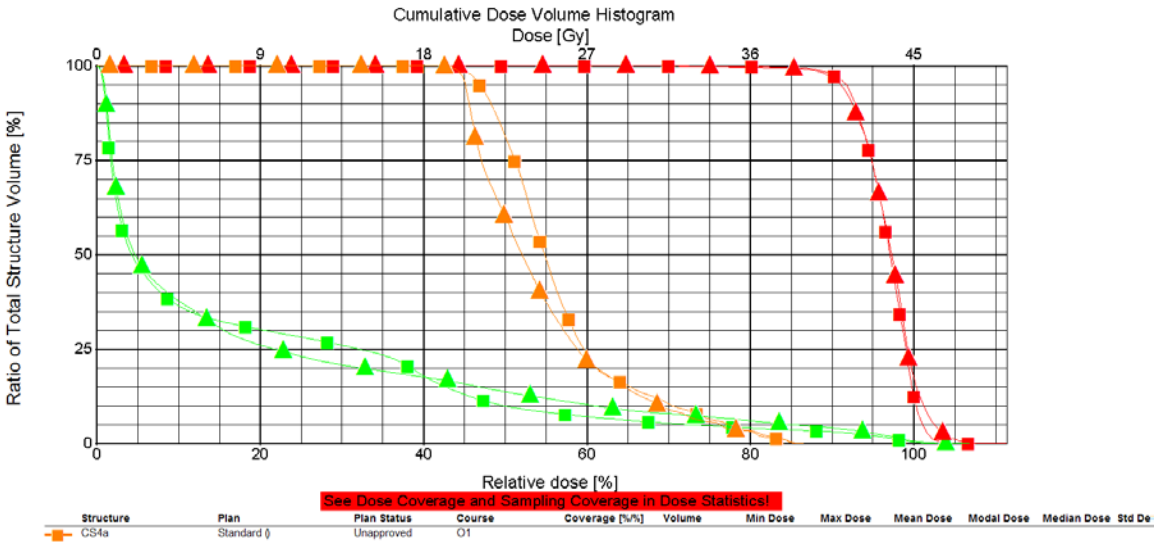

Figure H.52: cDVH of equispaced IMRT plan vs. optimized IMRT plan using Method 2 algorithm with rotated MCNP simulation data, and sela=6 and selb=5 for the square target geometry

The triangle data points represent the optimized IMRT plan and the square data points represent the equispaced IMRT plan.

H.2 L-Shaped Target Geometry

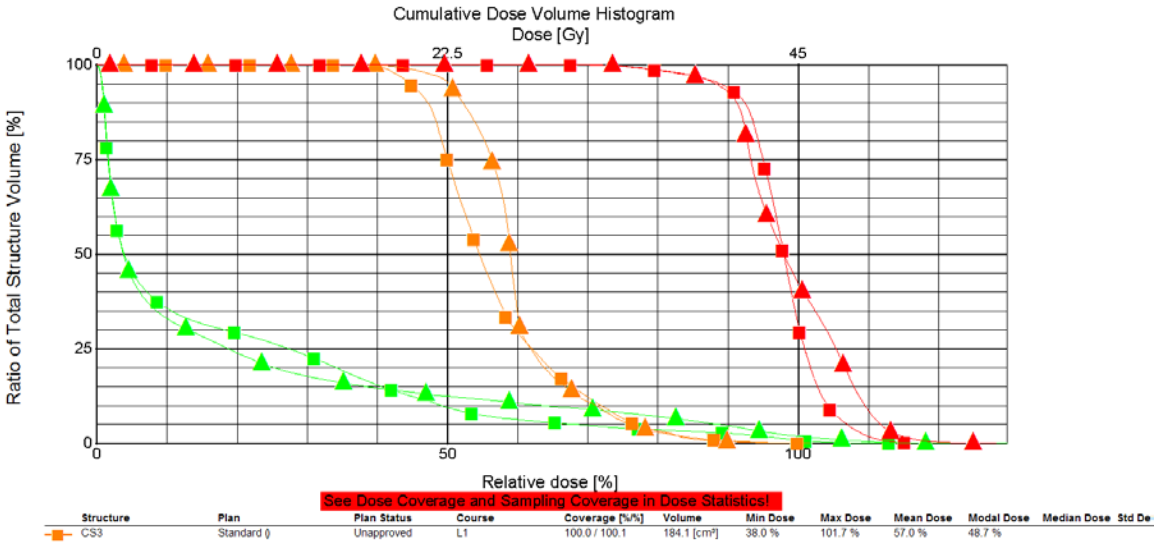

Figure H.53: cDVH of equispaced IMRT plan vs. optimized IMRT plan using Method 2 algorithm with rotated MCNP simulation data, and sela=4 and selb=2 for the L-shaped target geometry

The triangle data points represent the optimized IMRT plan and the square data points represent the equispaced IMRT plan.

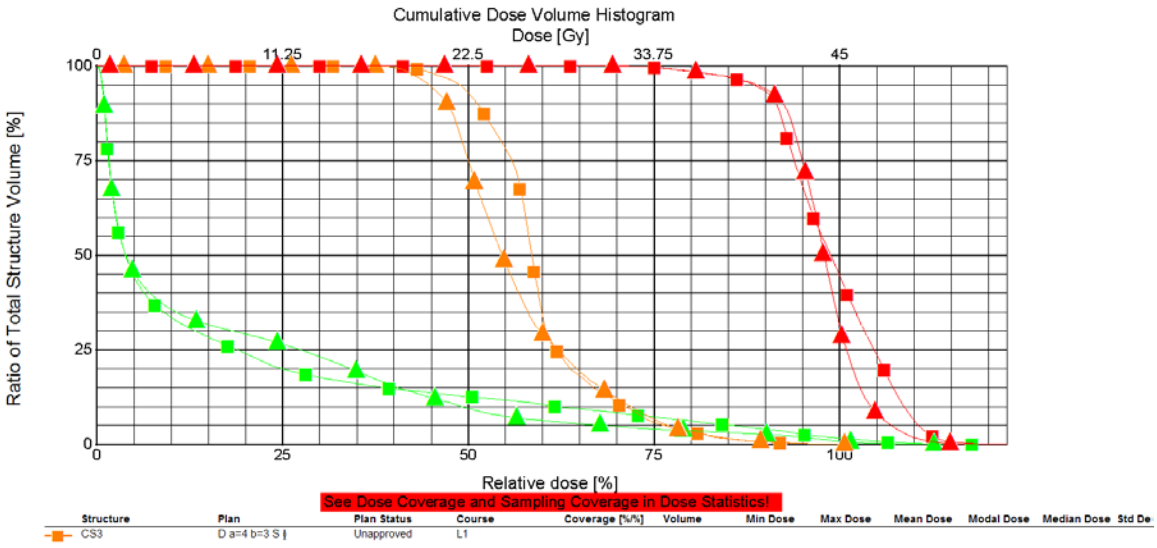

Figure H.54: cDVH of equispaced IMRT plan vs. optimized IMRT plan using Method 2 algorithm with rotated MCNP simulation data, and sela=4 and selb=3 for the L-shaped target geometry

The square data points represent the optimized IMRT plan and the triangle data points represent the equispaced IMRT plan.

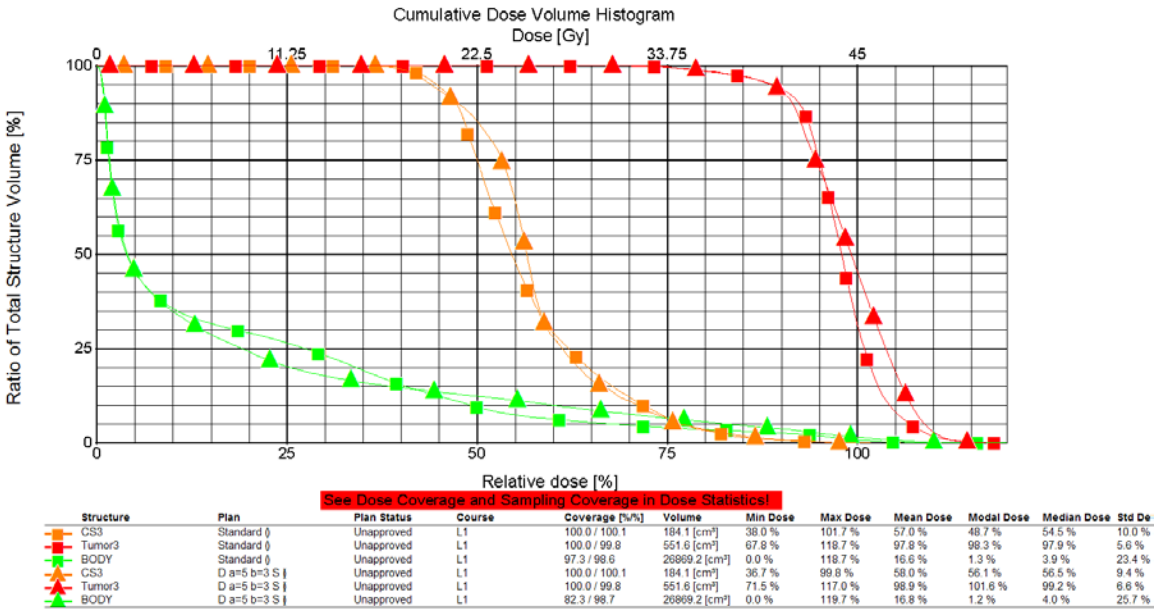

Figure H.55: cDVH of equispaced IMRT plan vs. optimized IMRT plan using Method 2 algorithm with rotated MCNP simulation data, and sela=5 and selb=3 for the L-shaped target geometry

The triangle data points represent the optimized IMRT plan and the square data points represent the equispaced IMRT plan.

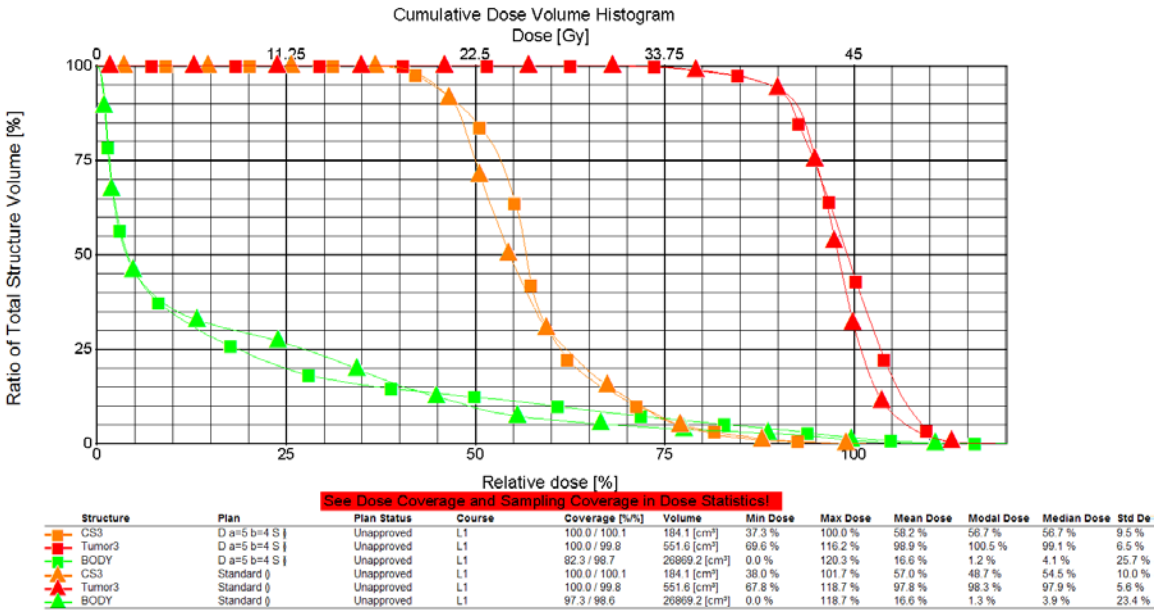

Structure	Plan	Plan Status	Course	Coverage [%/%]	Volume	Min Dose	Max Dose	Mean Dose	Modal Dose	Median Dose	Std De
CS3	D a=5 b=4 S	Unapproved	L1	100.0 / 100.1	184.1 [cm³]	37.3 %	100.0 %	58.2 %	56.7 %	56.7 %	9.5 %
Tumor3	D a=5 b=4 S	Unapproved	L1	100.0 / 99.8	551.6 [cm³]	69.6 %	116.2 %	98.9 %	100.5 %	99.1 %	6.5 %
BODY	D a=5 b=4 S	Unapproved	L1	82.3 / 98.7	26869.2 [cm³]	0.0 %	120.3 %	16.6 %	1.2 %	4.1 %	25.7 %
CS3	Standard ()	Unapproved	L1	100.0 / 100.1	184.1 [cm³]	38.0 %	101.7 %	57.0 %	48.7 %	54.5 %	10.0 %
Tumor3	Standard ()	Unapproved	L1	100.0 / 99.8	551.6 [cm³]	67.8 %	118.7 %	97.8 %	98.3 %	97.9 %	5.6 %
BODY	Standard ()	Unapproved	L1	97.3 / 98.6	26869.2 [cm³]	0.0 %	118.7 %	16.6 %	1.3 %	3.9 %	23.4 %

Figure H.56: cDVH of equispaced IMRT plan vs. optimized IMRT plan using Method 2 algorithm with rotated MCNP simulation data, and sela=5 and selb=4 for the L-shaped target geometry

The square data points represent the optimized IMRT plan and the triangle data points represent the equispaced IMRT plan.

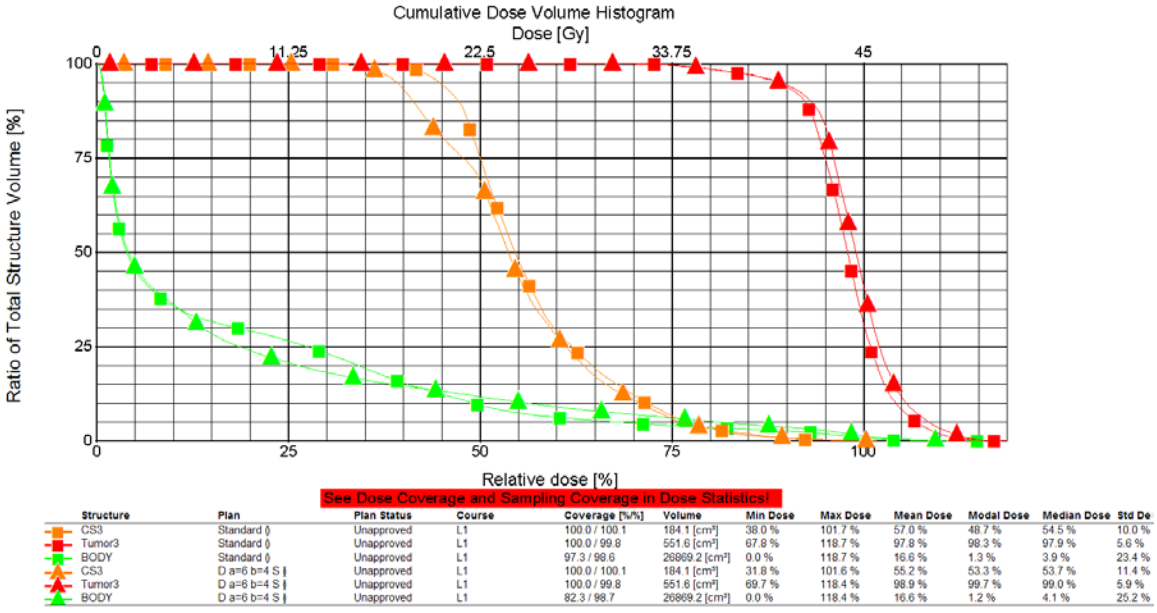

Structure	Plan	Plan Status	Course	Coverage [%/%]	Volume	Min Dose	Max Dose	Mean Dose	Modal Dose	Median Dose	Std De
CS3	Standard ()	Unapproved	L1	100.0 / 100.1	184.1 [cm³]	38.0 %	101.7 %	57.0 %	48.7 %	54.5 %	10.0 %
Tumor3	Standard ()	Unapproved	L1	100.0 / 99.8	551.6 [cm³]	67.8 %	118.7 %	97.8 %	98.3 %	97.9 %	5.6 %
BODY	Standard ()	Unapproved	L1	97.3 / 98.6	26869.2 [cm³]	0.0 %	118.7 %	16.6 %	1.3 %	3.9 %	23.4 %
CS3	D a=6 b=4 S	Unapproved	L1	100.0 / 100.1	184.1 [cm³]	31.8 %	101.6 %	55.2 %	53.3 %	53.7 %	11.4 %
Tumor3	D a=6 b=4 S	Unapproved	L1	100.0 / 99.8	551.6 [cm³]	69.7 %	118.4 %	98.9 %	99.7 %	99.0 %	5.9 %
BODY	D a=6 b=4 S	Unapproved	L1	82.3 / 98.7	26869.2 [cm³]	0.0 %	118.4 %	16.6 %	1.2 %	4.1 %	25.2 %

Figure H.57: cDVH of equispaced IMRT plan vs. optimized IMRT plan using Method 2 algorithm with rotated MCNP simulation data, and sela=6 and selb=4 for the L-shaped target geometry

The triangle data points represent the optimized IMRT plan and the square data points represent the equispaced IMRT plan.

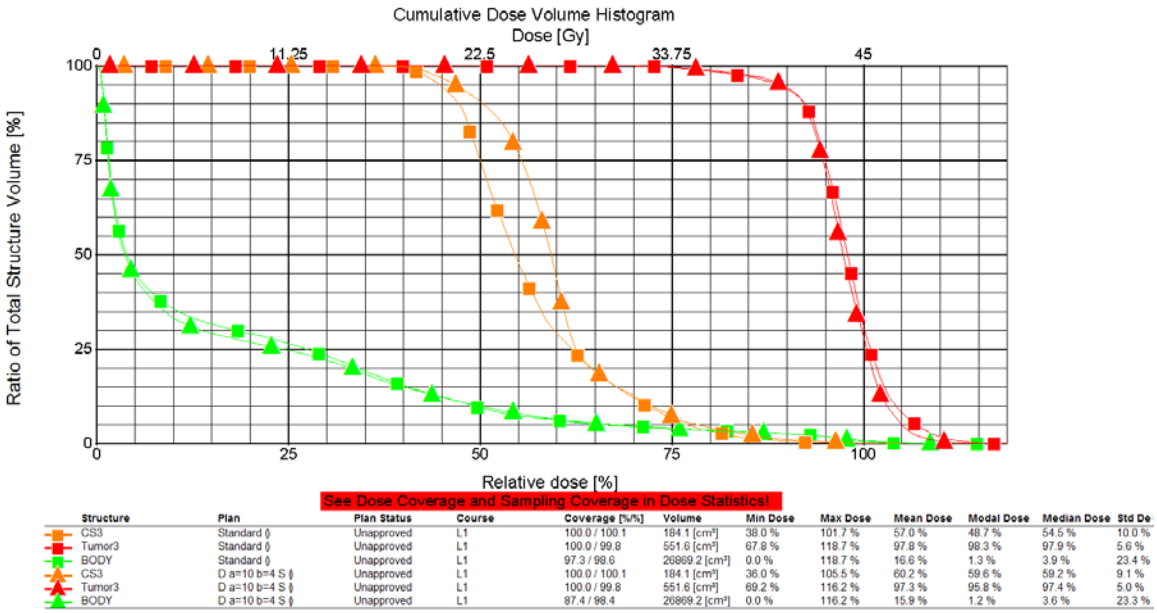

Structure	Plan	Plan Status	Course	Coverage [%/%]	Volume	Min Dose	Max Dose	Mean Dose	Modal Dose	Median Dose	Std De
CS3	Standard ()	Unapproved	L1	100.0 / 100.1	184.1 [cm³]	38.0 %	101.7 %	57.0 %	48.7 %	54.5 %	10.0 %
Tumor3	Standard ()	Unapproved	L1	100.0 / 99.8	551.6 [cm³]	67.8 %	118.7 %	97.8 %	98.3 %	97.9 %	5.6 %
BODY	Standard ()	Unapproved	L1	97.3 / 98.6	26869.2 [cm³]	0.0 %	118.7 %	16.6 %	1.3 %	3.9 %	23.4 %
CS3	D a=10 b=4 S ()	Unapproved	L1	100.0 / 100.1	184.1 [cm³]	36.0 %	105.5 %	60.2 %	59.6 %	59.2 %	9.1 %
Tumor3	D a=10 b=4 S ()	Unapproved	L1	100.0 / 99.8	551.6 [cm³]	69.2 %	116.2 %	97.3 %	95.8 %	97.4 %	5.0 %
BODY	D a=10 b=4 S ()	Unapproved	L1	87.4 / 98.4	26869.2 [cm³]	0.0 %	116.2 %	15.9 %	1.2 %	3.6 %	23.3 %

Figure H.58: cDVH of equispaced IMRT plan vs. optimized IMRT plan using Method 2 algorithm with rotated MCNP simulation data, and sela=10 and selb=4 for the L-shaped target geometry

The triangle data points represent the optimized IMRT plan and the square data points represent the equispaced IMRT plan.

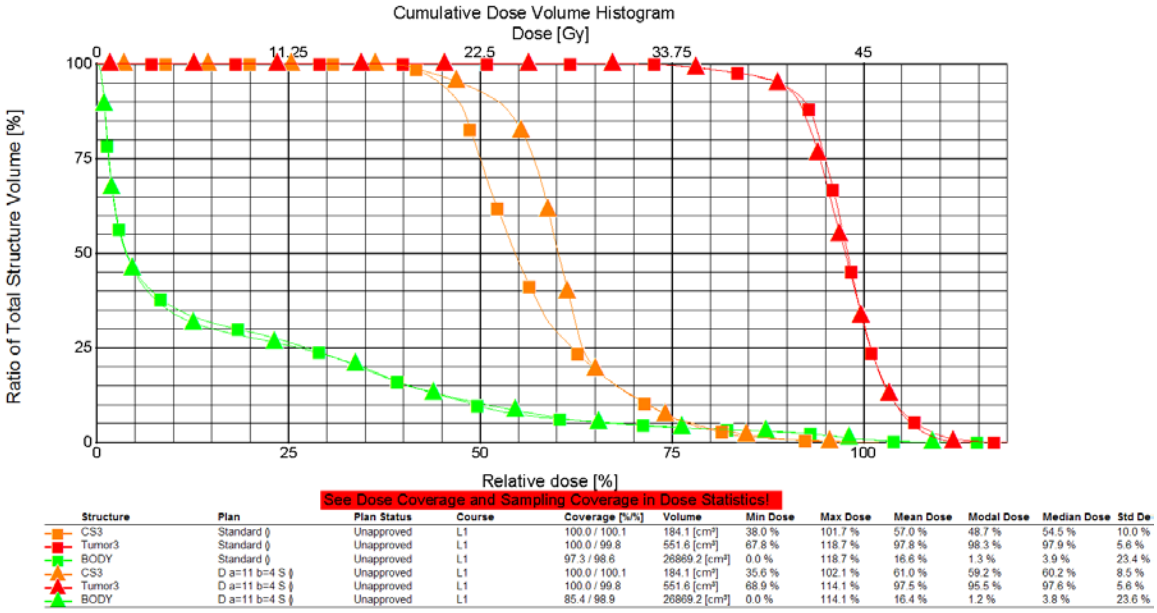

Structure	Plan	Plan Status	Course	Coverage [%/%]	Volume	Min Dose	Max Dose	Mean Dose	Modal Dose	Median Dose	Std De
CS3	Standard ()	Unapproved	L1	100.0 / 100.1	184.1 [cm³]	38.0 %	101.7 %	57.0 %	48.7 %	54.5 %	10.0 %
Tumor3	Standard ()	Unapproved	L1	100.0 / 99.8	551.6 [cm³]	67.8 %	118.7 %	97.8 %	98.3 %	97.9 %	5.6 %
BODY	Standard ()	Unapproved	L1	97.3 / 98.6	26869.2 [cm³]	0.0 %	118.7 %	16.6 %	1.3 %	3.9 %	23.4 %
CS3	D a=11 b=4 S ()	Unapproved	L1	100.0 / 100.1	184.1 [cm³]	35.6 %	102.1 %	61.0 %	59.2 %	60.2 %	8.5 %
Tumor3	D a=11 b=4 S ()	Unapproved	L1	100.0 / 99.8	551.6 [cm³]	68.9 %	114.1 %	97.5 %	95.5 %	97.6 %	5.6 %
BODY	D a=11 b=4 S ()	Unapproved	L1	85.4 / 98.9	26869.2 [cm³]	0.0 %	114.1 %	16.4 %	1.2 %	3.8 %	23.6 %

Figure H.59: cDVH of equispaced IMRT plan vs. optimized IMRT plan using Method 2 algorithm with rotated MCNP simulation data, and sela=11 and selb=4 for the L-shaped target geometry

The triangle data points represent the optimized IMRT plan and the square data points represent the equispaced IMRT plan.

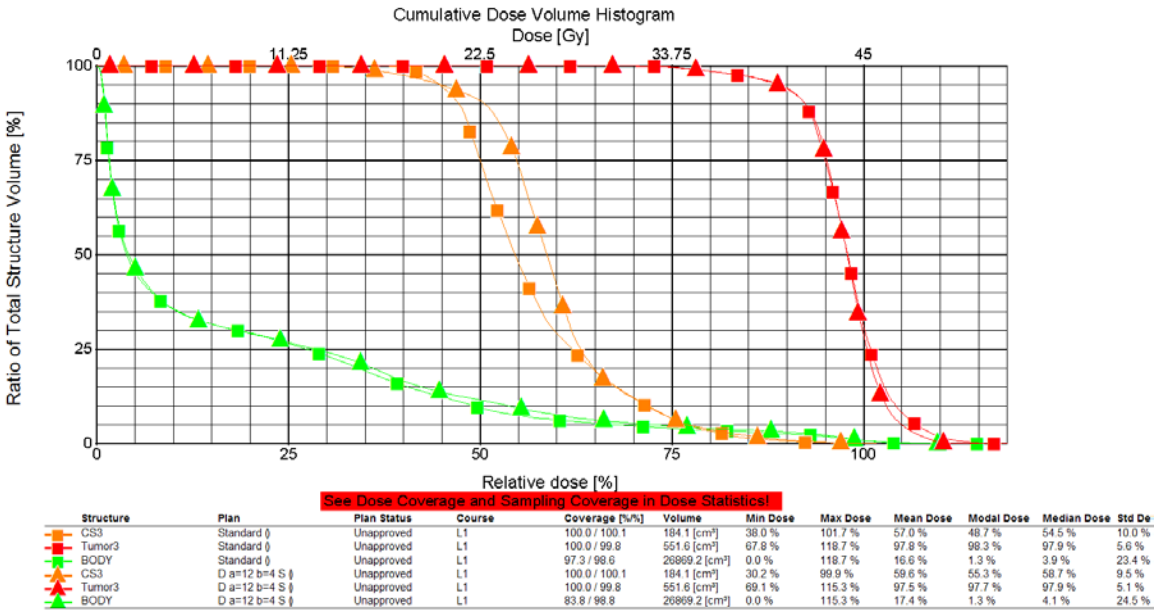

Structure	Plan	Plan Status	Course	Coverage [%/%]	Volume	Min Dose	Max Dose	Mean Dose	Modal Dose	Median Dose	Std De
CS3	Standard ()	Unapproved	L1	100.0 / 100.1	184.1 [cm³]	38.0 %	101.7 %	57.0 %	48.7 %	54.5 %	10.0 %
Tumor3	Standard ()	Unapproved	L1	100.0 / 99.8	551.6 [cm³]	67.8 %	118.7 %	97.8 %	98.3 %	97.9 %	5.6 %
BODY	Standard ()	Unapproved	L1	97.3 / 98.6	26869.2 [cm³]	0.0 %	118.7 %	16.6 %	1.3 %	3.9 %	23.4 %
CS3	D a=12 b=4 S ()	Unapproved	L1	100.0 / 100.1	184.1 [cm³]	30.2 %	99.9 %	59.6 %	55.3 %	58.7 %	9.5 %
Tumor3	D a=12 b=4 S ()	Unapproved	L1	100.0 / 99.8	551.6 [cm³]	69.1 %	115.3 %	97.5 %	97.7 %	97.9 %	5.1 %
BODY	D a=12 b=4 S ()	Unapproved	L1	83.8 / 98.8	26869.2 [cm³]	0.0 %	115.3 %	17.4 %	1.3 %	4.1 %	24.5 %

Figure H.60: cDVH of equispaced IMRT plan vs. optimized IMRT plan using Method 2 algorithm with rotated MCNP simulation data, and sela=12 and selb=4 for the L-shaped target geometry

The triangle data points represent the optimized IMRT plan and the square data points represent the equispaced IMRT plan.

H.3 U-Shaped Target Geometry

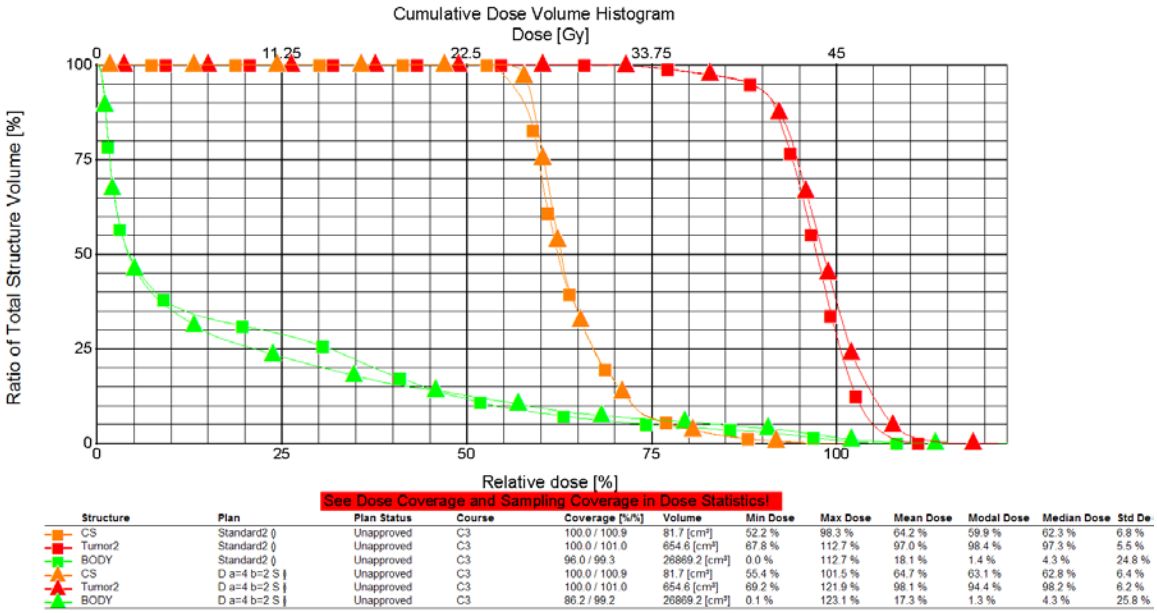

Structure	Plan	Plan Status	Course	Coverage [%/%]	Volume	Min Dose	Max Dose	Mean Dose	Modal Dose	Median Dose	Std De
CS	Standard2 ()	Unapproved	C3	100.0 / 100.9	81.7 [cm³]	52.2 %	98.3 %	64.2 %	59.9 %	62.3 %	6.8 %
Tumor2	Standard2 ()	Unapproved	C3	100.0 / 101.0	654.6 [cm³]	67.8 %	112.7 %	97.0 %	98.4 %	97.3 %	5.5 %
BODY	Standard2 ()	Unapproved	C3	96.0 / 99.3	26869.2 [cm³]	0.0 %	112.7 %	18.1 %	1.4 %	4.3 %	24.8 %
CS	D a=4 b=2 S	Unapproved	C3	100.0 / 100.9	81.7 [cm³]	55.4 %	101.5 %	64.7 %	63.1 %	62.8 %	6.4 %
Tumor2	D a=4 b=2 S	Unapproved	C3	100.0 / 101.0	654.6 [cm³]	69.2 %	121.9 %	98.1 %	94.4 %	98.2 %	6.2 %
BODY	D a=4 b=2 S	Unapproved	C3	86.2 / 99.2	26869.2 [cm³]	0.1 %	123.1 %	17.3 %	1.3 %	4.3 %	25.8 %

Figure H.61: cDVH of equispaced IMRT plan vs. optimized IMRT plan using Method 2 algorithm with rotated MCNP simulation data, and sela=4 and selb=2 for the U-shaped target geometry

The triangle data points represent the optimized IMRT plan and the square data points represent the equispaced IMRT plan.

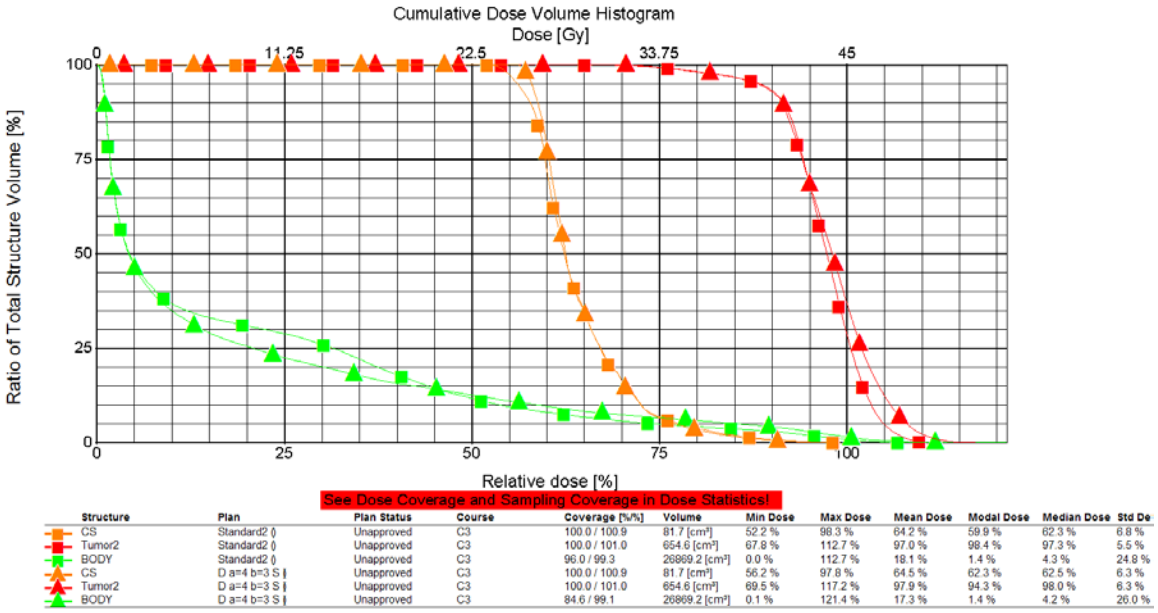

Figure H.62: cDVH of equispaced IMRT plan vs. optimized IMRT plan using Method 2 algorithm with rotated MCNP simulation data, and sela=4 and selb=3 for the U-shaped target geometry

The triangle data points represent the optimized IMRT plan and the square data points represent the equispaced IMRT plan.

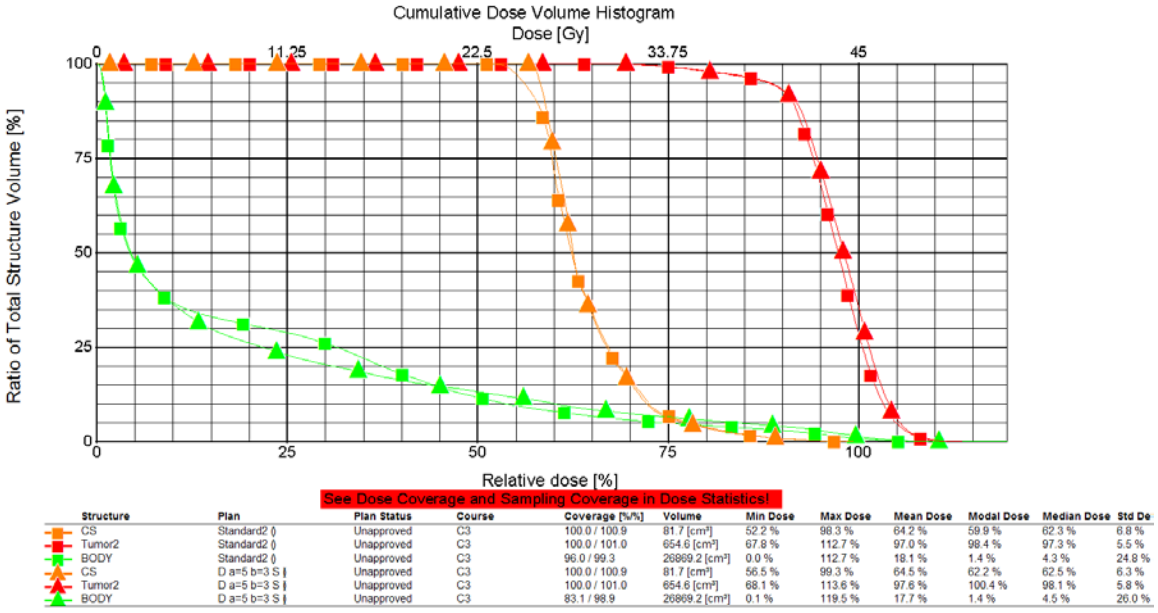

Figure H.63: cDVH of equispaced IMRT plan vs. optimized IMRT plan using Method 2 algorithm with rotated MCNP simulation data, and sela=5 and selb=3 for the U-shaped target geometry

The triangle data points represent the optimized IMRT plan and the square data points represent the equispaced IMRT plan.

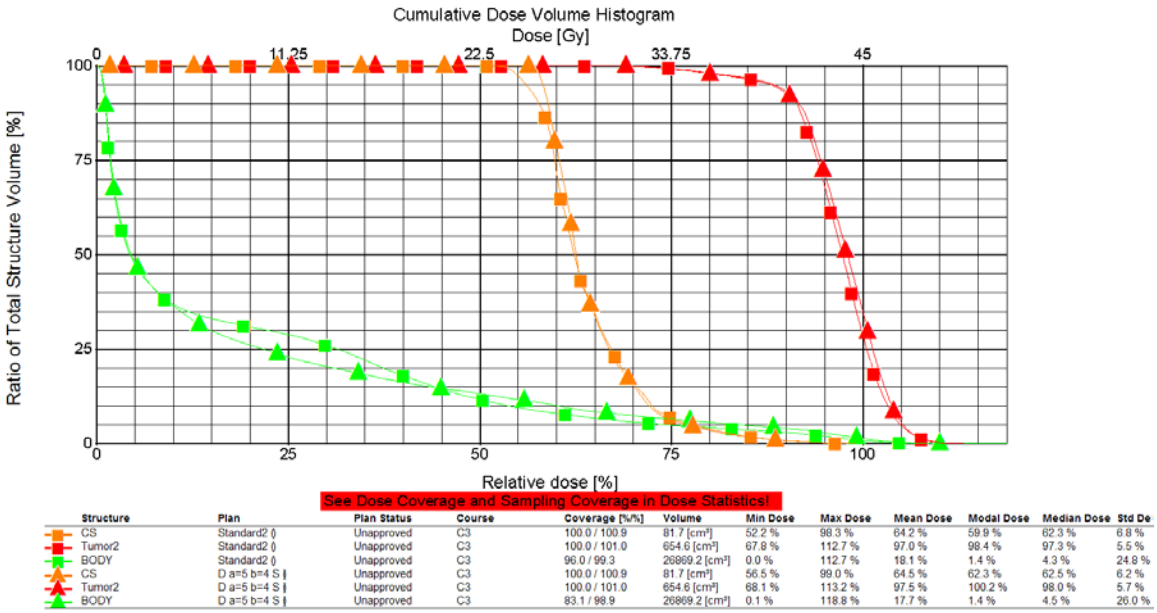

Structure	Plan	Plan Status	Course	Coverage [%/%]	Volume	Min Dose	Max Dose	Mean Dose	Modal Dose	Median Dose	Std De
CS	Standard2 ()	Unapproved	C3	100.0 / 100.9	81.7 [cm³]	52.2 %	98.3 %	64.2 %	59.9 %	62.3 %	6.8 %
Tumor2	Standard2 ()	Unapproved	C3	100.0 / 101.0	654.6 [cm³]	67.8 %	112.7 %	97.0 %	98.4 %	97.3 %	5.5 %
BODY	Standard2 ()	Unapproved	C3	96.0 / 99.3	26869.2 [cm³]	0.0 %	112.7 %	18.1 %	1.4 %	4.3 %	24.8 %
CS	D a=5 b=4 S	Unapproved	C3	100.0 / 100.9	81.7 [cm³]	56.5 %	99.0 %	64.5 %	62.3 %	62.5 %	6.2 %
Tumor2	D a=5 b=4 S	Unapproved	C3	100.0 / 101.0	654.6 [cm³]	68.1 %	113.2 %	97.5 %	100.2 %	98.0 %	5.7 %
BODY	D a=5 b=4 S	Unapproved	C3	83.1 / 98.9	26869.2 [cm³]	0.1 %	118.8 %	17.7 %	1.4 %	4.5 %	26.0 %

Figure H.64: cDVH of equispaced IMRT plan vs. optimized IMRT plan using Method 2 algorithm with rotated MCNP simulation data, and sela=5 and selb=4 for the U-shaped target geometry

The triangle data points represent the optimized IMRT plan and the square data points represent the equispaced IMRT plan.

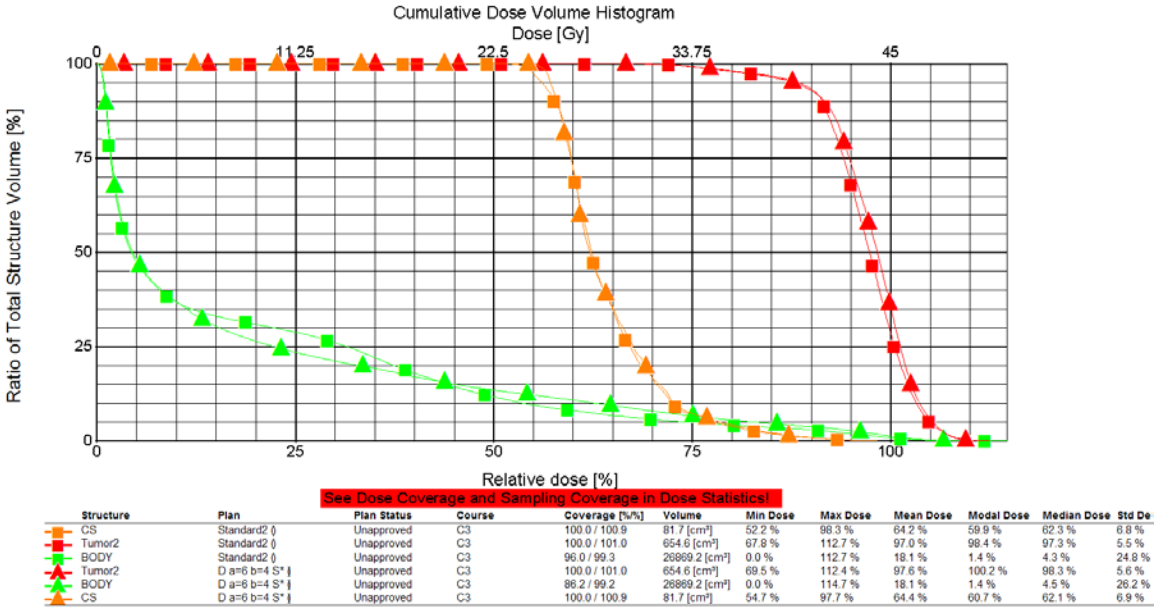

Structure	Plan	Plan Status	Course	Coverage [%/%]	Volume	Min Dose	Max Dose	Mean Dose	Modal Dose	Median Dose	Std De
CS	Standard2 ()	Unapproved	C3	100.0 / 100.9	81.7 [cm³]	52.2 %	98.3 %	64.2 %	59.9 %	62.3 %	6.8 %
Tumor2	Standard2 ()	Unapproved	C3	100.0 / 101.0	654.6 [cm³]	67.8 %	112.7 %	97.0 %	98.4 %	97.3 %	5.5 %
BODY	Standard2 ()	Unapproved	C3	96.0 / 99.3	26869.2 [cm³]	0.0 %	112.7 %	18.1 %	1.4 %	4.3 %	24.8 %
Tumor2	D a=6 b=4 S*	Unapproved	C3	100.0 / 101.0	654.6 [cm³]	69.5 %	112.4 %	97.6 %	100.2 %	98.3 %	5.6 %
BODY	D a=6 b=4 S*	Unapproved	C3	86.2 / 99.2	26869.2 [cm³]	0.0 %	114.7 %	18.1 %	1.4 %	4.5 %	26.2 %
CS	D a=6 b=4 S*	Unapproved	C3	100.0 / 100.9	81.7 [cm³]	54.7 %	97.7 %	64.4 %	60.7 %	62.1 %	6.9 %

Figure H.65: cDVH of equispaced IMRT plan vs. optimized IMRT plan using Method 2 algorithm with rotated MCNP simulation data, and sela=6 and selb=4 for the U-shaped target geometry

The triangle data points represent the optimized IMRT plan and the square data points represent the equispaced IMRT plan.

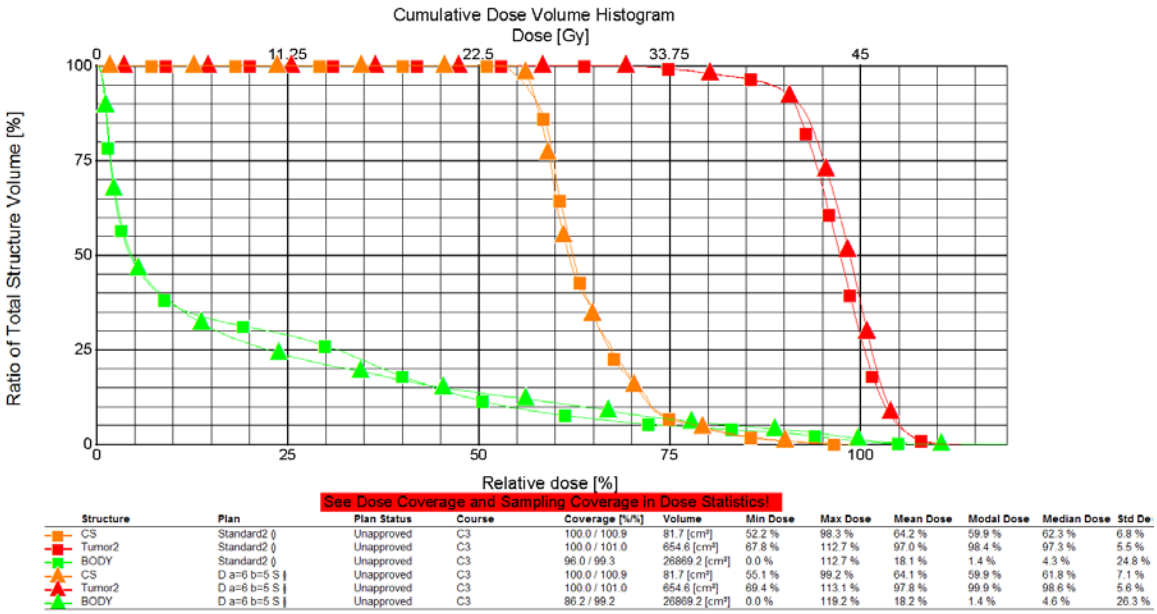

Structure	Plan	Plan Status	Course	Coverage [%/%]	Volume	Min Dose	Max Dose	Mean Dose	Modal Dose	Median Dose	Std De
CS	Standard2 ()	Unapproved	C3	100.0 / 100.9	81.7 [cm³]	52.2 %	98.3 %	64.2 %	59.9 %	62.3 %	6.8 %
Tumor2	Standard2 ()	Unapproved	C3	100.0 / 101.0	654.6 [cm³]	67.8 %	112.7 %	97.0 %	98.4 %	97.3 %	5.5 %
BODY	Standard2 ()	Unapproved	C3	96.0 / 99.3	26869.2 [cm³]	0.0 %	112.7 %	18.1 %	1.4 %	4.3 %	24.8 %
CS	D a=6 b=5 S	Unapproved	C3	100.0 / 100.9	81.7 [cm³]	55.1 %	99.2 %	64.1 %	59.9 %	61.8 %	7.1 %
Tumor2	D a=6 b=5 S	Unapproved	C3	100.0 / 101.0	654.6 [cm³]	69.4 %	113.1 %	97.8 %	99.9 %	98.6 %	5.6 %
BODY	D a=6 b=5 S	Unapproved	C3	86.2 / 99.2	26869.2 [cm³]	0.0 %	119.2 %	18.2 %	1.4 %	4.6 %	26.3 %

Figure H.66: cDVH of equispaced IMRT plan vs. optimized IMRT plan using Method 2 algorithm with rotated MCNP simulation data, and sela=6 and selb=5 for the U-shaped target geometry

The triangle data points represent the optimized IMRT plan and the square data points represent the equispaced IMRT plan.

REFERENCES

1. Pugachev A, Xing L. 2001. Psuedo beam's-eye-view as applied to beam orientation selection in intensity-modulated radiation therapy. Int. J. Radiation Oncology Biol. Phys. 51(5):1361-1370.

2. Pugachev AB, Boyer AL, Xing L. 2000. Beam orientation optimization in intensity-modulated treatment planning. Medical Physics 27(6):1238-1245.

3. Holder A, Salter B. A tutorial on radiation oncology and optimization. Trinity Universisty, Department of Mathematics. Available from: http://lagrange.math.trinity.edu/tumath/research/reports/report86.pdf via the INTERNET. Accessed 2007 Feb 25.

4. Stein J, et al. 1997. Number and orientations of beams in intensity-modulated radiation therapy. Medical Physics 24(2):149-160.

5. Pugachev A, Xing L. 2001. Psuedo beam's-eye-view as applied to beam orientation selection in intensity-modulated radiation therapy. Int. J. Radiation Oncology Biol. Phys. 51(5):1361-1370.

6. Pugachev AB, Boyer AL, Xing L. 2000. Beam orientation optimization in intensity-modulated treatment planning. Medical Physics 27(6):1238-1245.

7. Stein J, et al. 1997. Number and orientations of beams in intensity-modulated radiation therapy. Medical Physics 24(2):149-160.

8. X-5 Monte Carlo Team. (University of California). MCNP—A General Monte Carlo N-Particle Transport Code, Version 5. Volume I: Overview and Theory. Revised 2004 June 30. Los Alamos, NM: Los Alamos National Laboratory; 2003 Apr 24. Report LA-UR-03-1987. Contract W-7405-ENG-36. v p. Available from: LANL, Los Alamos, NM.

9. X-5 Monte Carlo Team. (University of California). MCNP—A General Monte Carlo N-Particle Transport Code, Version 5. Volume I: Overview and Theory. Revised 2004 June 30. Los Alamos, NM: Los Alamos National Laboratory; 2003 Apr 24. Report LA-UR-03-1987. Contract W-7405-ENG-36. 1.1 p. Available from: LANL, Los Alamos, NM.

10. Bucci MK, Bevan A, Roach III M. 2005. Advances in Radiation Therapy: Conventional to 3D, to IMRT, to 4D, and Beyond. CA Cancer J Clin 55:117-134. Available: http://caonline.amcancersoc.org/cgi/content/full/55/2/117 via the INTERNET. Accessed 2007 Feb 8.

11. Intensity-Modulated Radiation Therapy Collaborative Working Group. 2001. Intensity-Modulated Radiotherapy: Current Status and Issues of Interest. Int. J. Radiation Oncology Biol. Phys. 51(4):880-914.

12. Ezzell G, et al. 2003. Guidance document on delivery, treatment planning, and clinical implementation of IMRT: Report of the IMRT subcommittee of the AAPM radiation therapy committee. Medical Physics. 30(8):2089-2115.

13. Intensity-Modulated Radiation Therapy Collaborative Working Group. 2001. Intensity-Modulated Radiotherapy: Current Status and Issues of Interest. Int. J. Radiation Oncology Biol. Phys. 51(4):880-914.

14. Intensity-Modulated Radiation Therapy Collaborative Working Group. 2001. Intensity-Modulated Radiotherapy: Current Status and Issues of Interest. Int. J. Radiation Oncology Biol. Phys. 51(4):880-914.

15. Intensity-Modulated Radiation Therapy Collaborative Working Group. 2001. Intensity-Modulated Radiotherapy: Current Status and Issues of Interest. Int. J. Radiation Oncology Biol. Phys. 51(4):880-914.

16. Ezzell G, et al. 2003. Guidance document on delivery, treatment planning, and clinical implementation of IMRT: Report of the IMRT subcommittee of the AAPM radiation therapy committee. Medical Physics. 30(8):2089-2115.

17. Ezzell G, et al. 2003. Guidance document on delivery, treatment planning, and clinical implementation of IMRT: Report of the IMRT subcommittee of the AAPM radiation therapy committee. Medical Physics. 30(8):2089-2115.

18. Shepard DM, Ferris MC, Olivera GH, Mackie TR. 1999. Optimizing the Delivery of Radiation Therapy to Cancer Patients. SIAM Review. 41(4):721-744. Available: http:/www.siam.org/journals/sirev/41-4/34203.html via the INTERNET. Accessed 2007 Feb 25.

19. Chilton AB, Shultis JK, Faw RE. Principles of Radiation Shielding. Englewood Cliffs, NJ: Prentice Hall; 1984. 337 p.

20. Cho SH, et al. 2005. photon dosimetry data and reference phase space data for the 6 MV photon beam from Varian Clinac 2100 series linear accelerators. Medical Physics 32(!):137-148.

21. X-5 Monte Carlo Team. (University of California). MCNP—A General Monte Carlo N-Particle Transport Code, Version 5. Volume I: Overview and Theory. Revised 2004 June 30. Los Alamos, NM: Los Alamos National Laboratory; 2003 Apr 24. Report LA-UR-03-1987. Contract W-7405-ENG-36. 2-82 p. Available from: LANL, Los Alamos, NM.

22. X-5 Monte Carlo Team. (University of California). MCNP—A General Monte Carlo N-Particle Transport Code, Version 5. Volume II: MCNP Users Guide. Revised 2004 June 30. Los Alamos, NM: Los Alamos National Laboratory; 2003 Apr 24. Report LA-CP-03-0245. Contract W-7405-ENG-36. 3-97 p. Available from: LANL, Los Alamos, NM.

23. International Commission on Radiological Protection. ICRP Publication 74: Conversion coefficient for use in radiological protection against external radiation, 74. Annals of ICRP [elsevier online] 1997; 23(2). Available from: http://www.sciencedirect.com.gtel.gatech.edu:2048/science/journal/01466453 via the INTERNET. Accessed 2007 Feb 26.

24. X-5 Monte Carlo Team. (University of California). MCNP—A General Monte Carlo N-Particle Transport Code, Version 5. Volume II: MCNP Users Guide. Revised 2004 June 30. Los Alamos, NM: Los Alamos National Laboratory; 2003 Apr 24. Report LA-CP-03-0245. Contract W-7405-ENG-36. 3-99. Available from: LANL, Los Alamos, NM.

25. X-5 Monte Carlo Team. (University of California). MCNP—A General Monte Carlo N-Particle Transport Code, Version 5. Volume I: Overview and Theory. Revised 2004 June 30. Los Alamos, NM: Los Alamos National Laboratory; 2003 Apr 24. Report LA-UR-03-1987. Contract W-7405-ENG-36. 2-112. Available from: LANL, Los Alamos, NM.

26. X-5 Monte Carlo Team. (University of California). MCNP—A General Monte Carlo N-Particle Transport Code, Version 5. Volume I: Overview and Theory. Revised 2004 June 30. Los Alamos, NM: Los Alamos National Laboratory; 2003 Apr 24. Report LA-UR-03-1987. Contract W-7405-ENG-36. 2-109. Available from: LANL, Los Alamos, NM.

27. Shultis JK, Faw RE. An MCNP Primer [monograph online]. Manhattan, KS: Kansas State University, Dept. of Mechanical and Nuclear Engineering; 2006. Available from: http://ww2.mne.ksu.edu/~jks/MCNPprmr.pdf via the INTERNET. Accessed 2007 Feb 26.